MULTI-SCALAR REMOTE SENSING OF THE NORTHERN MIXED PRAIRIE VEGETATION

A Thesis Submitted to the College of

Graduate Studies and Research

in Partial Fulfillment of the Requirements

for the Degree of Doctor of Philosophy

in the Department of Geography and Planning

University of Saskatchewan

Saskatoon

By

Arun Govind

PERMISSION TO USE

In presenting this thesis in partial fulfilment of the requirements for a Postgraduate degree from the University of Saskatchewan, I agree that the Libraries of this University may make it freely available for inspection. I further agree that permission for copying of this thesis in any manner, in whole or in part, for scholarly purposes may be granted by the professor or professors who supervised my thesis work or, in their absence, by the Head of the Department or the Dean of the College in which my thesis work was done. It is understood that any copying or publication or use of this thesis or parts thereof for financial gain shall not be allowed without my written permission. It is also understood that due recognition shall be given to me and to the University of Saskatchewan in any scholarly use which may be made of any material in my thesis.

Requests for permission to copy or to make other use of material in this thesis in whole or part should be addressed to:

Head of the Department of Geography and Planning
University of Saskatchewan
Saskatoon, Saskatchewan S7N 5C8

ABSTRACT

Optimal scale of study and scaling are fundamental to ecological research, and have been made easier with remotely sensed (RS) data. With access to RS data at multiple scales, it is important to identify how they compare and how effectively information at a specific scale will potentially transfer between scales. Therefore, my research compared the spatial, spectral, and temporal aspects of scale of RS data to study biophysical properties and spatio-temporal dynamics of the northern mixed prairie vegetation.

I collected ground cover, dominant species, aboveground biomass, and leaf area index (LAI) from 41 sites and along 3 transects in the West Block of Grasslands National Park of Canada (GNPC; +49°, -107°) between June-July of 2006 and 2007. Narrowband (VI_n) and broadband vegetation indices (VI_b) were derived from RS data at multiple scales acquired through field spectroradiometry (1 m) and satellite imagery (10, 20, 30 m). VIs were upscaled from their native scales to coarser scales for spatial comparison, and time-series imagery at ~5-year intervals was used for temporal comparison.

Results showed VI_n, VI_b, and LAI captured the spatial variation of plant biophysical properties along topographical gradients and their spatial scales ranged from 35-200 m. Among the scales compared, RS data at finer scales showed stronger ability than coarser scales to estimate ground vegetation. VI_n were found to be better predictors than VI_b in estimating LAI. Upscaling at all spatial scales showed similar weakening trends for LAI prediction using VI_b, however spatial regression methods were necessary to minimize spatial effects in the RS data sets and to improve the prediction results. Multiple endmember spectral mixture analysis (MESMA) successfully captured the spatial heterogeneity of vegetation and effective modeling of sub-pixel spectral variability to produce improved vegetation maps. However, the efficiency of spectral unmixing was found to be highly dependent on the identification of optimal type and number of region-specific endmembers, and comparison of spectral unmixing on imagery at different scales showed spectral resolution to be important over spatial resolution. With the development of a comprehensive endmember library, MESMA may be used as a standard tool for identifying spatio-temporal changes in time-series imagery. Climatic variables were found to affect the success of unmixing, with lower success for years of climatic extremes. Change-detection analysis showed the success of biodiversity conservation practices of GNPC since establishment of the park and suggests that its management strategies are effective in maintaining vegetation heterogeneity in the region.

Overall, my research has advanced the understanding of RS of the northern mixed prairie vegetation, especially in the context of effects of scale and scaling. From an eco-management perspective, this research has provided cost- and time-effective methods for vegetation mapping and monitoring. Data and techniques tested in this study will be even more useful with hyperspectral imagery should they become available for the northern mixed prairie.

ACKNOWLEDGMENTS

My sincere thanks and gratitude to my supervisor, Dr. Scott Bell, for his guidance, mentoring, patience, and the research facilities he provided to me throughout my graduate study. I am extremely thankful to him for the research opportunity and support that enabled me to secure scholarships and bursaries.

Thank you to my advisory committee members: Dr. Eric Lamb, Dr. Xulin Guo, Dr. Weiping Zeng, and Dr. Dirk de Boer for providing feedback to my research, reviewing manuscripts, and devoting their valuable time for committee meetings. Dr. O.W. Archibold, Dr. Jeff Thorpe, and Dr. Maureen Reed provided research consultation. Xulin provided inputs to my research proposal and field work. Eric provided statistical consultation for data analyses. Dr. Joseph Piwowar, Dr. Greg McDermid, Dr. O.W. Archibold, and Dr. Xulin Guo shared instruments for my field work. Thank you to my external reviewer, Dr. Scott W. Mitchell, for his critical review of my thesis and his constructive comments that greatly improved my thesis.

Field work was successful only due to the hard work and enthusiasm of Randy Bonin, Jesse Nielsen, Yuhong He, and Chunhua Zhang. Thank you for pulling through long days and hikes, wilderness, and tough field conditions. Robert Sissons (Grasslands National Park of Canada) offered advice for field work.

I am grateful to Dr. Alec Aitken and Dr. Dirk de Boer for providing me the sessional teaching opportunity with the Dept. of Geography and Planning. Thanks to Dr. Cherie Westbrook, Phyllis Baynes, Brenda Britton, and Bernice Bratten at the Dept. of Geography and Planning.

Financial support from Saskatchewan Environment, Nature Saskatchewan, and University of Saskatchewan is greatly appreciated.

Software support teams at Exelis VIS Inc. (Alberto Meroni, Mari Minnari, Peg Shippert) and ESRI (Lauren Scott) were resourceful to my technical questions. Free or subsidized data sets

from United States Geological Survey (USGS), GeoBase, and Information Services Corporation (ISC) is appreciated. Dr. John Wilmshurt (Parks Canada) shared geospatial data sets.

Dr. P. Ilangovan and Dr. N. Krishnan (Madurai Kamaraj University) and Dr. Umamaheswaran K. and Dr. N. Sheela (Kerala Agricultural University) supported me to pursue studies in Canada.

Many thanks to my parents, M.P. Govindankutty and P. Girija, and my brother, Ajit Govind, and sister-in-law, Jyoti Kumari, for their love and support. Thanks to Teri Zimmerman, Raynell Connelly and the Connellys, and Karen Malanowich.

DEDICATION

This thesis is dedicated to my parents. Thank you for all your love and support.

TABLE OF CONTENTS

LIST OF TABLES

LIST OF FIGURES

LIST OF ACRONYMS

a	Gain
AB	Alberta
ACCP	Accelerated Canopy Chemistry Program
A_s	Contributing catchment area
AIC	Akaike Information Criterion
AIC_c	Corrected Akaike Information Criterion
AISA	Airborne Imaging Spectrometer for Applications
ALI	Advanced Land Imager
ANN	Artificial neural network
ASD	Analytical Spectral Devices
ASTER	Advanced Spaceborne Thermal Emission and Reflection Radiometer
ATSAVI	Adjusted-transformed soil-adjusted vegetation index
AVHRR	Advanced very high resolution radiometer on NOAA
AVIRIS	Airborne Visible/Infrared Imaging Spectrometer
b	Offset
β_0	Intercept
B	Slope
B	Blue
CASI	Compact Airborne Spectrographic Imager
CBERS	China Brazil Earth Resources Satellite
CHRIS	Compact High Resolution Imaging Spectrometer
CoB	Count Based Endmember Selection
DEM	Digital elevation model
DMC	Disaster Monitoring Constellation
EAR	Endmember Average root mean square error
ε	Random error term
em	Endmember
EMR	Electromagnetic radiation
EnMAP	Environmental Mapping and Analysis Program
ENVI	ENvironment for Visualiazing Images
EO-1	Earth Observing
EROS	Earth Resources Observation and Science Center
ESRI	Environmental Systems Research Insitute
ETM+	Enhanced Thematic Mapper Plus
FCC	False Color Composite
FLAASH	Fast Line-of-sight Atmospheric Analysis of Spectral Hypercubes
fPAR	Fraction of absorbed photosynthetically active radiation
G	Green
GIS	Geographic Information Systems
GIScience	Geographic Information Science
GLCF	Global Landcover Facility
GME	Geospatial Modelling Environment
GMES	Global Monitoring for Environment and Security

GNPC	Grasslands National Park of Canada
GPS	Global positioning system
GV	Green vegetation
GWR	Geographically weighted regression
HERO	Hyperspectral Environment and Resource Observer
HRG	High Resolution Geometry
HRVIR	High Resolution Visible and Infra Red
HYDICE	HYperspectral Digital Imagery Collection Experiment
HyspIRI	Hyperspectral Infrared Imager
IFOV	Instantaneous field of view
ITTVIS	ITT Visual Information Services
JPL	Jet Propulsion Laboratory
L	Canopy background adjustment factor
LAI	Leaf area index
L-ATSAVI	Litter-corrected adjusted-transformed soil-adjusted vegetation index
Ln	Natural logarithm
LDCM	Landsat Data Continuity Mission
LiDAR	Light Detection and Ranging
LM	Lagrange Multiplier
LTER	Long-term ecosystem monitoring and research
MASA	Minimum Average Spectral Angle
MAUP	Modifiable areal unit problem
MB	Manitoba
MESMA	Multiple endmember spectral mixture analysis
MLC	Maximum likelihood classifier
MNF	Minimum noise fraction
MODIS	Moderate resolution imaging spectrometer on Terra
MODTRAN	Moderate Resolution Transmittance
µm	Micrometer
MSAVI	Modified soil-adjusted vegetation index
MSS	Multispectral Scanner
MVC	Maximum value composites
MW	Microwave
NAD83	North American Datum 1983
NASA	National Aeronautics and Space Administration
NDVI	Normalized difference vegetation index
NDWI	Normalized difference wetness index
NIR	Near-infrared
NPP	Net primary productivity
NPV	Non-photosynthetic vegetation
OLS	Ordinary least squares
OSAVI	Optimized soil-adjusted vegetation index
PAR	Photosynthetically active radiation
PASSAGE	Pattern Analysis, Spatial Statistics and Geographic Exegesis
PCA	Principal component analysis
PPI	Pixel Purity Index

R	Red
RGB	Red-Green-Blue
RMSE	Root mean square error
ROI	Regions of interest
RS	Remote sensing / remotely sensed
SA	Spatial autocorrelation
SAGA	System for Automated Geoscientific Analyses
SAM	Spatial Analysis for Macroecology
SAMS	Spectra Analysis and Management System
SAVI	Soil-adjusted vegetation index
SGIC	Saskatchewan Geospatial Imagery Collaborative
SK	Saskatchewan
$\gamma(h)$	Semivariance
SPECCHIO	Spectral Input/Output
SMA	Spectral mixture analysis
SPECNET	Spectral Network
ρ	Spectral reflectance
SD	Standard deviation
SPOT	Satellite Pour l'Observation de la Terre
SPSS	Statistical Product for Social Sciences
SR	Spatial regression
SVI	Spectral vegetation indices
SWIR	Shortwave infrared
TIR	Thermal infrared
TM	Thematic Mapper
TSAVI	Transformed soil-adjusted vegetation index
TVs	Terrain variables
USGS	United States Geological Survey
UTM	Universal Transverse Mercator
VI	Vegetation index
VI_b	Broadband VI
VI_n	Narrowband VI
VMESMA	Variable multiple endmember spectral mixture analysis
VIF	Variation inflation factor
VIS	Visible
VLU	Vegetation landscape units
WI	Wetness index

CHAPTER 1

1.1 INTRODUCTION

Effective ecosystem management requires proper understanding of ecosystem processes and patterns at multiple spatial and temporal scales. Scientists often require information on: (i) the scale of variation of processes and patterns, (ii) how effectively data at a specific scale will potentially transfer between scales (scaling), (iii) the implications of scaling, or (iv) how processes or factors at different scales may be linked, i.e. how data at dissimilar scales may be integrated for analysis and decision-making. Ecological data is often collected at large-scales (smaller area; point- or landscape-level) using field-based methods at fixed sampling intervals and extrapolated for small-scale (larger area; regional- or ecosystem-level) predictions, decision-making, and management action. Observations and measurements can be taken only with some degree of generalization at coarser scales, however may be obtained with higher detail at finer scales. A dense sampling interval may include many observations effected by the same spatial process, while sparse sampling interval may select observations with no detectable spatial dependence (Miller et al., 2007). Hence, the conclusions derived at one scale cannot be expected to be relevant at another scale (Wiens, 1989; Wu, 1999). Therefore, these differences of scale at the collection, integration, or extrapolation stages pose problems and lead to implications if the selection of scale of study is based on convenience rather than relevance (Wessman, 1992).
To circumvent issues with scale, studies recommend that ecosystem patterns and processes are ideally examined at their optimum scale (O'Neill et al., 1986). However, it is challenging to identify the optimum scale of study due to the non-linear and multi-factorial ecological complexities (Hay et al., 2003). Therefore, a multi-scale approach (Hay et al. 2001, 2003) might be useful to understand the limitations of the selection of an arbitrary scale, identify the domains of scale, analyze scales at which patterns or processes change, or help link ecosystem processes occurring at varying scales. Realizing these challenges, ecologists are increasingly resorting to methods such as remote sensing (RS), aerial photography, and light detection and ranging (LiDAR) for their ability to provide multi-scalar data that are readily integrated with field data and analyzed at multiple scales using geographic information systems (GIS).

RS is the technique of remotely acquiring information about ground features, processes, or phenomena using sensors mounted on platforms (satellite, aircraft, unmanned aerial vehicles, and field instruments). RS has proved to be an invaluable source of vegetation, ecological, and earth-observation data at multiple spatial, spectral, and temporal scales. RS is used to study and monitor vegetation (land cover) in terrestrial ecosystems for their ability to provide data in non-destructive, repeatable, and cost-effective ways (Kerr and Ostrovsky, 2003; Cohen and Goward , 2004; Wulder et al., 2008; Roy et al., 2014). RS can provide diverse qualitative and quantitative information on plant cover, biomass, leaf area index (LAI), and plant pigment and moisture content that are useful to understand vegetation distribution and dynamics, plant productivity, or even predicting natural disasters (fire, drought). Also, RS data being in the digital format can be manipulated by resampling, classifying, or transforming into categorical and continuous data sets such as thematic maps, vegetation index (VI) maps, biophysical maps, or modeled information, georeferenced, and integrated with raster, vector, and terrain geospatial layers in GIS for multi-criteria analysis and decision-making. Currently, there are remote sensors with spatial scales ranging from sub-meter to several kilometers, spectral scales ranging from one band to several bands, and temporal scales ranging from daily to weekly. Scalar details of popular environmental monitoring satellites are given in Jensen (2000), Rogan and Chen (2004), and Kerr and Ostrovsky (2003).

With RS data available at several scales, it is important to identify how they compare against each other and the advantages and limitations of the scales of specific RS data. More importantly, how effectively data at a specific scale will potentially transfer between scales. Therefore, my research compared multi-scalar RS data of different spatial, spectral, and temporal scales for understanding the biophysical properties, spatial patterns, and identifying the temporal dynamics of the northern mixed prairie vegetation.

1.2 DEFINITIONS OF SCALE AND SCALING

Ecosystem-processes, patterns and their causal factors operate at different scales. Therefore, scale of analysis can significantly affect the identification, interpretation, and conclusion of ecological processes and patterns. E.g., temperature and precipitation occur at regional- to

global-scales, while evapotranspiration and photosynthesis occur at plant canopy-scales. Similarly, microclimate and edaphic factors affect plant distribution at local-scales, while temperature and precipitation affect vegetation distribution at regional-scales. Uncertainties arise when arbitrarily upscaling information from finer to coarser scales without properly understanding the scales and the domains at which processes operate. Therefore, the choice of the scale of study and the effects of scaling have been fundamental topics of debate and active research in ecology (Turner, 1989; Urban, 2005; Wessman, 1992), geography (Atkinson and Tate, 2000), RS (Woodcock, 1987), and GIScience (Goodchild, 2001). Wessman (1992) and Hay et al. (2001, 2003) provides discussion on scale and scaling in ecology and RS.

I adopt the following working definitions of scale throughout this dissertation.

1.2.1 Scale

Scale is defined as the window of perception; the filter or measuring tool through which the landscape may be observed or studied (Levin, 1992; Turner et al., 1989). Scale can have spatial or temporal dimension, i.e. the size of an area or the length of time under consideration when analyzing an ecological problem (Turner et al., 1989). Scale may imply: 1) the representation of the size and shape of the observation, 2) the size and shape of the study area, 3) the characterization of agents or factors, or 4) the process area. Scaling refers to the transfer of information between scales (spatial or temporal), and may be from a finer to a coarser scale (upscaling or bottom-up approach), or from a coarser to a finer scale (downscaling or top-down approach). Scale and scaling are important in ecology as new patterns and processes emerge as the scale changes. Wu et al. (2006) and Dungan et al. (2002) provide discussion on scale and types of scale.

1.2.2 Scale as in ecology and geography

Scale can be divided into cartographic scale and ecological scale, and these differ fundamentally. Cartographic (map) scale denotes the ratio of the distance on the map product to the actual ground distance. Large-scale implies patterns and processes that occur and operate over a smaller area (point, patch, landscape), while small-scale implies processes and patterns that occur and operate over a larger area (regional, biome, global). Ecological scale is defined in terms of grain

and extent. Grain refers to the resolution or the sample unit size of the study, and extent refers to the areal or temporal expanse of interest. Scale can also be coarse, medium, or fine. Fine scale refers to minute resolution or smaller study area, while coarse scale refers to broad resolution or larger study area.

Scale is further classified into intrinsic, measurement, or modeling. Intrinsic scale is the scale at which the pattern, process, or phenomenon actually operates and has a fixed extent (e.g. photosynthesis rate of a leaf). Measurement scale is the scale at which observations or sampling is taken and can be varied (e.g. size of a sampling plot or transect). Modeling scale is the scale at which the analysis is performed. Preferably, effective scale detection requires the analysis scale to match with the intrinsic scale of the pattern, process, or phenomenon under study (Wu et al., 2006). Since the latter is unknown *a priori*, different observations at multiple scales are ideal for an effective study.

1.2.3 Scale as in remote sensing

Scale is used in RS and GIScience to classify remote sensors and their data into spatial (ground coverage) and temporal (frequency of acquisition) scales. Marceau and Hay (1999) suggest scale as a function of the instantaneous field of view (IFOV) of the remote sensor, i.e. indicating the ground area imaged by the sensor at a given instant of time. Spatial resolution denotes the spatial scale; the smallest object that can be resolved to a pixel by the remote sensor. Spatial resolution signifies the grain and IFOV denotes the extent. In GIScience, scale-detection is the determination of the appropriate resolution of the spatial data. Woodcock (1987) suggests that the appropriate scale for RS observations is a function of the type of environment and the kind of information desired out of the analysis. Ideally, the resolution of predictor variables should match the ecological scale at which they are associated with the response variable. See Section 1.3.2 for implications of scale in remote sensing, especially in heterogenous environments. However, compromises to selection of data scale are often made due to data availability, costs, computational limits, or decided by the coarsest dataset used in the study. Common methods for scale detection in RS include graphs of local variance (Woodcock, 1987), semivariogram analysis (Rahman, 2003; Davidson, 2002; Zhang, 2007; Govind, current study), power spectrum and wavelet analysis (He, 2007), and image segmentation (Karl and Maurer, 2010; Hay et al., 2001, 2003).

1.3 REMOTE SENSING OF VEGETATION: STATE OF SCIENCE

RS for earth observation and land use-land cover change monitoring became popular since the launch of the Landsat satellite in 1972 (Rouse et al., 1974; Tucker, 1979; Cohen and Goward, 2004; Williams et al., 2006; Wulder et al., 2008, 2012; Roy et al., 2014). Several RS platforms, both in the optical (passive) and microwave (active) region, with increased spatial, spectral, and temporal resolutions have become available and proven to be highly useful in vegetation studies involving mapping, analysis, and monitoring. The major use of RS is its ability to provide time-series data sets to identify environmental and land use-land cover changes due to natural, anthropogenic-, environmental-, or climate-induced factors.

The Landsat program offer medium-resolution multispectral sensors such as the MSS (Multispectral Scanner), TM (Thematic Mapper), and ETM+ (Enhanced Thematic Mapper Plus). Similarly, the SPOT (Système Probatoire d'Observation de la Terre) instruments such as Vegetation, HRVIR (High Resolution Visible Infra Red) and HRG (High Resolution Geometrical), and the IRS (Indian Remote Sensing) sensors such as LISS (Linear Imaging Self Scanner), ResourceSat, and Cartosat have been used in small- and large-scale vegetation studies. Coarse-resolution satellites such as the NOAA AVHRR (Advanced Very High Resolution Radiometer), Terra MODIS (Moderate Resolution Imaging Spectroradiometer), and ASTER (Advanced Spaceborne Thermal Emission and Reflection Radiometer) have been successfully exploited for global remote sensing of vegetation and earth-observation. Also worth noting are opportunities for regional studies with DMC (Disaster Monitoring Constellation) and CBERS (China Brazil Earth Resources Satellite) satellites. Fine-resolution satellites such as GeoEye, WorldView, Pleaides, QuickBird, IKONOS, and RapidEye are useful for local vegetation studies. Vegetation-specific sensors are being developed; incorporation of the red-edge band in RapidEye and WorldView. Jensen (2000) provides acronyms and details of popular satellites, their sensors, and scope of applications.

Hyperspectral RS is a recent technology with immense potential for ecosystem studies due to hundreds of narrow spectral bands as opposed to few broad bands for multispectral RS (Ustin et

al., 2004; Kokaly et al., 2009). Hyperspectral sensors include AVIRIS (Airborne Visible/Infrared Imaging Spectrometer), AISA (Airborne Imaging Spectrometer for Applications), HYDICE (HYperspectral Digital Imagery Collection Experiment), CHRIS (Compact High Resolution Imaging Spectrometer), CASI (Compact Airborne Spectrographic Imager), HyMap, EnMap, and the Hyperion and ALI (Advanced Land Imager) sensors on EO-1 (Earth Observing). LiDAR is a complementary RS technology that is useful for obtaining canopy structure, canopy height, plant cover, leaf area index (LAI), and aboveground plant biomass (Lefsky, 2002). Hyperspectral RS and LiDAR are rapidly finding applications in ecology, forestry, and precision agriculture. Milton et al. (2007), Schaepman et al. (2009), and Goetz (2009) provide reviews on progress in hyperspectral RS and its applications in earth science. Usefulness of the fusion of LiDAR with hyperspectral, multispectral, or microwave RS data is being explored.

Remote sensors acquire spectral data along five major portions (regions) of the electromagnetic radiation (EMR) spectrum: (i) visible (VIS) (blue (B; 0.45-0.52 µm); green (G; 0.52-0.60 µm), red (R; 0.62-0.69 µm)), (ii) near infrared (NIR; 0.70-0.90 µm), (iii) shortwave infrared (SWIR; 0.9-2.5 µm), (iv) thermal infrared (TIR; 6.0-15.0 µm), and (v) microwave (MW; 0.10-100 cm). Spectral responses of different types of vegetation, soil, and water have been researched extensively. Green plant canopies absorb B and R due to chlorophyll pigments but reflect in the G and NIR region due to moisture content and internal leaf structure (Blackburn, 1998; Sims and Gamon, 2002; Homolova´, 2013). Spectral vegetation indices (SVI), combinations of reflectance in two more wavelengths (bands) have been developed to transform spectral data into biologically meaningful variables. SVI are computed as differences, ratios, or linear combinations of reflectance to represent biophysical, biochemical, or physiological characteristics (Sims and Gamon, 2002). SVI such as normalized difference vegetation index (NDVI) and simple ratio (SR) have been shown to have a strong relationship to aboveground cover, biomass, net primary productivity (NPP), pigment concentration, moisture content, and leaf area index (LAI) (Thenkabail et al., 2000). Broadband VI (VI_b) are generally used to represent “greenness” and vegetation “health”. Narrowband VI (VI_n) are specifically used to denote content of leaf pigment and moisture (Kokaly et al., 2009; Sims and Gamon, 2002). Haboudane (2004), Ollinger (2011), and Hatfield (2008) provide exhaustive list of SVI commonly used in vegetation studies.

1.3.1 Applications of multi-scalar RS data products

The common RS derivatives include true or false color composite maps, classification maps for land use-land cover, SVI maps, modeled maps for biomass, LAI, NPP, and fraction of photosynthetically active radiation (fPAR). These maps have been derived for local-, regional-, or global-level to understand vegetation distribution, patterns, and dynamics. Fine resolution imagery are used to identify and count the number of tree in an area, estimate acreage of wetlands and crop fields, or point-pattern analysis. Spectral resolution of imagery is useful to identify intra- and inter-species differences in spectral signatures and infer biophysical characteristics. Temporal resolution helps to identify plant phenological differences arising due to seasonal or environmental variability. Spectral patterns at the leaf- and canopy-level have been explored for types and concentration of plant pigment, moisture content, and phenology and how they translate into spectral response functions (Hatfield et al., 2008; Ollinger, 2011; Pinter et al., 2003). Hyperspectral RS is useful to understand plant biophysical properties such as foliar pigment and water content, photosynthetic ability, phenological changes, and physiological stress (Blackburn, 1998; Ustin et al., 2004; Goetz, 2009; Schaepman et al., 2009). Applications of hyperspectral imagery in precision agriculture include identification of crop productivity, nutrient deficiency, pest and disease damage, and environmental or physiological stress. Hatfield (2008) and Pinter et al. (2003) provide reviews on RS applications in precision agriculture.

1.3.2 Implications of scale in remote sensing

Often, the scale of study is decided by the data, the analysis scale, or by the coarsest data scale used in the analysis. Studies are frequently attempted with a single data scale for the sake of convenience and logistical- or cost-constraints. Therefore, problems may arise when an arbitrary RS data scale is chosen to study ecosystem properties and patterns as it introduces incongruence between scales at RS imaging and field sampling, i.e. mismatch between the sampling scale of ground measurements to the data scale of the RS data. Information may be masked if the intrinsic scale is finer than the measurement scale, or inferences may be incorrect if the data scale is finer than the intrinsic scale (Miller et al., 2007). Often, the selection of spatial scale may depend on the capability of the image to resolve ground objects. Coarser-scale data might spatially aggregate the ground variance, thereby reducing spatial heterogeneity and masking finer

spatial variations. Finer-scale data might have high spatial autocorrelation (SA; i.e. similarity in pairs of the values of nearby locations; Tobler, 1970), costly, or simply difficult to acquire, process, or store. Therefore, observations made by the imposition of an arbitrary scale has a "smoothening or coarsening effect" on the patterns and processes being studied and their ability to give the ideal inference. This further affects the types of patterns that can be observed, limits the scales within which the observations can occur (scale domains), or restricts ability for scaling information (scaling threshold). RS data also suffers from the modifiable areal unit problem (MAUP; Hay et al. 2001) whereby the scale of data analysis influences the outcome when the same analysis is applied to the same data but at different aggregation shemes. MAUP effect can be either due to scale (aggregation) or zone (grouping). In the former, different results may be obtained when the same data analysis is applied on different aggregation units (changes in scale). Scale can be problematic during imaging. The spectral information from ground features is recorded by the remote sensor into pixels that are arranged into a spatial matrix. Ideally, spectral information from a single feature is recorded into a single pixel (a pure pixel) that can be spatially referenced to the ground. In highly heterogeneous environments, the reflectance from background materials combine with the reflectance from green vegetation to form a composite (mixed) spectra that is recorded by the sensor. Thus, spectral information from several ground features are non-linearly mixed (Somers et al., 2011) and imaged into a single pixel (a mixed pixel). 'Mixed pixels' are an issue with coarse-scale imagery and the spectral variability on the landscape is not effectively captured into image pixels. These mixed pixels do not correspond to actual ground cover and the values recorded for the space represented by that pixel are not solely determined by what is on the ground in that discrete space, unless the cover fractions are separated within the mixed pixel. Therefore, with coarser resolution, the ability of the remote sensor to resolve ground objects is compromised and pixels do not adequately represent the optimal scales of boundaries of natural patterns and processes. When fine resolution sensors are used, they record the same land cover into multiple pixels (i.e. more noise and less variance). Thereby, problems of spatial autocorrelation (SA; Ji and Peters, 2004) are introduced, which violate the conditions of predictive global regression models. Statistical assumptions of correlation and regression (e.g. independence of observations) are not met when data shows SA, thus requiring 'corrections' to incorporate and adjust for spatial effects in the prediction models.

Hence, studying ecosystem processes and patterns only at finest scales limits our ability to generalize patterns or processes at coarser RS scales. Further, comparison of results is difficult if studies employ different scales that have been selected based on convenience rather than relevance. With the current availability of RS data from various platforms and at multiple spatial scales, researchers are faced with the challenge of selecting appropriate RS data scale to answer specific research objectives. A multi-scalar study allows for the understanding of the effects and implications of scale and upscaling observations.

1.4 ECOLOGICAL CONTEXT – PRAIRIE CONSERVATION AND MANAGEMENT

Grasslands, referred as the 'Great Plains', are ecosystems dominated > 90% in land cover by grasses. Grasslands occur in all continents except Antarctica and dominate the land cover in the interior of the North America (Coupland, 1950). The major types of grasslands in North America are the tall grass prairie, the mixed grass prairie, and the short grass prairie (Briggs et al., 2008). Within the Great Plains, the tall grass prairie extends from Canada and Minnesota south to Texas, the mixed grass prairie from Saskatchewan and Alberta and eastern North Dakota south to Texas, and the short grass prairie extends from western Texas and New Mexico north to eastern Montana (Samson and Knopf, 1994). Fig. 1.1 shows the geographic extents of the three major grassland types in North America. The mixed grass prairie is the largest grassland type in North America and is further divided into the northern and the southern mixed prairie.

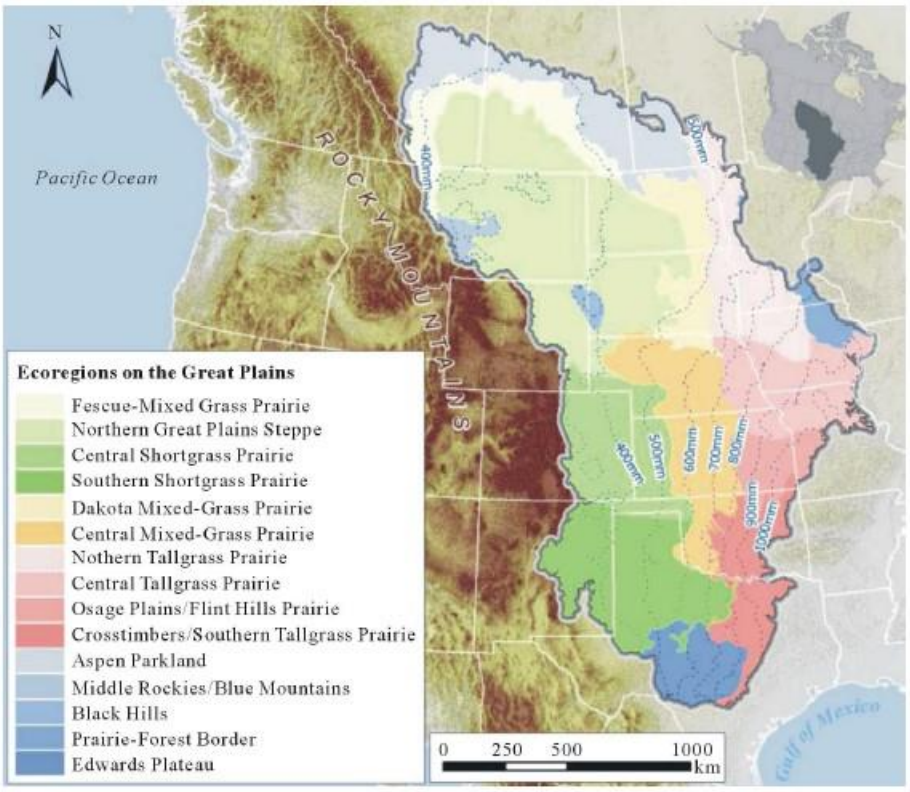

Fig. 1.1 Types and distribution of grasslands within North America (Adapted from: Li and Guo, 2014).

The North American grasslands are recognized as one of the most diverse terrestrial ecosystems on Earth, with a rich geological and paleontological history and habitat to several endangered and threatened species (Gauthier et al., 2003; Dolan, 1999). The original extent of the grasslands is estimated at ~25-40% (~162 million hectares) of the Earth's land surface, however their area has declined to currently occupy ~20% (Samson and Knopf, 1994). In Canada, significant decline of the mixed prairie have been reported for Saskatchewan (SK), Alberta (AB), and Manitoba (MB), with >80-90% reduction in SK and AB (Samson and Knopf, 1994). Grasslands are significant carbon sinks, highly agriculturally productive, and rich sources of natural resources (Gauthier et al., 2003). Economically, the grasslands have a 500-year history of intensive human exploitation for grain- and forage-cultivation, ranching, and livestock grazing (Lauenroth et al., 1999). Oil and mineral exploration are the recent human-induced pressures.

Climate, topography, soil, fire, and grazing are the main factors responsible for the origin, maintenance, and structure of the grasslands. Climatic gradients are the primary factor for the distribution of the grassland types, with a latitudinal temperature gradient, and a moisture (precipitation) gradient due to topography from the west to the east (Coupland, 1950). Vegetation growth in the mixed prairie is largely dependent on the availability of soil moisture, and therefore future temperature and precipitation trends are highly important. Besides human disturbances, climate change is believed to be the biggest long-term threat in this ecosystem. Among the terrestrial ecosystems, the Great Plains are predicted to be the worst hit by global climate change, and scientists forecast a temperature increase of 0.5-1°C per decade (Samson and Knopf, 1996). A few of the predicted impacts include warming, changes in vegetation type, composition and structure, and invasion of exotic plants.

Considering the necessity for grassland restoration and conservation (see Samson and Knopf (1994)) and the need for methods that are small-scale, cost-effective, continuous, and sustainable, RS seems to be the most promising approach. Several RS data sets are now available at multiple spatial, and temporal scales that permit inventorying, management, and monitoring of grasslands.

1.4.1 Synthesis of remote sensing research in the northern mixed prairie

Many of the previous vegetation RS studies have focused on forestry or agricultural applications. Grasslands have been given less importance even though they are ecologically and economically important. Previous research in the northern mixed prairie has explored RS for studying plant biophysical characteristics (Guo, 2000; He, 2008; Li et al., 2014), modeling plant productivity (Davidson, 2002; Mitchell, 2003), identifying suitable indices to characterize vegetation (He at al., 2006; Li and Guo, 2010), estimating photosynthetic rates (Black, 2007), quantifying dead plant component (Yang and Guo, 2011; Xu et al., 2014), studying vegetation heterogeneity (Guo et al., 2004; Zhang, 2008), understanding effects of grazing (Li and Guo, 2010; Yang and Guo, 2011; Yang et al., 2012; Virk, 2012; Virk and Mitchell, 2014), predicting plant water content (Davidson et al., 2006), vegetation mapping using pixel-based and neural network classifiers (Zhou, 2008), and identifying vegetation changes due to climate (Mitchell and Csillag, 2001; Mitchell, 2003; Li and Guo, 2012; Li and Guo, 2014).

These researchers report that RS of the northern mixed prairie is challenging due to several reasons. Vegetation, even though sparse, occurs in several layers (Coupland, 1950). Vegetation growth in the region is highly limited by temperature and availability of soil moisture, which leads to short-term differences in phenology (Li and Guo, 2012). The dominant native prairie grasses are perennials with very quick but short vegetative growth period (~170 days), however shrubs and a few invasive grasses are perennial. The northern mixed prairie is dominated by grasses of different photosynthetic pathways and different phenology. Similar to other semi-arid ecosystems (Okin et al., 2001), non-linear mixing is an issue in the mixed prairie as vegetation cover is generally sparse and predominantly occurs with large amount of non-photosynthetic vegetation (NPV), litter, and soil. SVIs, such as the soil-adjusted VI (SAVI) have been recommended to minimize background effects (Qi et al., 1994), especially improved versions such as the adjusted-transformed (ATSAVI) and the litter-corrected ATSAVI (L-ATSAVI; He et al., 2006; Li and Guo, 2010). Yang and Guo (2011; 2014) and Xu et al. (2014) used RS approaches to study the dead plant component in northern mixed prairie.

1.5 STUDY AREA

1.5.1 History and land use

This research was conducted at the Grasslands National Park of Canada (GNPC; Parks Canada), situated at the Saskatchewan-Montana border (49° N, 107° W). GNPC covers 906 km^2 and is composed of the East Block and the West Block (Fig. 1.2). GNPC established in 1984 is the first and the only park in Canada with a strong mandate for grassland conservation and preservation of the remnant native prairie. Prior to the first land acquisition by the Park in 1984, agriculture, livestock and ranching were widely practiced in the region. Though the Park is protected from human disturbances since its establishment, prairie eco-restoration strategies such as prescribed burning and natural grazing by bison (introduced in 2006) are followed. This region is home to several endangered and species-at-risk, and this region has therefore been adopted for biodiversity conservation and long-term ecosystem monitoring and research (LTER). The Park also provides palaeological evidence of dinosaur fossils, heritage of First Nations and history of ranching and homesteading by European settlers. Ranching and agriculture are still practiced

around the GNPC area and Parks Canada is actively pursuing acquisition of private lands for conservation.

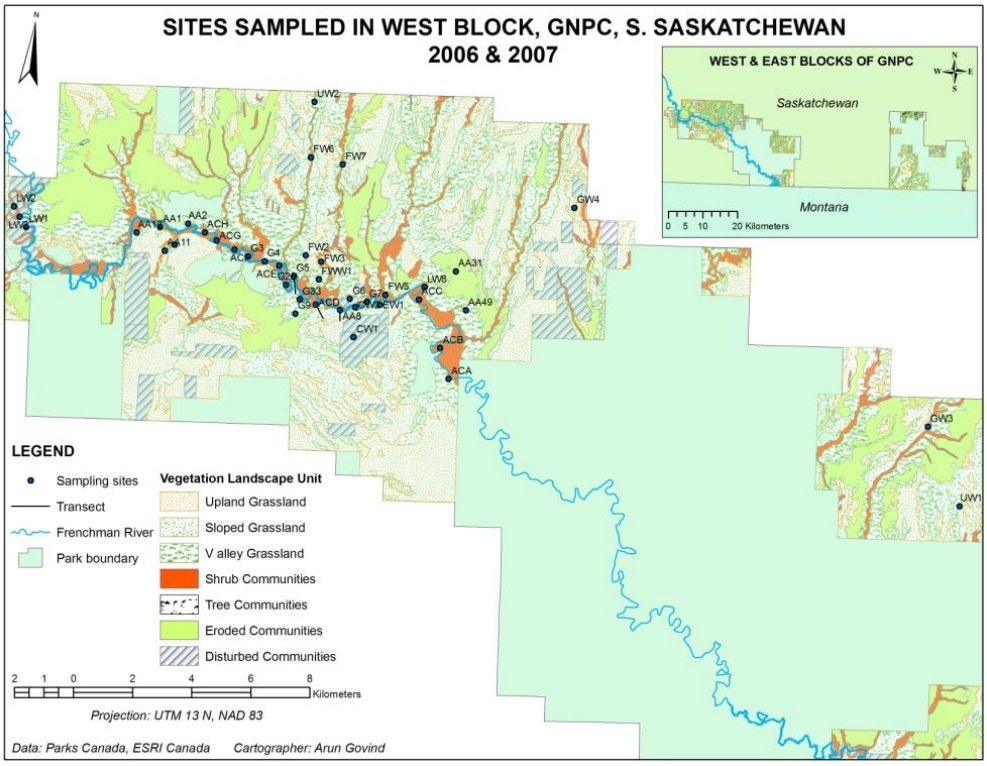

Fig. 1.2 Map showing the location of Grasslands National Park of Canada (GNPC), its East and West Blocks, and the vegetation landscape units (VLU; Michalsky and Ellis, 1994).

1.5.2 Climate, topography, soil and physical features

The northern mixed prairie has the continental semi-arid type of climate with great extremes of temperature between winter and summer seasons, and low annual precipitation. The mean annual temperature is 3.8°C and annual precipitation <325 mm, with the majority of the precipitation is between May to September. The predominant soils are primarily of glacial origin and the common soil types include chernozems, solonetzs, and regosols (Saskatchewan Institute of Pedology, 1992). Chernozems are the most dominant soil and followed by solonetz as the second major. The region has a rolling topography and the average elevation is ~800 m. Topography directly controls water and soil erosion and determines the spatial distribution and patterns of vegetation. Also, topography along with elevation determines local climatic conditions. Important rivers flowing in the GNPC area are the North and the South Saskatchewan River. The

Frenchman River, flowing from the north-west to the south-east, is the major waterbody in the GNPC area and is part of the Missouri river watershed.

1.5.3 Vegetation types and distribution

The northern mixed prairie is dominated 85% by grasses and consists of a mixture of mid-height and short grasses. They differ in their photosynthetic pathway types and peak season of growth and maturity. Coupland (1950, 1961, 1992) and Singh et al. (1983) have elaborately discussed the ecology and vegetation of the northern mixed prairie. The dominant vegetation communities in the northern mixed prairie include *Stipa-Agropyron*, *Stipa-Bouteloua*, *Stipa-Bouteloua-Agropyron*, *Agropyron-Koeleria*, and *Bouteloua-Agropyron* (Coupland, 1992). Michalsky and Ellis (1994) completed a vegetation inventory within the GNPC and broadly classified the vegetation on the basis of elevation and degree of slope into upland, sloped, and lowland grassland (Fig. 1.2). The dominant grasses include western wheat grass (*Agropyron smithii*), northern wheat grass, and blue grama (*Bouteloua gracilis*). Shrubs, forbs, and microphytic vegetation such as moss and lichens also occur and limited by topography and availability of soil moisture. Forbs, shrubs, and sedges are of lower coverage and mostly seen in the sloped land and lowlands. Low precipitation, high summer temperatures, and warm, dry, high winds make soil moisture the limiting factor for plant growth. Localized variations in soil moisture created by topography determine the composition and density of vegetation. Coupland (1950) discusses the distribution of vegetation communities in the northern mixed prairie based on soil type, topography, and soil moisture. Specifically in the GNPC area, the dominant grasses include needle and thread (*Hesperostipa comata*), blue grama (*Bouteloua gracilis*), northern wheat grass (*Elymus lanceolatus*), western wheat grass (*Pascopyrum smithii*), june grass (*Koeleria macrantha*). Common shrubs in the region consists of sagebrush (*Artemisia cana*), buckbrush (*Symphoricarpos occidentalis*), winterfat (*Krascheninnikovia lanata*), thorny buffaloberry (*Shepherdia argentea*), wood rose (*Rosa woodsii*), creeping juniper (*Juniperus horizontalis*), rabbit brush (*Chrysothamnus nauseosus*), and willow (*Salix* sp.). The common forbs include prairie sage (*Artemisia ludoviciana*), pasture sage (*Artemisia frigida*), moss phlox (*Phlox hoodii*), spike moss (*Selaginella densa*), and prickly pear (*Opuntia polycantha*). Invasive species such as crested wheat grass (*Agropyron cristatum*) and smooth brome (*Bromus inermis*), introduced through human activities, are of high management priority. Plant names are adapted from Harms

(2006). Vegetative growth for most grasses begins in late March to early April, and the quick and short vegetative growth is completed by late June, with senescence in August or September.

1.6 KNOWLEDGE GAPS

My research aims to fill some of the important knowledge gaps in the context of RS of the northern mixed prairie vegetation. Previous vegetation RS studies have focused solely on the upland prairie, arguing it to be the important vegetation in the northern mixed prairie. However, ecologists and conservationists now agree that preserving and managing vegetation in the lowland prairie might be the best strategy for conserving the endangered and species-at-risk fauna and for maintaining the ecological integrity of the prairies. The lowland prairie has the shrubs which have been recognized as critical habitat for several endangered fauna. There is lack of knowledge of the biophysical properties and spectral characteristics of the lowland prairie. Further, most previous RS studies have used RS data at a single or few spatial scales, i.e. studies have not attempted a multi-scalar approach and compared how effectively data at specific scales will potentially transfer between scales. RS data at multiple scales are currently available, therefore it is important to compare the effects of scale for RS of vegetation and how patterns, interpretations, or inferences vary with change in data scales. Performance of vegetation indices have been tested at one or two scales, however there is lack of information on over what range of scales they are effective. High spatial heterogeneity of the northern mixed prairie vegetation has been acknowledged (Zhang, 2008), however none of the previous studies have attempted methods to incorporate sub-pixel spectral variability. Though the issue of mixed pixels and linear mixing of the vegetation spectrum has been recognized in these semi-arid ecosystems, none of the past studies has explicitly attempted to address this problem. None of the previous studies has accounted for the effects of sub-pixel spectral variability of the mixed prairie vegetation or how they might be incorporated in image classification for land cover mapping. Though studies have used NDVI images from coarse-resolution sensors such as AVHRR (250 m) to identify changes, however research (He et al (2007) has shown that the optimum sampling scale for vegetation studies is between 10-50 m. Hence, spatio-temporal changes need to be re-examined using medium-resolution data sets such as Landsat.

1.7 RESEARCH QUESTION

My fundamental hypothesis was that multi-scalar RS information of vegetation can be successfully exploited to reveal important spatial patterns, biophysical characteristics, and dynamics of the northern mixed prairie vegetation. The general question that motivated this study was to identify the spatial data scale of RS data product that is most effective in studying the patterns and the dynamics of vegetation in the northern mixed prairie, and whether the identified patterns are comparable irrespective of the scale of the RS data product used in the study. Grasslands National Park of Canada (GNPC) was selected as a representative area for the northern mixed prairie, and all my experiments were based in this study area.

1.8 THESIS STRUCTURE

This thesis is divided into five chapters. Though each chapter focuses on specific research objectives, they are intended to build upon each other in a logical progression to accomplish the main research hypothesis. Each manuscript has an abstract, literature review and background research, discussion of materials and methods, results and findings, discussion and conclusions, and list of references cited.

The introductory chapter provides working definitions of scale and scaling and how they are conceptualized and applied in ecology, geography, and remote sensing. The different views and classifications of scales as used in ecology and geography, and also how the concept of scale applies in ecology, geography, RS, and GIScience are discussed. I further provide brief introduction to the state of science of vegetation RS and include a synthesis of the RS research in the northern mixed prairie along with the research gaps that motivated the current study. The importance of grasslands and the need for their conservation and restoration are also described to justify my research.

In Chapter 2, I discuss the spatial scales and spatial variation of plant biophysical properties along topographical gradients in the northern mixed prairie. SVI derived from RS data at four

data scales: 1, 10, 20, and 30 m were compared with field estimates. Semivariogram analysis was used on RS estimates to identify the spatial scales of variation of plant biophysical properties.

In Chapter 3, I discuss spatial scale and effects of upscaling RS information for studying the northern mixed prairie vegetation. RS data sets were upscaled from their native scales to common coarser scales of 40, 50 and 60 m to understand the effects of upscaling and how they compare. Analysis integrated spatial regression methods to account for spatial effects.

In Chapter 4, I used multiple endmember spectral mixture analysis (MESMA) and tested its feasibility for vegetation mapping in the northern mixed prairie. Comprehensive region-specific endmember spectral libraries for green vegetation (GV), non-photosynthetic vegetation (NPV), and soil were developed and used to create 2- and 3-endmember models. These endmember models were used to unmix three multispectral images of differing spatial scales (10, 20, and 30 m) to estimate sub-pixel fractions of GV, NPV, and soil in the study area.

In Chapter 5, I further tested MESMA for spatio-temporal change-detection on time-series Landsat-5 TM imagery. 2-endmember models were developed using endmember spectra for GV, NPV, and soil for unmixing seven Landsat-5 TM scenes at phenologically comparable time-points. Time-series NDVI images were also derived to compare with the MESMA images. Bi-temporal change differencing was performed by subtracting each historical year from the base year to identify the spatio-temporal changes to land cover in the study area.

In Chapter 6, I provide summary and conclusions from my study and outline possible future research opportunities.

1.9 REFERENCES

Atkinson, P.A., and Tate, N.J. 2000. Spatial scale problems and geostatistical solutions: A Review. *The Professional Geographer*, 52(4): 607-623.

Black, S.C. 2006. *Estimation of grass photosynthesis rates in mixed grass prairie using field and remote sensing approaches.* M.Sc. Thesis, University of Saskatchewan, Saskatoon.

Blackburn, G.A. 1998. Quantifying chlorophylls and carotenoids at leaf and canopy scales: An evaluation of some hyperspectral approaches.

Briggs, J.M., Knapp, A.K., and Collins, S.L. 2008. Steppes and Prairies. *Encyclopedia of Ecology*, 3373-3382.

Cohen, W.B., and Goward, S.N. 2004. Landsat's role in ecological applications of remote sensing. *BioScience*, 54(6): 535-545.

Coupland, R.T. 1950. Ecology of mixed prairie in Canada. *Ecological Monographs*, 20(4): 271-315.

Coupland, R.T. 1961. A reconsideration of grassland classification in the Northern Great Plains of North America. *Journal of Ecology*, 49(1): 135-167.

Coupland, R.T. 1992. Mixed prairie. In Coupland, R.T. (Ed.) *Natural Grasslands - Introduction and Western Hemisphere. Ecosystems of the World*. New York, Elsiver.

Davidson, A. 2001. *Integrating field sampling and remotely sensed data for monitoring the function and composition of the northern mixed grass prairie.* Ph.D. Thesis, University of Toronto, Toronto.

Davidson, A., and Csillag, F. 2001. The influence of vegetation index and spatial resolution on a two-date remote sensing-derived relation to C_4 species coverage. *Remote Sensing of Environment*, 75(1): 138-151.

Davidson, A., Wang, S., and Wilmshurst, J. 2006. Remote sensing of grassland-shrubland vegetation water content in the shortwave domain. *International Journal of Applied Earth Observation and Geoinformation*, 8(4): 225-236.

Dolan, C.C. 1999. The national grassland and disappearing biodiversity: can the prairie dog save us from an ecological desert? *Environmental Law*, 29(1): 213-234.

Dungan, J.L., Perry, J.N., Dale, M.R.T., Legendre, P., Citron-Pousty, S., Fortin, M.J., Jakomulska, A., Miriti, M., and Rosenberg, M.S. 2002. A balanced view of scale in spatial statistical analysis. *Ecography*, 25(5): 626-640.

Goetz, A.F.H. 2009. Three decades of hyperspectral remote sensing of the Earth: A personal view. *Remote Sensing of Environment*, 113: S5–S16.

Goodchild, M.F. 2001. Models of scale and scales of modelling. In: Tate, N.J., Atkinson, P.M. (Eds.), Modelling Scale in Geographical Information Science. John Wiley & Sons, Chichester.

Guo, X., Price, K.P., and Stiles, J.M. 2000. Biophysical and spectral characteristics of three land management practices on cool and warm season grasslands in eastern Kansas. *Natural Resources Research*, 9(4): 321-331.

Guo, X., Wilmshurst, J., Fargey, P., and Richard, P. 2004. Measuring spatial and vertical heterogeneity of grasslands using remote sensing techniques. *Journal of Environmental Informatics*, 3(1): 24-32.

Haboudane, D., Miller, J.R., Pattery, E., Zarco-Tejad, P.J., and Strachan, I.B. 2004. Hyperspectral vegetation indices and novel algorithms for predicting green LAI of crop canopies: modeling and validation in the context of precision agriculture. *Remote Sensing of Environment*, 90(3): 337-352.

Harms, V.L. 2006. *Annotated catalogue of Saskatchewan vascular plants*. 116 pp.

Hatfield, J.L., Gitelson, A.A., Schepers, J.S., and Walthall, C.L. 2008. Application of spectral remote sensing for agronomic decisions. *Agronomy Journal*, 100: S-117-S-131.

Hay, G.J., Marceau, D.J., Dube, P., and Bouchard, A. 2001. A multiscale framework for landscape analysis: Object-specific analysis and upscaling. *Landscape Ecology*, 16(6): 471-490.

Hay, G.J., Blaschke, T., Marceau, D.J., and Bouchard, A. 2003. A comparison of three image-object methods for the multiscale analysis of landscape structure. *ISPRS Journal of Photogrammetry and Remote Sensing*, 57(5-6): 327-345.

He, Y. 2008. *Modeling grassland productivity through remote sensing products.* Ph.D. Thesis, University of Saskatchewan, Saskatoon.

He, Y., Guo, X., and Wilmshurst, J.F. 2006. Studying mixed grassland ecosystems I: suitable hyperspectral vegetation indices. *Canadian Journal of Remote Sensing*, 32(2): 98-107.

He, Y., Guo, X., and Si, B.C. 2007. Detecting grassland spatial variation by a wavelet approach. *International Journal of Remote Sensing*, 28(7): 1527-1545.

He, Y., Guo, X., and Wilmshurst, J.F. 2007. Comparison of different methods for measuring leaf area index in a mixed grassland. *Canadian Journal of Plant Science*, 87(4): 803-813.

He, Y., Guo, X., and Wilmshurst, J.F. 2009. Reflectance measures of grassland biophysical structure. *International Journal of Remote Sensing*, 30(10): 2509-2521.

Homolova´, L., Malenovsky, Z., Clevers, J.G.P.W., and Garcı´a-Santos, G. 2013. Review of optical-based remote sensing for plant trait mapping. *Ecological Complexity*, 15: 1-16

Jensen, J.R. 2000. Remote Sensing of the Environment: an Earth Perspective. Prentice Hall, Saddle River, New Jersey.

Karl, J.W., and Maurer, B.A. 2010. Spatial dependence of predictions from image segmentation: A variogram-based method to determine appropriate scales for producing land-management information. *Ecological Informatics*, 5(3): 194-202.

Kerr, J., and Ostrovsky, M. 2003. From space to species: ecological applications for remote sensing. *Trends in Ecology & Evolution*, 18(6): 299-305.

Kokaly, R.F., Asner, G.P., Ollinger, S.V., Martin, M.E., and Wessman, C.A. 2009. Characterizing canopy biochemistry from imaging spectroscopy and its application to ecosystem studies. *Remote Sensing of Environment*, 113: S78-S91.

Lauenroth, W.K., Burke, I.C., and Gutmann, M.P. 1999. The structure and function of ecosystems in the central north american grassland region. *Great Plains Research*, 9(2): 223-259.

Lefsky, M.A., Cohen, W.B., Parker, G.G., and Harding, D.J. 2002. Lidar remote sensing for ecosystem studies. *Bioscience*, 52(1): 19-30.

Levin, S.A. 1992. The problem of pattern and scale in ecology. *Ecology*, 73: 1943-1967.

Li, M., and Guo, X. 2014. Long term effect of major disturbances on the northern mixed grassland – A review. *Open Journal of Ecology*, 4: 214-233.

Li, S., Li, Z., and Guo, X. 2014. Remote sensing of leaf area index (LAI) and a spatiotemporally parameterized model for mixed grasslands. *International Journal of Applied Science and Technology*, 4(1): 46-61.

Li, Z., and Guo, X. 2010. A suitable vegetation index for quantifying temporal variations of LAI in semi-arid mixed grassland. *Canadian Journal of Remote Sensing*, 36(6): 709-721.

Li, Z., and Guo, X. 2010. Topographic effects on vegetation biomass in semiarid mixed grassland under climate change using AVHRR NDVI. *British Journal of Environment and Climate Change*, 4(2): 229-242.

Li, Z., and Guo, X. 2012. Detecting climate effects on vegetation in northern mixed prairie using NOAA AVHRR 1-km time-series NDVI data. *Remote Sensing*. 4(1): 120-134.

Marceau, D.J. 1999. The scale issue in social and natural sciences. *Canadian Journal of Remote Sensing*, 25(4): 347-356.

Marceau, D.J., and Hay, G.J. 1999. Remote sensing contributions to the scale issue. *Canadian Journal of Remote Sensing*, 25(4): 357-366.

Michalsky, S.J., and Ellis, R.A. 1994. *Vegetation of Grasslands National Park*. DA Westworth and Associates, Calgary.

Miller, J., Franklin, J., and Aspinall, R. 2007. Incorporating spatial dependence in predictive vegetation models. *Ecological Modelling*, 202(3-4): 225-242.

Milton, E.J., Schaepman, M.E., Anderson, K., Kneubühler, M., and Fox, N. 2009. Progress in field spectroscopy. *Remote Sensing of Environment*, 113(1): S92-S109.

Mitchell, S.W. 2003. *Does Pattern Matter? Spatio-temporal modelling strategies to predict grassland productivity dynamics, Grasslands National Park, Saskatchewan*. Ph.D. Thesis, University of Toronto, Toronto.

Mitchell, S.W., and Csillag, F. 2001. Assessing the stability and uncertainty of predicted vegetation growth under climatic variability: northern mixed grass prairie. *Ecological Modelling*, 139(2-3): 101-121.

Okin, G.S., Roberts, D.A., Murray, B., and Okin, W.J. 2001. Practical limits on hyperspectral vegetation discrimination in arid and semiarid environments. *Remote Sensing of Environment*, 77(2): 212-225.

Ollinger, S.V. 2011. Sources of variability in canopy reflectance and the convergent properties of plants. *New Phytologist*, 189(2): 375-394.

O'Neill, R.V., Johnson, A.R., and King, A.W. 1989. A hierarchical framework for the analysis of scale. *Landscape Ecology*, 3(3-4): 193-205.

Pinter, P.J., Hatfield, J.L., Schepers, J.S., Barnes, E.M., Moran, M.S., Daughtry, C.S.T., and Upchurch, D.R. 2003. Remote sensing for crop management. *Photogrammetric Engineering & Remote Sensing*, 69(6): 647-664.

Qi, J., Chehbouni, A., Huete, A.R., Kerr, Y.H., and Sorooshian, S. 1994. A modified soil adjusted vegetation index. *Remote Sensing of Environment*, 48(2): 119-126.

Rahman, A.F., Gamon, J.A., Sims, D.A., and Schmidts, M. 2003. Optimum pixel size for hyperspectral studies of ecosystem function in southern California chaparral and grassland. *Remote Sensing of Environment*, 84(2): 192-207.

Rogan, J., and Chen, D.M. 2004. Remote sensing technology for mapping and monitoring land-cover and land-use change. *Progress in Planning*, 61: 301-325.

Rouse, J.W., Haas, R.H., Schell, J.A., and Deering, D.W. 1974. *Monitoring vegetation systems in the great plains with ERTS.* Proceedings, Third Earth Resources Technology Satellite-1 Symposium, Greenbelt: NASA SP-351: 301-317.

Roy, D.P., Wulder, M.A., Loveland, T.R., Woodcock, C.E., Allen, R.G., Anderson, M.C., Helder, D., Irons, J.R., Johnson, D.M., Kennedy, R., Scambos, T.A., Schaaf, C.B., Schott, J.R., Sheng, Y., Vermote, E.F., Belward, A.S., Bindschadler, R., Cohen, W.B., Gao, F., Hipple, J.D., Hostert, P., Huntington, J., Justice, C.O., Kilic, A., Kovalskyy, V., Lee, Z.P., Lymburner, L., Masek, J.G., McCorkel, J., Trezza, R., Vogelmann, J., Wynne, R.H., and Zhu, Z. 2014. Landsat-8: Science and product vision for terrestrial global change research. *Remote Sensing of Environment*, 145: 154-172.

Saskatchewan Institute of Pedology. 1992. Grasslands National Park Soil Survey, University of Saskatchewan, Saskatoon.

Samson, F., and Knopf, F. 1994. Prairie conservation in North America. *Bioscience*, 44(6): 418-421.

Samson, F., and Knopf, F. 1996. Prairie conservation: Preserving North America's most endangered ecosystem. Island Press. Washington D.C. and Covello, California, USA.

Schaepman, M.E., Ustin, S.L., Plaza, A.J., Painter, T.H., Verrelst, J., and Liang, S. 2009. Earth system science related imaging spectroscopy – An assessment. *Remote Sensing of Environment*, 113(1): S123-S137.

Sims, D.A., and Gamon, J.A. 2002. Relationships between leaf pigment content and spectral reflectance across a wide range of species, leaf structures and developmental stages. *Remote Sensing of Environment*, 81(2-3): 337-354.

Singh, J.S., Lauenroth, W.K., Heitschmidt, R.K., and Dodd, J.L. 1983. Structural and functional attributes of the vegetation of northern mixed prairie of North America. *The Botanical Review*, 49(1): 117-149.

Somers, B., Asner, G.P., Tits, L., and Coppin, P. 2011. Endmember variability in spectral mixture analysis: A review. *Remote Sensing of Environment*, 115(7): 1603-1616.

Thenkabail, P.S., Smith, R.B., and Pauw, E.D. 2000. Hyperspectral vegetation indices and their relationships with agricultural crop characteristics. *Remote Sensing of Environment*, 71(2): 158-182.

Tucker, C. 1979. Red and photographic infrared linear combinations for monitoring vegetation. *Remote Sensing of Environment*, 8(2): 127-150.

Turner, M.G. 1989. Landscape Ecology: The effect of pattern on process. *Annual Review of Ecology and Systematics*, 20: 171-197.

Turner, M.G., Dale, V.H., and Gardner, R.H. 1989. Predicting across scales: Theory development and testing. *Landscape Ecology*, 3(3-4): 245-252.

Urban, D.L. 2005. Modeling ecological processes across scales. *Ecology*, 86(8): 1996-2006.

Ustin, S.L., Roberts, D.A., Gamon, J.A., Asner, G.P., and Green, R.O. 2004. Using imaging spectroscopy to study ecosystem processes and properties. *Bioscience*, 54(6): 523-534.

Virk, R. 2012. *Impacts of cattle grazing on spatio-temporal variability of soil moisture and above-ground live plant biomass in mixed grasslands.* Ph.D. Thesis, Carleton University, Ottawa.

Virk, R., and Mitchell, S.W. 2014. Effect of different grazing intensities on the spatial-temporal variability in above-ground live plant biomass in North American mixed grasslands. *Canadian Journal of Remote Sensing*, 40(6): 423-439.

Wessman, C.A. 1992. Spatial scales and global change: Bridging the gap from plots to GCM grid cells. *Annual Review of Ecology and Systematics*, 23: 175-200.

Wiens, J.A., and Milne, B.T. 1989. Scaling of 'landscapes' in landscape ecology, or landscape ecology from a beetle's perspective. *Landscape Ecology*, 3(2): 87-96.

Williams, D.L., Goward, S.N., and Arvidson, T.J. 2006. Landsat: Yesterday, Today, and Tomorrow. *Photogrammetric Engineering & Remote Sensing*, 72(10): 1171-1178.

Woodcock, C.E. 1987. The factor of scale in remote sensing. *Remote Sensing of Environment*, 21(3): 311-332.

Wu, J. 1999. Hierarchy and scaling: extrapolating information along a scaling ladder. *Canadian Journal of Remote Sensing*, 25(4): 367-380.

Wu, J., Jones, K.B., Li, H., and Loucks, O.L. 2006. *Scaling and uncertainty analysis in ecology: Methods and applications*. Springer, 3-15.

Wulder, M.A., White, J.C., Goward, S.N., Masek, J.G., Irons, J.R., Herold, M., Cohen, W.B., Loveland, T.R., and Woodcock, C.E. 2008. Landsat continuity: Issues and opportunities related to Landsat continuity. *Remote Sensing of Environment*, 112(3): 955-969.

Wulder, M.A., Masek, J.G., Cohen, W.B., Loveland, T.R., and Woodcock, C.E. 2012. Opening the archive: How free data has enabled the science and monitoring promise of Landsat. *Remote Sensing of Environment*, 122: 2-10.

Xu, D., Guo, X., Li, Z., Yang, X., and Yin, H. 2014. Measuring the dead component of mixed grassland with Landsat imagery. *Remote Sensing of Environment*, 142: 33-43.

Yang, X., and Guo, X. 2011. Investigating vegetation biophysical and spectral parameters for detecting light to moderate grazing effects: a case study in mixed grass prairie. *Central European Journal of Geosciences*. 3(3): 336-348.

Yang, X., and Guo, X. 2014. Quantifying responses of spectral vegetation indices to dead materials in mixed grasslands. *Remote Sensing*. 6(5): 4289-4304.

Yang, X., Guo, X. and Fitzsimmons, M. 2012. Assessing light to moderate grazing effects on grassland production using satellite imagery. *International Journal of Remote Sensing*. 33(16): 5087-5104.

Zhang, C., and Guo, X. 2006. Application of RADARSAT imagery to grassland biophysical heterogeneity assessment. *Canadian Journal of Remote Sensing*, 32(4): 281-287.

Zhang, C., and Guo, X. 2007. Measuring biological heterogeneity in the northern mixed prairie: a remote sensing approach. *The Canadian Geographer*, 51(4): 462-474.

Zhang, C. 2008. *Monitoring biological heterogeneity in a northern mixed prairie using hierarchical remote sensing methods.* Ph.D. Thesis, University of Saskatchewan, Saskatoon.

Zhou, W. 2007. *Assessing remote sensing application on rangeland insurance in Canadian Prairies.* M.Sc. Thesis, University of Saskatchewan, Saskatoon.

CHAPTER 2

MULTI-SCALAR COMPARISON OF PLANT BIOPHYSICAL PROPERTIES ALONG TOPOGRAPHICAL GRADIENTS IN A MIXED PRAIRIE

ABSTRACT

Multi-scale approaches have been suggested to optimally study ecosystem patterns and processes. Remotely sensed (RS) data being available at multiple scales could be utilized to detect spatial scales of plant biophysical properties and identify optimum scales of imagery. In this study, canopy reflectance, plant cover, and leaf area index (LAI) were collected from 41 sites and along three transects in the Grasslands National Park of Canada in 2006 and 2007. Spectral reflectance from field spectroradiometer and three satellite images were used to derive narrowband VI (VI_n) and broadband VI (VI_b) vegetation indices at four spatial data scales (1, 10, 20, and 30 m). Regression analyses were run at four scales to compare the ability of VI_n or VI_b to estimate plant cover and LAI, and semivariograms were used to estimate spatial scales of LAI, VI_n, and VI_b. Results show that RS data at all data scales successfully captured the spatial variation of biophysical properties along topographical gradients. An inverse relationship was observed for plant cover, LAI, and VI to topographic gradients. VI at all spatial scales showed significant relationships to plant cover and LAI, however VI at finer scales showed the strongest relationship. The spatial scales of variation were different for VI_n, VI_b, and LAI and ranged between 35 and 200 m, and imagery scale finer than 20 m is recommended as ideal for studying the mixed prairie vegetation. Ecologists need to be cautious that an arbitrary scale selection for their study and scalar analysis using a single biophysical property may have implications to their study.

2.1 INTRODUCTION

Identification and selection of the appropriate scale to study any ecosystem process or pattern is one of the fundamental and challenging problems in ecology and geography (Levin, 1992; Turner et al., 1989; Goodchild, 1997). Marceau (1999) defined scale as the spatial dimensions at which entities, patterns, or processes are observed or characterized. Turner et al. (1989) defined scale as having two dimensions: spatial (areal extent of an object) or temporal (time interval of process). Since ecosystem processes and patterns and their causal factors are scale-dependent, they are ideally examined at the appropriate scale (Denny et al., 2004; Parsons et al., 2004) or within their domains of scale (Wiens and Milne, 1989) to correctly analyze ecosystem- and landscape-level processes. Seldom are the patterns and processes studied at the optimum scale. As discussed by Dungan et al. (2002), often the scale of study is arbitrarily fixed by the sampling process or measurement unit (measurement scale), decided by the method used for data collection (sampling scale), limited by the scale of the study data sets (data scale), or defaulted to the coarsest data used in the analysis (analysis scale). Often, there is a requirement to extrapolate information for predicting processes or patterns at alternate scales (Turner et al., 1989). Localized or broad-scale factors may interact across spatial scales, creating problems when information at a specific scale is arbitrarily upscaled (Urban et al., 1987; Royer and Minshall, 2003; Dalgaard et al., 2003; Turner, 1990). Wiens and Milne (1989) suggested that landscape structures are best defined in ways that are relevant to the organism and should be independent of the measurement scale used. By considering multiple scale selections that are relevant to the pattern or the process, the biases and errors that arise due to the imposition of an arbitrary scale are reduced. By identifying the appropriate scale, it might be possible to infer how the organism perceives the environment at different scales and allows insight into how scales affect the organism's response over the landscape (Milne et al., 1989). Milne (1989) suggested that the differences in landscape heterogeneity might be apparent only when the same landscape is analyzed at different scales. Therefore, by adopting a multi-scalar conceptualization of landscapes and by conducting multi-scalar studies it might be possible to define the domains of scale that apply to specific patterns, processes, or phenomena (Weins and Milne, 1989). Further, problems arise when data at finer- or coarser- spatial scales are used to study ecosystem

properties and patterns (Miller et al., 2007). Finer-scale data might have high spatial autocorrelation, be costly, or simply be difficult to acquire, process, and store. Coarser-scale data might spatially aggregate the ground variance, thereby reducing spatial heterogeneity and masking finer spatial variations. Observations and measurements can be taken only with some level or degree of generalization at coarser scales, but may be obtained with higher detail at finer scales. To address the above scale issues, ecologists have advocated a multi-scalar approach which provides the advantages of integrating the complexity of patterns while permitting a simultaneous consideration of the ecosystem patterns and their scalar variations.
Remotely sensed (RS) data are increasingly being used by ecologists due to their cost-effectiveness and synoptic ability to provide a variety of ecological information at multiple spatial data scales ranging from sub-meter to few kilometers. RS-derived data products such as classified thematic maps, vegetation index (VI) maps, and land use-land cover maps can be readily integrated with other geospatial layers in geographic information systems (GIS) for comprehensive, multi-criteria ecosystem analysis and for effective decision-making. RS data of finer spatial resolution are now commercially available: 0.4 m (GeoEye), 0.5 m (WorldView, QuickBird), 1 m (IKONOS), 2.5-20 m (SPOT), 5 m (RapidEye), and 22 m (DMC; Disaster Monitoring Constellation). However, these data sources are costly, image only smaller areas, or have limited availability. Publically available RS data such as Landsat, NOAA AVHRR, and Terra MODIS, though with coarser spatial resolution (30 m or more) are more cost-effective, image larger areas, and readily available. Hence, given the wide variety of RS data currently available, ecologists are faced with the challenge of selecting RS data with spatial scales that are appropriate for their study-at-hand and with high benefit-cost ratio. See Marceau (1999) for review on the effects of scale and scaling in the context of remote sensing.

Vegetation indices (VI), transformed from spectral reflectance of ground features imaged by remote sensors, have proven to be useful as indirect indicators of plant abundance, greenness, photosynthetic pigment content, aboveground biomass, green-leaf area, photosynthetically active radiation, productivity, and vegetation health (Thenkabail et al., 2000; Blackburn, 2007; Ollinger, 2011). VIs are useful to understand the spatial patterns of vegetation arising due to gradients of environment, moisture, topography, soil fertility, or land management. Therefore, VI as key indicators of plant biophysical properties can be exploited for estimating spatial scales and

further used for designing field sampling and data collection, selecting optimum pixel size of imagery, and for developing future remote sensors.

Continued and regular monitoring of ecosystems with high priority for conservation, such as the northern mixed prairie, is important and requires access to cost-effective RS data at multiple spatial and temporal scales. RS has been utilized in the northern mixed prairie for studying vegetation heterogeneity (Zhang, 2008), modeling primary productivity (Davidson, 2002; Mitchell, 2003; He, 2008), and understanding effects of grazing (Li and Guo, 2010; Yang and Guo, 2011). However, very few studies have attempted the use of multi-scale RS data in tandem; most studies have used one or two data scales (Zhang and Guo, 2007; Davidson, 2001). This limits our understanding of upscaling information from the plot-level to the landscape-level. With the availability of several RS data sets, park managers, conservationists, and ecologists are interested in how RS data sets can be effectively exploited for monitoring the northern mixed prairie vegetation. Thus, there is incongruence between spatial scales, i.e. traditional field collection and RS imaging (i.e. mismatch between the sampling scale of ground measurements to the scale of RS imagery). Hence, studying ecosystem processes and patterns only at finest scales limits our ability to generalize patterns or processes at coarser scales. Therefore, multi-scalar studies allows for the understanding of the effects and implications of upscaling observations, and the current availability of RS data at several spatial scales allows the adoption of a multi-scalar study approach.

2.1.1 Research questions

The research objectives in the study are:

(i) To describe the spatial variation of plant biophysical variables along topographical gradients in the northern mixed prairie;
(ii) How effectively do VIs derived from RS data of varying spatial data scales compare against field estimates of vegetation?
(iii) Is there a dominant spatial scale for plant biophysical variables in the northern mixed prairie that can be identified through RS data sets?

2.2 DATA AND METHODS

2.2.1 Study area

The West Block of Grasslands National Park of Canada (GNPC; 49° 12' N, 107°24' W) in Southern Saskatchewan was chosen as the study area (Fig. 2.1). GNPC falls within the northern mixed prairie of the North American Great Plains and was established in 1984 to conserve remnant native mixed prairie within Canada. GNPC experiences a continental, semi-arid climate with mean annual temperature of 3.8 °C and total yearly precipitation ~325 mm. The region is characterized by rolling topography consisting of upland, sloped land, and lowland prairie, thereby making the vegetation growth in the area largely dependent on topography and soil moisture. ~85% of the vegetation in the GNPC is dominated by native prairie grasses, and the remainder is comprised of forbs, low and tall shrubs, and exotic grasses (Michalsky and Ellis, 1994). Upland prairie is dominated by grasses such as needle and thread (*Hesperostipa comata*), western wheat grass (*Pascopyrum smithii*), blue grama (*Bouteloua gracilis*), and northern wheat grass (*Elymus lanceolatus*). Lowlands are dominated by western wheat grass, shrubs such as sagebrush (*Artemisia cana*), buckbrush (*Symphoricarpos occidentalis*), willows (*Salix* sp.), and exotic grasses such as crested wheat grass (*Agropyron cristatum*) and smooth brome (*Bromus inermis*) (plant names adapted from Harms (2006)). The peak plant growth occurs in June and July (Zhang and Guo, 2007) and the average plant growing season is ~170 days (Csillag et al., 2001).

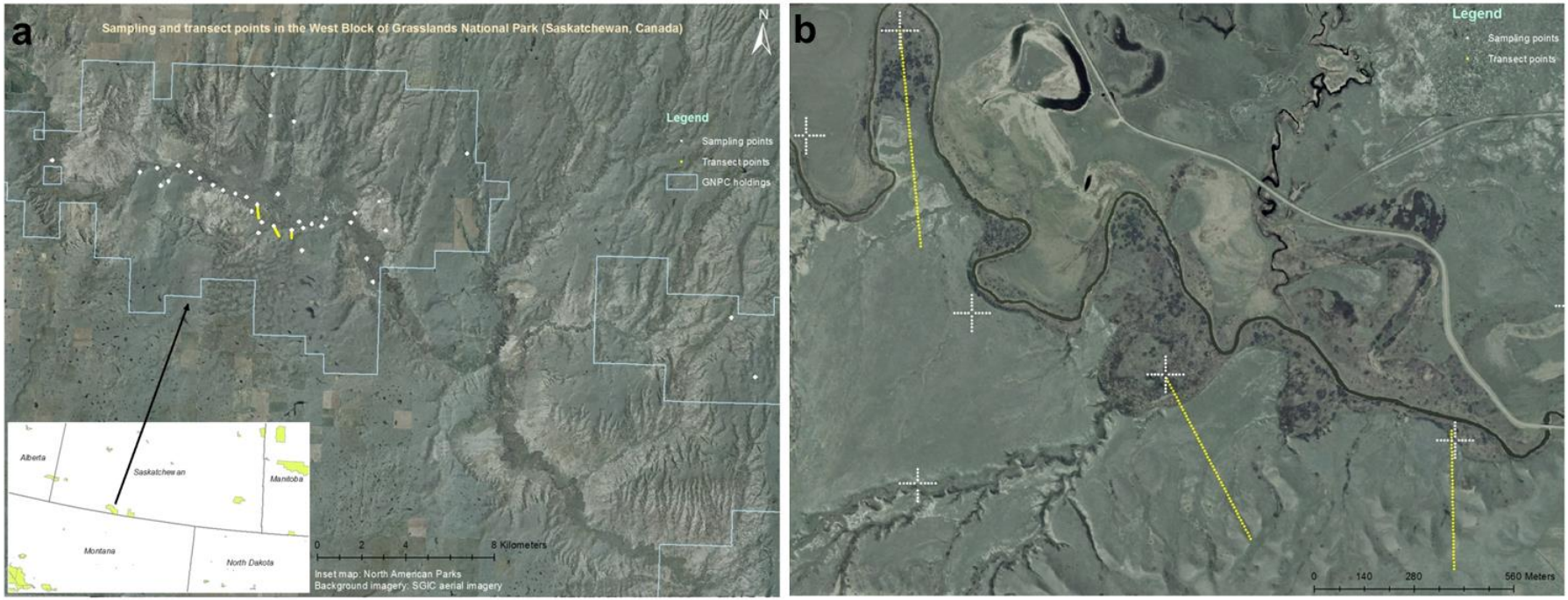

Fig. 2.1 Map of the study area, sampling sites, and transects (2.1a). The inset map shows the West and East blocks of GNPC (proposed boundary of GNPC and its holdings as of 2006; Parks Canada *pers comm*), ortho aerial imagery (Source: SGIC; Saskatchewan Geospatial Imagery Collaborative), and North American Parks (Source: ArcGIS Online, ESRI). Zoomed-in map shows the sampling design for plots and transects (2.1b).

2.2.2 Sites, sampling methods, and field data

Field data were collected within a two-week period in mid-June 2006 and early-July 2007 from 41 randomly distributed sites and along three transects (Fig. 2.1a and 2.1b). These sites were selected based on a stratified sampling scheme and represented a wide variety of vegetation communities and topographic positions (Fig. 2.1-2.2). Site data were used to understand spatial variation at smaller scales (larger area) and transect data were used to understand spatial variation at smaller scales (smaller area). At each site (of size 100 m*100 m), a quadrat of 50 cm x 50 cm dimension was laid out at 10 m sampling intervals in the N-S and E-W directions (Fig. 2.1b). Transects were laid out from the lowland to the upland prairie and were ~400-650 m long (Fig. 2.1b and 2.2b). Plant cover, leaf area index (LAI), and canopy spectral reflectance were collected at each quadrat using the methods outlined below.

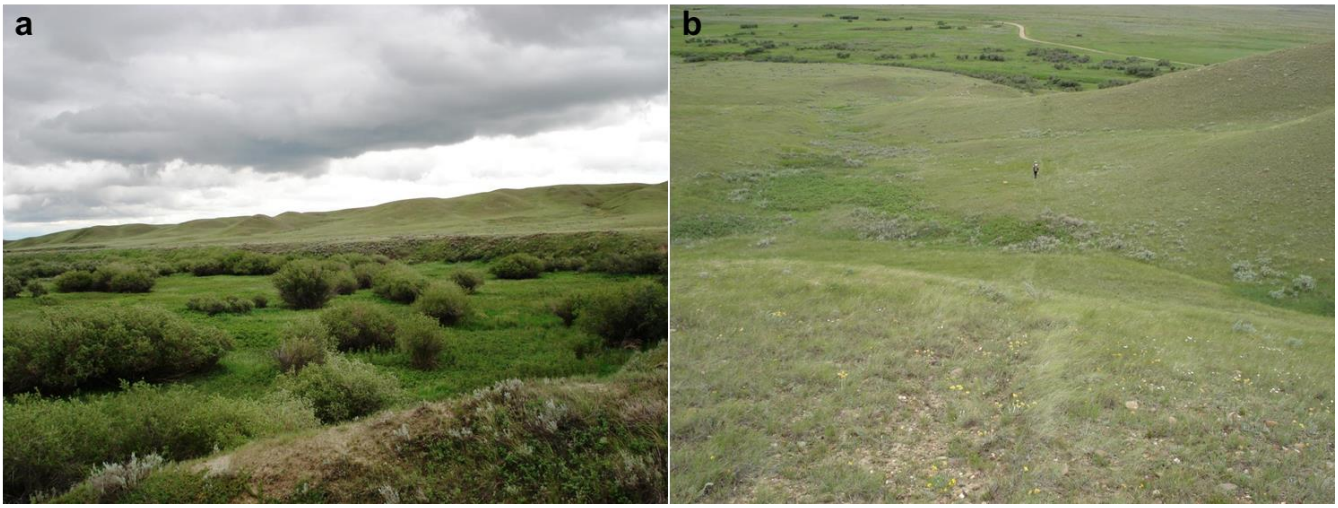

Fig. 2.2 Spatial heterogeneity in the study area (2.2a) - lowland (front), sloped land (middle), and upland prairie (back) can been seen in the photo. Overview of the study area and one of the sampling transects (2.2b).

Plant cover was visually estimated using the Daubenmire method (Daubenmire, 1959) in which cover was classified into seven groups: graminoids, shrubs, forbs, cacti, lichens and moss, rock, and bare ground. The individual cover values were expressed in percentages and summed to obtain the total cover for a single vegetation layer within a quadrat (maximum 100% cover).

Leaf area index (LAI) was used to calculate plant area index and is an index of canopy density that relates surface area of the canopy to the ground area below the canopy (Ross, 1981). LAI measurements were taken using a LiCOR® LAI-2000 Plant Canopy Analyzer in 2006 and with a Decagon® Accupar (Lincoln, Nebraska) in 2007; both these instruments work on the same principle and provide similar estimates (see Hyer and Goetz, 2004). LAI-2000 and Accupar measure LAI as the ratio (therefore unitless) of the amount of light intercepted by the canopy and then falling on the sensor (below canopy) to the amount of light (photosynthetically active radiation; PAR) falling directly on the sensor (above canopy). LAI was measured with the LiCOR LAI-2000 by using the shadow method (see He et al., 2007). In the shadow method, the shadow of the person is used to avoid sunlight falling directly on the sensor, or that the below canopy readings do not include any sunlight that is reflected or transmitted by the foliage, or minimize changing sky conditions. LAI values at each corner of the quadrat were averaged. Comparison of the working and measurements estimated with LAI-2000 and Accupar instruments can be seen in Hyer and Goetz (2004).

Aboveground biomass was collected by clipping the vegetation within a 50 cm x 20 cm quadrat (a GNPC stipulation) at the ground-level. The clipped vegetation was stored in air-sealed bags and immediately weighed in the field to estimate fresh (wet) biomass. Fresh biomass was sorted in the lab into different groups (grass, shrubs, forbs, and standing dead) and sorted-biomass was oven-dried until a constant weight at a temperature of 60^{o} C for 48 hours was reached to estimate the dry weight for each respective group. Dominant species and species composition in each quadrat were visually identified. Additionally, mean plant height and litter depth were measured by averaging the height or depth values at each quadrat corner.

2.2.3 Remote sensing at multiple scales

Reflectance data were collected for sites and transects using field RS and satellite RS to calculate three types of VI (Table 2.1) at four data scales (1, 10, 20, 30 m) to describe the spatial patterns of vegetation and to estimate the spatial scale of variation of plant biophysical properties. Narrowband VI (VI_n) were derived from field RS to use at the finest spatial scale, and broadband VI (VI_b) calculated from satellite RS were used at the coarsest scale. It was of interest to identify the RS platform that could best capture the spatial variation of plant biophysical properties at both fine and coarse scales. Also of interest was to identify whether the trends of spatial variation

of plant biophysical properties obtained from different RS platforms corresponded with the vegetation patterns observed through field work.

Field remote sensing

Canopy spectral reflectance measurements were collected using an ASD® FieldSpec FR Pro spectroradiometer (Analytical Spectral Devices, Boulder, Colorado) with a spectral resolution of 3 nm in the 350-1000 nm and 10 nm in the 1000-2500 nm region. Spectra were collected perpendicular to the quadrat at a height of 1 m with a 25^{o} field of view probe (corresponding to a pixel size ~1 m^2 on the ground) and under low wind and stable atmospheric conditions. All canopy reflectance measurements were collected between 10:00 and 14:00 hours and calibrated to a Spectralon reference panel (Labsphere, New Hampshire) before every measurement.

Satellite remote sensing

Satellite images at three data scales (native pixel size and date of acquisition are given in parentheses): SPOT-5 HRG1 (10 m; 27 July 2006), SPOT-4 HRVIR1 (20 m; 28 June 2006), and Landsat-5 TM (30 m; 17 July 2006) were acquired for the study area. Using ENVI 4.7 (ITTVIS Inc., Boulder, Colorado), the images were individually georeferenced using a high-resolution SPOT-5 HRG1 PAN (5 m; 28 June 2007) image, orthorectified, projected to UTM 13N-NAD83 and resampled using the nearest neighbour scheme to their native pixel size. Further, the Landsat-5 and SPOT-4 images were co-registered to the SPOT-5 HRG1 image as it had the highest ground accuracy. Further, images were processed from raw digital numbers (DN) to surface reflectance values after the Fast Line-of-Sight Atmospheric Analysis of Spectral Hypercubes (FLAASH; Anderson et al., 1999) atmospheric correction.

2.2.4 Auxiliary data

A digital elevation model (DEM; Source: *www.geobase.ca*) with 20 m resolution was used to extract elevation, slope, and aspect for all sampling points in the study area. Additionally, maps

of species richness, soil cover (Saskatchewan Institute of Pedology, 1992), and vegetation cover (Michalsky and Ellis, 1994) were used.

2.2.5 Data processing and analyses

Processing of spectral reflectance and calculation of vegetation indices

VI are combinations of surface reflectance in two or more wavelengths and used to highlight specific plant biophysical properties (Haboudane, 2004). Three VI_n and VI_b (Table 2.1) were computed: Normalized Difference Vegetation Index (NDVI), Normalized Difference Wetness Index (NDWI), and Adjusted Transformed Soil Adjusted Vegetation Index (ATSAVI).VI_n were computed using reflectance (ρ) in the 670, 800, 860, and 1240 nm wavelengths. Comparable VI_b were calculated for each satellite image using spectral reflectance (ρ) in the red (R), near-infrared (NIR), and shortwave infrared (SWIR) bands. NDVI is commonly used to represent "greenness" (vegetation abundance) and as an indirect estimate of LAI. NDWI is used to represent "wetness" (canopy moisture). Though several VI are mentioned in the literature (Hattfield, 2008; Thenkabail et al., 2000), previous research (He et al., 2006) showed ATSAVI as the most effective VI for representing plant biophysical properties in the northern mixed prairie, therefore ATSAVI was also calculated. The locations of field measurements were converted to point vectors in ESRI® ArcGIS 9.3.1 (ESRI, California) and used to spatially extract VI_b from corresponding pixels in each satellite image.

Table 2.1 Vegetation index (VI) used in the study, formulae, references, and major use.

Vegetation index		Formula	Reference	Usefulness
VI_n	$NDVI_n$	$\frac{\rho_{800} - \rho_{670}}{\rho_{800} + \rho_{670}}$	Rouse (1974)	Greenness, leaf area index, vegetation abundance
	$NDWI_n$	$\frac{\rho_{860} - \rho_{1240}}{\rho_{860} + \rho_{1240}}$	Gao (1996)	Canopy moisture content
	$ATSAVI_n$	$\frac{a(\rho_{800} - a\rho_{670} - b)}{a\rho_{800} + \rho_{670} - ab + X(1+a^2)}$	Baret and Guyot (1991)	Minimizes soil background effects
VI_b	$NDVI_b$	$\frac{\rho_{NIR} - \rho_R}{\rho_{NIR} + \rho_R}$	Rouse (1974)	Greenness, leaf area index, vegetation abundance
	$NDWI_b$	$\frac{\rho_{NIR} - \rho_{SWIR}}{\rho_{NIR} + \rho_{SWIR}}$	Gao (1996)	Canopy moisture content
	$ATSAVI_b$	$\frac{1.219 \times (\rho_{NIR} - 1.219 \times \rho_R - 0.029)}{1.219 \times \rho_{NIR} + \rho_R - 1.219 \times 0.029 + 0.08 \times (1 + 1.219^2)}$	Baret and Guyot (1992)	Minimizes soil background effects

Note: NDVI (Normalized Difference Vegetation Index), NDWI (Normalized Difference Vegetation Index), and ATSAVI (Adjusted Transformed Soil Adjusted Vegetation Index). ρ (Spectral reflectance). Narrowband VI (VI_n) and broadband VI (VI_b). Satellite bands: R (Red), NIR (Near infrared), and SWIR (Shortwave infrared). Values for a (Gain) = 1.22, b (Offset) = 0.03, and L (Canopy background adjustment factor) = 0.5 were obtained from He et al. (2006).

Relationship of RS-derived estimates to field estimates

Plant cover, LAI, and VI were organized on the basis of elevation and slope into three topographic groups: upland, sloped land, and lowland. Upland had elevation >900 m above sea level (ASL) and slope <5%; sloped land 785-900 m and >3%; and lowland <785 m and <5%. Prior to all analyses, vegetation data were analyzed for outliers based on LAI and all outliers were removed from the data set. Note that a few lowland plots fell on the Frenchman River or its creeks in very dense shrub lowlands where LAI >5 or in sparse uplands where LAI <0.5, and these plots were either not sampled or removed from the analysis. Linear stepwise regression was used to determine the relationships between VI_n or VI_b to LAI and plant cover at different data scales. Linear stepwise regressions were also run between each VI_n to its corresponding VI_b. Note that only non-spatial regressions were used in this study. All statistical analyses were completed using SPSS 17.0 (Statistical Product for Social Sciences, SPSS Inc., Chicago, USA).

Also, analysis for presence of spatial autocorrelation (SA) was tested using Moran's *I* (Goodchild, 1986) for examining the similarity between values at pairs of sample locations as a function of spatial distance. Moran's *I* value ranges from -1 to +1 through 0 (values of -1, 0, and +1 indicating dispersed, random, and clustered pattern, respectively). SA analysis was performed on the plot-level data using the Spatial Statistics Tools in ESRI® ArcGIS. If Moran's *I* was found significant, the field and satellite measurements were upscaled to the site-level by averaging all the plot measurements within a site to see if it reduced the amount of SA. Linear regressions were re-run using the upscaled data to see if the trends were similar to those obtained at the original data scale.

Estimation of spatial scales

Methods to estimate spatial scale include semivariogram analysis, wavelet transformation, and geostatistics, among which semivariograms are the most popular. To identify the dominant spatial scale of plant biophysical variables, semivariogram analysis (Meisel and Turner, 1998; Legendre and Fortin, 1989) was performed on VI_n, VI_b, and LAI at data scales of 1, 10, 20, and 30 m.

In semivariogram analysis, the semivariance $\gamma(h)$ of a biophysical property between any pair of sampling points (quadrat locations or pixels) at a lag distance (h) can be expressed as:

$$\gamma(h) = \frac{1}{2}[z(x) - z(x+h)]^2 \quad (2.1)$$

where $z(x)$ is the biophysical value at a location with coordinate vector (x). Similarly, if there are $n(h)$ pairs of plant biophysical measurements within the study area that are separated by a lag h, their semivariance is given by:

$$\Gamma(h) = \frac{1}{2n}\sum_{i=1}^{n}[z(x_i) - z(x_i + h)]^2 \quad (2.2)$$

where $\Gamma(h)$ is an unbiased estimate of the population variance. Semivariance is a useful measure of dissimilarity between spatially distributed, regionalized biophysical variables (Rahman et al., 2003), i.e. dissimilar biophysical values with higher semivariance. The relationship between semivariance (Γ) and lag vectors (h) provides a semivariogram for the biophysical variable. A semivariogram graphically represents the spatial variability of any variable. In a semivariogram, semivariance increases with distance, and the specific lag distance (sill) at which the semivariance starts to flatten is called the range. Range shows the distance within which the biophysical variable is spatially dependent and is used to determine the spatial scale of that biophysical property.

Since the objective was to estimate spatial scales for plant biophysical variables for the entire study area rather than just for the sampling sites, semivariogram analysis was performed using the site and the transect data pooled together. The former represents a wide variety of vegetation communities but at a smaller scale (larger area), and the latter represents lesser vegetation communities but at a larger scale (smaller area). The hypothesis here is that the dominant spatial scale identified for any biophysical property (variable) should be comparable irrespective of the data scale that is used to estimate it.

Semivariograms were modeled with ordinary kriging and a spherical model (see Rahman et al. (2003) for detailed descriptions) in ESRI® ArcGIS Geostatistical Analyst. The spherical model is most commonly used in ecological studies. A lag size of 10 m was chosen to match the field sampling grid interval (ArcGIS Desktop 9.3 Help). To account for directional influences to spatial pattern (anisotropy), anisotropical semivariograms were estimated for different angles.

Parameters such as sill, range, and nugget were identified from each semivariogram. The range value estimated from each semivariogram gave the dominant spatial scale for a particular plant biophysical property extracted from the RS data for a specific data scale.

2.3 RESULTS AND DISCUSSION

2.3.1 Spatial variation of vegetation and plant biophysical variables

Note that the description of vegetation and their distribution trends are provided here only to give the reader an idea about the sampling sites; our field observations were consistent with existing knowledge and those reported by previous researchers (Zhang, 2006; He, 2010).

Spatial variation at a smaller scale

Plant cover, LAI, VI_n, and VI_b from the 41 sites were analyzed to understand the spatial variation of vegetation along topographical gradients at a smaller scale (larger area) (Table 2.2 and Fig. 2.3).

Table 2.2 Mean values for plant cover, LAI, and three VI_n at three topographic groups. LAI, NDVI, NDWI, and ATSAVI are unitless.

Topographic group	**Elevation (m)**	**Green plant cover (%)**	**LAI**	**Spectroradiometer (1 m)**		
				$NDVI_n$	**$NDWI_n$**	**$ATSAVI_n$**
Upland	913.2	49.50	0.695	0.39235	-0.13808	0.19678
Sloped	818.7	65.67	1.291	0.55150	-0.07384	0.32831
Lowland	773.5	60.12	2.263	0.67648	-0.04691	0.41774
Mean	785.5	60.79	2.050	0.64634	-0.05427	0.39565
S.D.	31.3	23.56	1.210	0.19973	+0.08083	0.16711

Analysis of plant cover showed that the cover of grasses and shrubs was greatest in the lowlands and forbs covered majority of the sloped land. Overall, the green plant cover (sum of grass,

shrub, and forbs) decreased with elevation, and the cover of litter, lichens, and rocks increased with elevation. Similarly, biomass decreased with elevation: the average fresh biomass was 177.95, 158.96, and 119.8 gm^{-2} in the lowland, sloped land, and upland, respectively. Shrubs contributed the major component of fresh biomass in the lowlands while grasses contributed the most in the uplands. These field observations are consistent with Zhang (2008).

Flanagan and Johnson (2005) suggested that the availability of soil moisture determines vegetation abundance and growth in semi-arid grasslands. In our study site, uplands with drier and medium- to coarse-textured soils had a higher cover of native prairie grasses and lower cover of forbs. Sloped lands had a higher cover of native grasses and forbs and moderate to low cover of shrubs, while lowlands with heavier and moister soils had a higher cover of shrubs and invasive grasses. Coupland (1950) has reported that the lowland plants favor larger, less-variable water resources, while the drier upland sites support drought-tolerant plants and adapted to utilize light summer showers. Similarly, Zhang et al. (2006) noticed higher backscatter for lowlands in radar imagery that are positively correlated with higher soil moisture and higher plant water content. Our field observations also confirmed that soil moisture has a major influence on vegetation cover.

Similar to Thorpe (2005) and Zhang and Guo (2007), plant height for grasses and shrubs decreased with elevation, whereas forb height was highest in the sloped lands. The plant height was 5.5-38 cm in the valley land (except in lowland sites dominated by tall shrubs where plant height was sometimes >1 m), 26-30 cm in the slope lands, 10-26 cm in the uplands. In general, height for grasses ranged from 26-38 cm, shrubs 10-36 cm, and forbs 5-27 cm over the entire study area. Species richness was higher in the uplands, while lower in the lowlands. Species richness of grasses were highest in the sloped lands, for shrubs highest in the lowlands, and highest for forbs in the uplands.

Spectral reflectance of vegetation is dependent on the amount of chlorophyll and water in the foliage, canopy architecture, LAI, and background effects (Asner, 1998; Asner et al., 1998). Therefore, the amount of NIR and R in the spectral reflectance is an indirect indication of the amount of plant chlorophyll or moisture content. Studies have shown the effectiveness of VI as indicators of structural and physiological vegetation properties such as LAI, aboveground biomass, absorbed PAR, and plant productivity (Thenkabail et al., 2000; Blackburn, 2007**)**.

Therefore, the trends for the spatial variation of LAI, VI_n, and VI_b were similar to the variation of plant cover and biomass. Comparison of three topographic groups showed that the biophysical values decreased with elevation (Table 2.2), and this trend occurs for all plant biophysical variables at all spatial data scales (Fig. 2.3). We obtained a higher mean LAI of 2.05 (± 1.22) for the study area (Table 2.2) than those reported by previous studies (LAI = 1.09 in He et al. (2006); 1.05 in Black and Guo (2007)). This is because most of our sampling points were in the dense lowland shrub habitats. Shrubs showed higher LAI values than native prairie grasses or forbs and the lowland grasses had higher LAI than the upland grasses (Govind *unpublished data*).

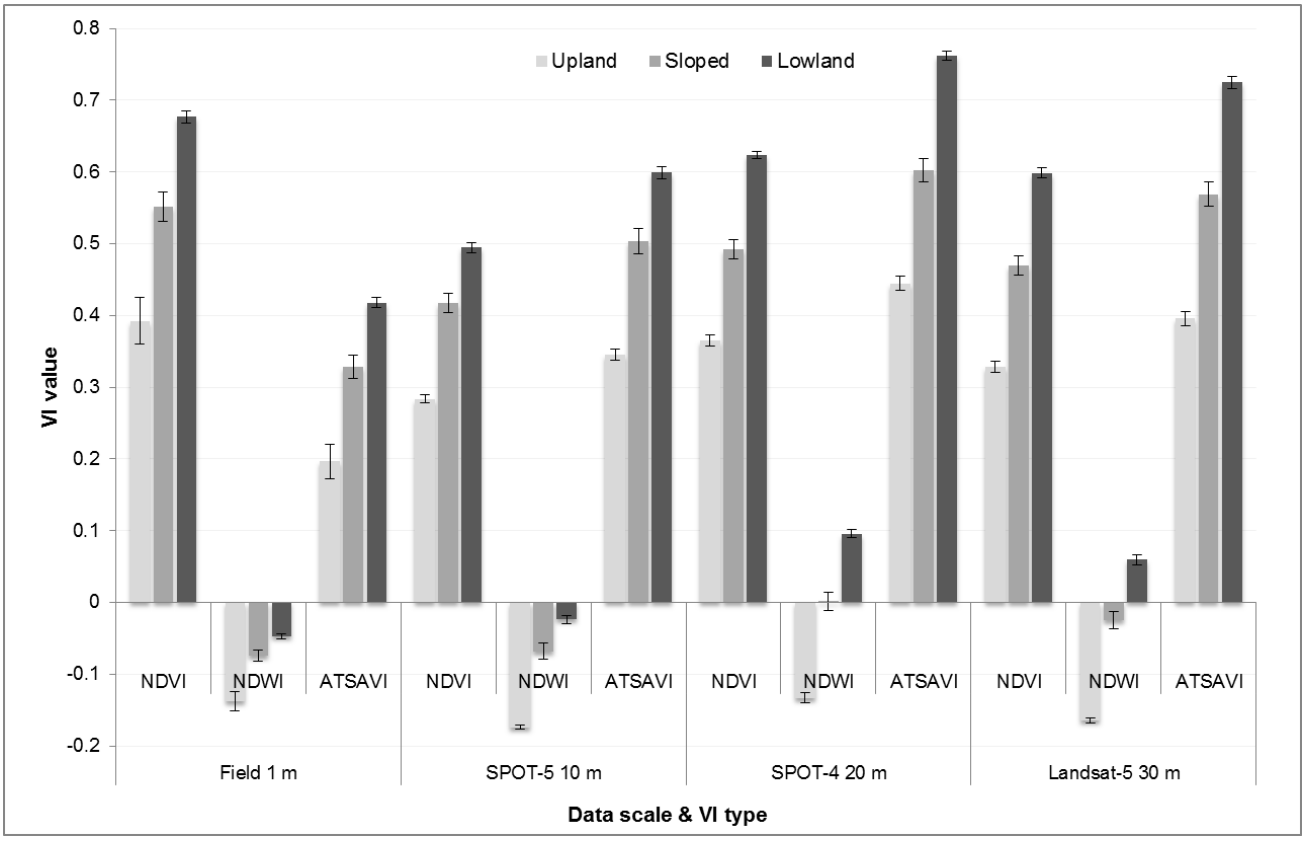

Fig. 2.3 Spatial variation of plant biophysical properties at three topographic groups (upland, sloped, lowland) across four spatial data scales (1, 10, 20, 30 m). Mean values (unitless) for VI (NDVI, NDWI, ATSAVI) are given on the y-axis, and x-axis shows the spatial data scale of the remote sensor: field and satellite (SPOT-5, SPOT-4, Landsat-5). Standard error bars are shown.

Spatial variation at a larger scale

Transect data was analyzed to understand the spatial variation of vegetation at a larger scale (smaller area). Significant negative correlations ($r > 0.5$, $p = 0.01$) were obtained between LAI and VI to elevation and soil moisture. Analysis of plant cover from the three transects showed similar trends as those discussed (section 3.1.1) with higher cover of grasses and shrubs in the lowlands, but higher forb cover in the uplands. Green plant cover increased from the upland to the lowland and varied from 83.7-96.3% for transect 1, 76.3-93.0% for transect 2, and 54.4-84.0% for transect 3. Dead and litter cover increased from the lowland to the upland.

Generally, height for grasses, shrubs, and forbs decreased from the lowland to the upland. Height for grasses ranged from 14.1-52.9 cm, for shrubs 15.0-71.4 cm, and for forbs 12.9-20.0 cm, with lower values in the uplands. Species composition and species richness was lower in the lowlands. This might be due to the competitive ability of some plants in the lowlands such as smooth brome and crested wheat which prevents other plants from surviving (Csillag et al., 2001). LAI and VI along transects decreased with elevation indicating that topographical variations even at larger scales, influence the spatial heterogeneity of vegetation in the northern mixed prairie. Strong relationships between topographic attributes influencing VI at several scales have been reported for other natural ecosystems such as the Mediterranean region of California (Deng et al., 2007).

2.3.2 Relationship between remotely sensed estimates and field estimates of vegetation

Significant relationships were found between VI and LAI at all spatial data scales (Table 2.3), indicating that VI can be used as indirect measure of biophysical properties such as vegetation greenness or wetness. VI_n were more effective than VI_b in estimating LAI (Table 2.3a and 2.3b), where the r^2 *adjusted* value for LAI-$NDVI_n$ is 0.48 ($p < 0.01$) while for LAI-$NDVI_b$ (SPOT-5) it is only 0.23 ($p < 0.01$). Also, the relationship between LAI to VI was weaker than the relationship between VI_n to its corresponding VI_b. E.g. for SPOT-5 (Table 2.3b), LAI-NDVI (r^2 *adj.* = 0.23, $p < 0.01$) and LAI-ATSAVI (r^2 *adj.* = 0.22, $p < 0.01$) are lower than $NDVI_n$-$NDVI_b$ (r^2 *adj.* = 0.38, $p < 0.01$) or $ATSAVI_n$-$ATSAVI_b$ (r^2 *adj.* = 0.37). However, NDWI is an exception; $NDWI_b$ at all data scales underestimated $NDWI_n$ (r^2 *adj.* only 0.19-0.22). The northern mixed prairie has large amounts of standing dead and plant litter that can lead to higher

LAI values but does not necessarily signify high amount of greenness and higher VI (Zhang and Guo, 2007). Regression analyses between VI_b to VI_n (Table 2.3b) indicate that the VI_b at their native data resolution inadequately capture the spatial variability of the vegetation on the landscape. The relationships were significant, however VI_b could explain only to a maximum of 37% ($NDVI_n$ - $NDVI_b$) of the variability of VI_n (Table 2.3b). This may be attributed to high background noise from standing dead, litter, or bare soil, or non-linear mixing seen in the northern mixed prairie (Davidson and Csillag, 2001; Yang and Guo, 2014). The satellite sensor (even at 10 m data scale) is imaging a 'mixed pixel' with spectral reflectance of several surface materials combined into a single pixel. This spatial aggregation leads to imaging mixed spectral signal and consequently any VI_b (based on NIR and R bands) will have less correspondence to their VI_n. This explains the low efficiency of VI in the northern mixed prairie and indicates the need to develop more robust VI for semi-arid regions.

Table 2.3 Abilities of VI_b to estimate LAI and VI_n at four spatial data scales (1, 10, 20, 30 m) using the original unscaled plot-level data (n = 686). Note: Criterion variables are given in the first column, and r^2 *adjusted* values are given. All relationships were significant at $p < 0.01$.

(a) Field remote sensing (1 m):

Biophysical variable	**Spectroradiometer (1 m)**		
	$NDVI_n$	$NDWI_n$	$ATSAVI_n$
LAI	0.48	0.36	0.47

(b) Satellite remote sensing (10, 20, 30 m):

Biophysical variable		**SPOT-5 (10 m)**			**SPOT-4 (20 m)**			**Landsat-5 (30 m)**		
		$NDVI_b$	$NDWI_b$	$ATSAVI_b$	$NDVI_b$	$NDWI_b$	$ATSAVI_b$	$NDVI_b$	$NDWI_b$	$ATSAVI_b$
Field	LAI	0.23	0.21	0.23	0.25	0.25	0.25	0.25	0.25	0.25
	$NDVI_n$	0.38			0.38			0.36		
	$NDWI_n$		0.22			0.19			0.21	
	$ATSAVI_n$			0.37			0.35			0.34

Further, the plot-level data was upscaled to the site-level to account for SA (section 2.2.5). With upscaling, Moran's *I* value for SA decreased from +0.34 (Z = 30.19) to +0.01 (Z = 0.89). Table 2.4 shows that the upscaled plot-level data showed better relationships to the field estimates: Table 2.4a and 2.4b shows stronger relationships: LAI-$NDVI_n$ (r^2 *adj.* = 0.66, $p < 0.01$) and LAI-$NDVI_b$ (SPOT-5) (r^2 *adj.* = 0.44, $p < 0.01$). Upscaling showed that the VI_b can now explain to a maximum of 74% ($ATSAVI_n$-$ATSAVI_b$) of the variability of VI_n. He et al. (2009) reported better relationship of ATSAVI over NDVI, however we did not obtain stronger relationships even after upscaling the plot-level data; this also agrees with Yang and Guo (2014). This may be attributed to LAI saturation at high NDVI values and typical of lowlands with dense shrub vegetation. It is interesting to note that the ability of VI_b to estimate VI_n (e.g. $NDVI_n$ and $ATSAVI_n$) decreased with increasing spatial data scales - the coefficient of determination for ATSAVI at 10, 20, and 30 m data scales are 0.74, 0.69, and 0.67, respectively (Table 2.4b). Note that we were successful in obtaining better relationships with local regression modeling by effectively incorporating spatial heterogeneity (see Chapter 3) instead of global regressions used in this study.

Relationships between LAI-VI or between VI_b -VI_n for transect-data (Table 2.5) showed better relationships than site-data (Table 2.3). This was expected as each transect, unlike the sites, covered smaller areas with relatively homogeneous vegetation. Though data from three transects were available, we report only the results of regression analyses of a single transect (Transect 1) for the sake of clarity.

Table 2.4 Abilities of VI_b to estimate LAI and VI_n at four spatial data scales (1, 10, 20, 30 m) using the scaled site-level data (n = 37). Note: Criterion variables given in the first column and r^2 *adjusted* values are given. All relationships were significant at $p < 0.01$.

(a) Field remote sensing (1 m):

Biophysical variable	**Spectroradiometer (1 m)**		
	$NDVI_n$	$NDWI_n$	$ATSAVI_n$
LAI	0.66	0.61	0.65

(b) Satellite remote sensing (10, 20, 30 m):

Biophysical variable		**SPOT-5 (10 m)**			**SPOT-4 (20 m)**			**Landsat-5 (30 m)**		
		$NDVI_b$	$NDWI_b$	$ATSAVI_b$	$NDVI_b$	$NDWI_b$	$ATSAVI_b$	$NDVI_b$	$NDWI_b$	$ATSAVI_b$
Field	LAI	0.44	0.39	0.44	0.43	0.46	0.44	0.45	0.42	0.44
	$NDVI_n$	0.72			0.70			0.68		
	$NDWI_n$		0.55			0.49			0.51	
	$ATSAVI_n$			0.74			0.69			0.67

Table 2.5 Abilities of VI_b to estimate LAI and VI_n at four spatial data scales (1, 10, 20, 30 m) using the transect data. Note: Criterion variables are given in the first column, and r^2 *adjusted* values are given. All relationships were significant at $p < 0.01$.

(a) Field remote sensing (1 m):

Biophysical variable	**Spectroradiometer (1 m)**		
	$NDVI_n$	$NDWI_n$	$ATSAVI_n$
LAI	0.57	0.37	0.63

(b) Satellite remote sensing (10, 20, 30 m):

	Data scale	**SPOT-5 (10 m)**			**SPOT-4 (20 m)**			**Landsat-5 (30 m)**		
		$NDVI_b$	$NDWI_b$	$ATSAVI_b$	$NDVI_b$	$NDWI_b$	$ATSAVI_b$	$NDVI_b$	$NDWI_b$	$ATSAVI_b$
Field	LAI	0.45	0.43	0.45	0.38	0.46	0.38	0.42	0.51	0.42
	$NDVI_n$	0.63			0.44			0.52		
	$NDWI_n$		0.50			0.50			0.53	
	$ATSAVI_n$			0.64			0.48			0.57

2.3.3 Spatial scales for plant biophysical properties

We found a strong relationship between VI and LAI, signifying their usefulness for estimating spatial scales of plant biophysical properties. Semivariograms were plotted for LAI, VI_n, and VI_b at four data scales: 1, 10, 20, and 30 m (Fig. 2.4a to 2.4e) using original unscaled plot-level data (n = 686).

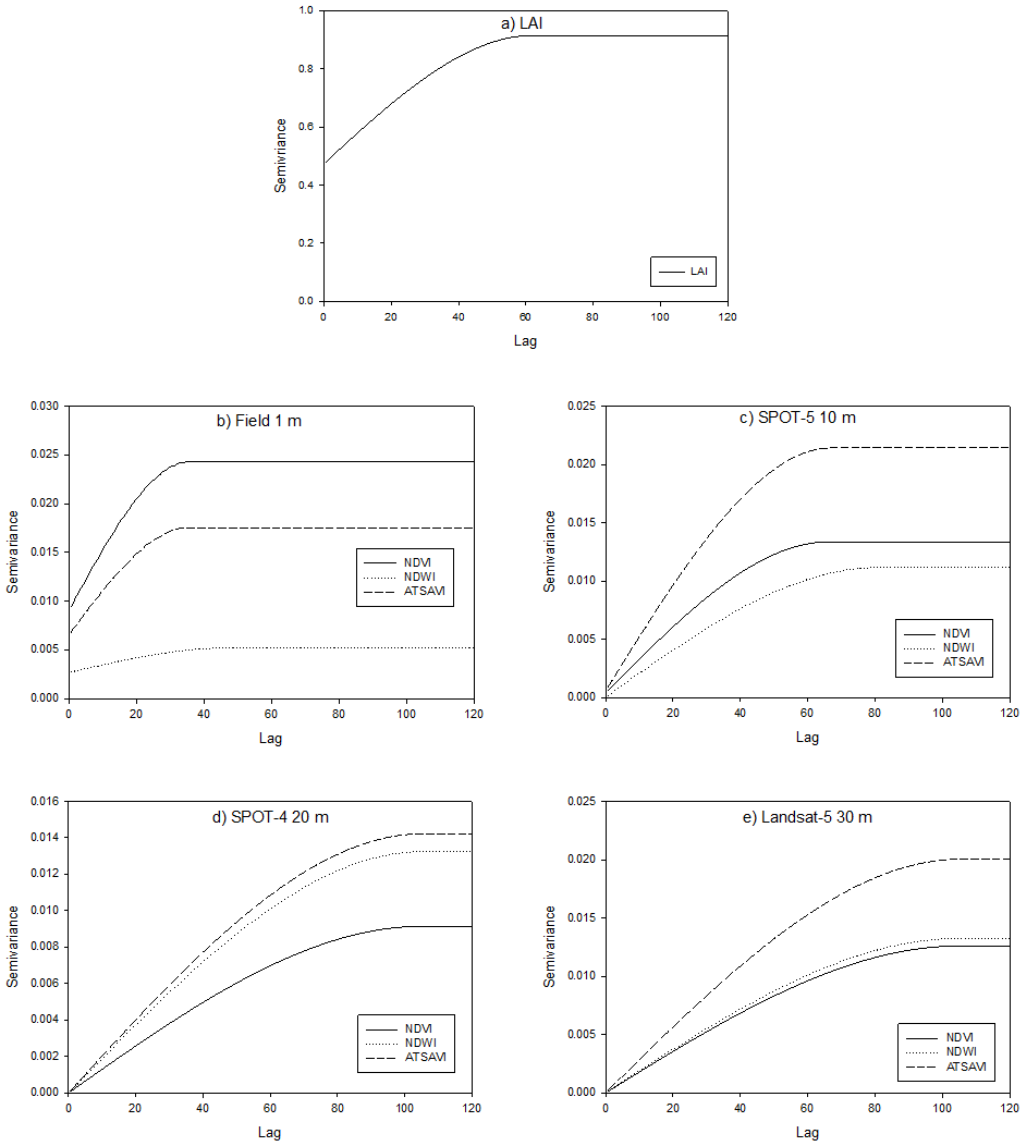

Fig. 2.4 Semivariograms for plant biophysical properties (LAI, VI_n, VI_b) at four spatial data scales (1, 10, 20, 30 m). a) Leaf area index (LAI), b) Field 1 m, c) SPOT-5 10 m, d) SPOT-4 20 m, e) Landsat-5 30 m. Lag is in meters (m). Note that only the fit of the spherical model (lines) for each semivariogram are shown, and the binned points (dots) are not shown for the sake of clarity.

Note that the semivariograms fitted for NDVI, NDWI, and ATSAVI at a specific data scale are plotted into a single graph, and plotted separately for LAI. In a semivariogram, the semivariance data pairs are shown by dots and the spherical model fit is shown by a solid line (see Fig. 2.5). The range value where each specific plant biophysical variable attained its sill was used to determine its spatial scale. The range values estimated across four data scales are summarized in Table 2.6.

Results show that the plant biophysical properties exhibit different spatial scales as indicated by their wide range values (35-115 m). Among the VI_n (Table 2.6a), lower spatial scales of 35 m were estimated for $NDVI_n$ and $ATSAVI_n$ than for $NDWI_n$ (46 m) or LAI (62 m). This same trend is seen in Table 2.6b at the 10 m (SPOT-5) data scale. It is interesting to note that the ranges estimated from VI_n were lower than that for LAI. The range values increase with increase in spatial data scales; spatial scales estimated from VI_n showed lower spatial scales (35-46 m) than those obtained from VI_b (66-105 m). E.g. in Table 2.6, the spatial scales estimated for NDVI at 1, 10, and 20 m are 35, 66, and 105 m, respectively. Similar range values of 55 m (for Landsat $NDVI_b$) and 66 m (for $NDVI_n$) have been obtained by Zhang and Guo (2007). For data scales beyond 20 m (SPOT-4), the estimated range values remain similar (Table 2.6b). The variances for VI_b are also lower than for LAI or VI_n. Therefore, it is clear from the semivariograms that spatial aggregation or a decrease in variance is evident with increasing spatial data scale. The semivariograms for LAI or VI_n always show some nugget variance (Fig. 2.4a, 2.4b, 2.5) and may be attributed to measurement errors, varying field of view, sun angle, or sky conditions (Rahman et al., 2003) that can change over several days of field work and also within a single field day. Interestingly, the semivariograms modeled for VI_b show almost zero nugget values. This might be because the satellite remote sensor is imaging a large area on the landscape in an instantaneous manner and therefore the measurement errors are minimal.

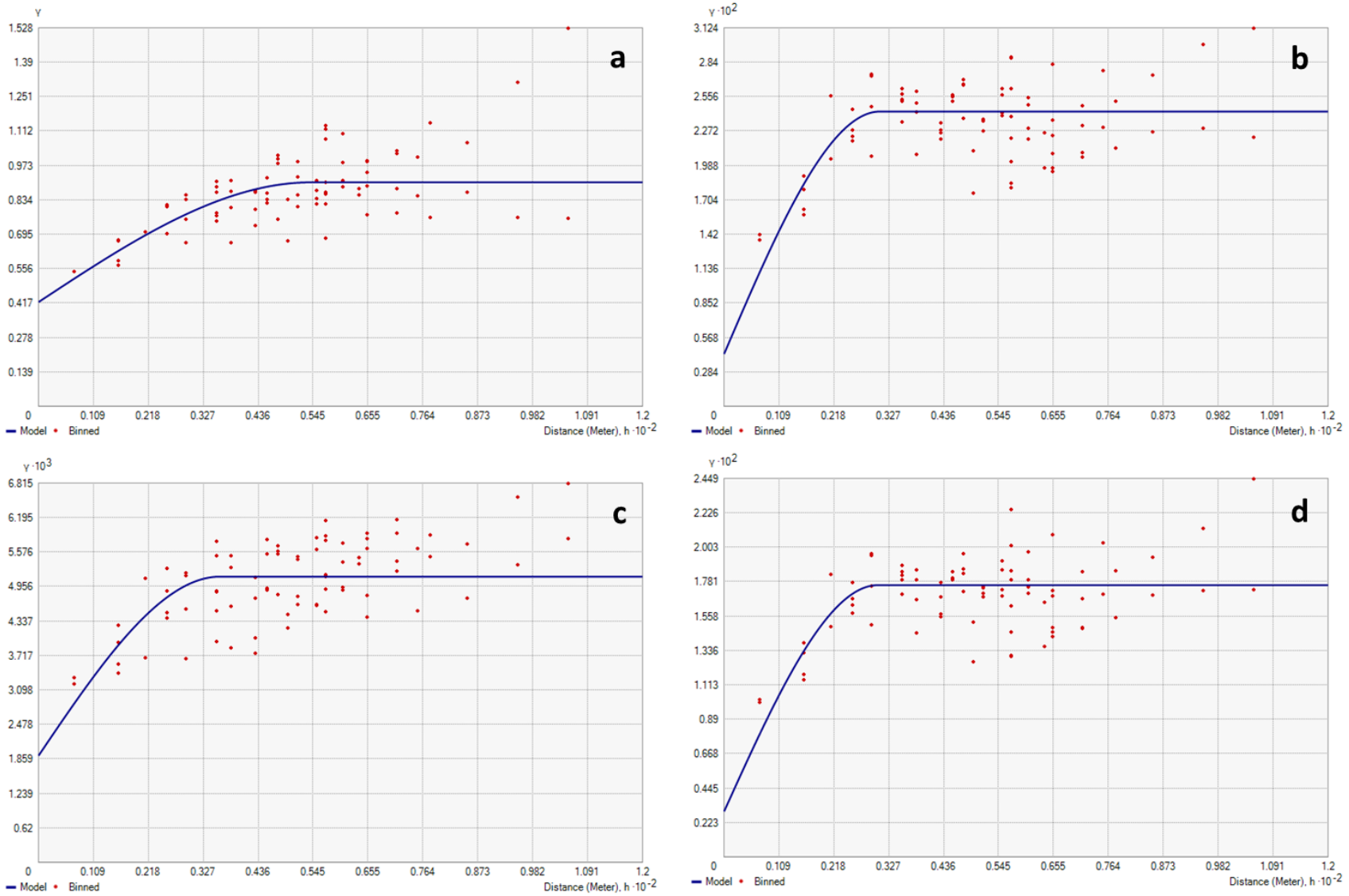

Fig. 2.5 Semivariograms for LAI (2.5a), $NDVI_n$ (2.5b), $NDWI_n$ (2.5c), $ATSAVI_n$ (2.5d) showing their binned points (dots) and spherical model fit (lines). Semivariance is given in y-axis and lag (distance) is shown in x-axis.

Table 2.6 Spatial scales (range) estimated from semivariograms for LAI, VI_n, VI_b at different data scales (1, 10, 20, 30 m) using original unscaled plot-level data (n = 686). Range values (spatial scales) are in meters.

(a) Field remote sensing (1 m):

Data scale	**Field (1 m)**			
	LAI	$NDVI_n$	$NDWI_n$	$ATSAVI_n$
Range	62	35	46	35

(b) Satellite remote sensing (10, 20, 30 m):

Data scale	**SPOT-5 (10 m)**			**SPOT-4 (20 m)**			**Landsat-5 (30 m)**		
	$NDVI_b$	$NDWI_b$	$ATSAVI_b$	$NDVI_b$	$NDWI_b$	$ATSAVI_b$	$NDVI_b$	$NDWI_b$	$ATSAVI_b$
Range	66	80	67	105	105	105	105	105	105

Table 2.7 shows the scales estimated for each plant biophysical variable from the pooled transect data (n = 1540). In general, the spatial scales from the transect data were higher than those from the site data (Table 2.6). This was expected since transects crossed terrains with relatively lower vegetation heterogeneity. Yet, the estimated spatial scales of 66 to 200 m fall within the range reported by Zhang and Guo (2007). In a semivariogram, the data pairs for the variable located close together on the semivariogram cloud have similar semivariance values (Fig. 2.5). It was seen that the data pairs with high semivariance for the plant biophysical variables were located in the sloped lands, indicating that high vegetation heterogeneity typically occurs on the sloped lands and therefore leading to significantly different biophysical values. This is further supported by our field observations. Rahman et al. (2003) suggests that grasslands have higher spatial scales as they are relatively homogeneous when compared to the patchy shrub vegetation. Therefore, it is possible to obtain higher range values in the uplands dominated by grasses than the sloped lands.

Table 2.7 Spatial scales (range) estimated from semivariograms for LAI, VI_n, VI_b at different data scales (1, 10, 20, 30 m) using transect data (n = 1540). Range values (spatial scales) are in meters.

(a) Field remote sensing (1 m):

Data scale	**Field (1 m)**			
	LAI	$NDVI_n$	$NDWI_n$	$ATSAVI_n$
Range	66	66	66	66

(b) Satellite remote sensing (10, 20, 30 m):

Data scale	**SPOT-5 (10 m)**			**SPOT-4 (20 m)**			**Landsat-5 (30 m)**		
	$NDVI_b$	$NDWI_b$	$ATSAVI_b$	$NDVI_b$	$NDWI_b$	$ATSAVI_b$	$NDVI_b$	$NDWI_b$	$ATSAVI_b$
Range	108	66	106	200	114	200	81	66	80

2.4 CONCLUSIONS

This study was successful in identifying the relationships between RS estimates and field estimates of vegetation. It also identified the effectiveness of VI_n and VI_b across several data scales and with upscaling to characterize the spatial heterogeneity of vegetation along topographical gradients. RS data at all spatial scales effectively captured the spatial heterogeneity of vegetation in the northern mixed prairie, however RS data at finer spatial data scales were more effective in estimating ground vegetation cover. Similar results have been reported by Davidson et al. (2006), who found that vegetation water content was better predicted at finer spatial scales than at coarser scales. The variations of LAI and VI along topographical gradients corresponded to the observed variation of vegetation cover and aboveground biomass. Higher values for LAI and VI seen at lower elevations in the study area leads to conclude that topography and soil moisture are the major driving factors determining plant growth in the northern mixed prairie. Coupland (1950) suggested that the soil moisture variation in the mixed prairie is mainly caused by topography and soil texture. Since soil moisture variations are indirectly the effect of topography, it can be concluded that topography is the main factor controlling plant growth and determining the spatial patterns of vegetation in the northern mixed prairie.

Semivariograms were useful in estimating the spatial scales of plant biophysical properties and showed different ranges (35-200 m) for VI_n, VI_b, and LAI. Spatial scales and spatial variation of plant biophysical properties estimated through RS and their comparison at multiple data scales is an important outcome of this study.

Contrary to He et al. (2006) but agreeing with Zhang (2008) and Yang and Guo (2014), our analyses did not suggest ATSAVI to be superior to NDVI for LAI estimation in the northern mixed prairie. ATSAVI was developed specifically to account for the background noise from soil and plant litter, and this may not be a major problem in lowlands. Most of our sampling sites were in the dense, lowland sites and therefore ATSAVI might still be more effective in the uplands.

The peak vegetative growth for the northern mixed prairie vegetation is between June and July, therefore our data set has some limitations as the satellite images tested are not for the exact month, i.e. not at exact phenological time points. Therefore, it is possible that the VI estimated by different remote sensors could be slightly affected by vegetation phenology. However, atmospheric-correction and transformation of spectral reflectance to VI should account for this issue.

Rahman et al. (2003) suggest that the optimum pixel sizes to study any ecosystem processes is half of the range value (spatial scale) of a biophysical property. Accordingly, based on the spatial scales estimated through this study, the optimum pixel size recommended for studying plant biophysical properties such as greenness and wetness in the northern mixed prairie would range from 20 m or finer to a maximum of 100 m. Pixel sizes coarser than 20 m would spatially aggregate the information on the landscape into a single pixel, thereby reducing the variance. The range values of biophysical variables can help researchers to identify spatial variability of different vegetation properties, with field or research design, or sampling protocols. Field sampling at scales coarser than the scale of vegetation properties will result in inefficient capture of the properties and characteristics on the landscape. Field sampling finer than the scale of vegetation properties may be unnecessary and waste of sampling resources.

A wide variety of RS data are currently available at varying spatial resolutions and costs, therefore park managers, ecologists, and decision makers must exercise caution in selecting the optimum data resolution while conducting ecological studies. Field RS can give significant insight into many important structural and physiological properties of vegetation. Though hyperspectral RS imagery is currently unavailable for the northern mixed prairie, our results demonstrate that narrowband RS data sets can significantly improve our understanding of the scales and vegetation properties in the northern mixed prairie. This continues to be a motivation for our future research.

2.5 ACKNOWLEDGEMENT

Randy Bonin, Chunhua Zhang, Yuhong He, and Jesse Nielsen assisted with field work. Univ. of Saskatchewan, Saskatchewan Ministry of Environment, and Nature Saskatchewan provided financial support. Eric Lamb provided comments on early drafts. Xulin Guo, Joseph Piwowar, and Greg McDermid provided field instruments. Imagery and GIS data were provided by U of S, Parks Canada, GeoBase, and USGS.

2.6 REFERENCES

Anderson, G.P., Pukall, B., Allred, C.L., Jeong, L.S., Hoke, M., Chetwynd, J.H., Adler-Golden, S.M., Berk, A., Bernstein, L.S., Richtsmeier, S.C., Acharya, P.K., and Matthew, M.W. 1999. FLAASH and MODTRAN4: state-of-the-art atmospheric correction for hyperspectral data. *IEEE Proceedings of Aerospace Conference,* pp. 177-181, Snowmass at Aspen, CO, USA.

Asner, G. 1998. Biophysical and biochemical sources of variability in canopy reflectance. *Remote Sensing of Environment,* 64(3): 234-253.

Asner, G., Wessman, C., and Archer, S. 1998. Scale dependence of absorption of photosynthetically active radiation in terrestrial ecosystems. *Ecological Applications,* 8(4): 1003-1021.

Baret, F., and Guyot, G. 1991. Potentials and limits of vegetation indices for LAI and APAR assessment. *Remote Sensing of Environment,* 35(2-3): 161-173.

Baret, F., Jacquemoud, S., Guyot, G., and Leprieur, C. 1992. Modeled analysis of the biophysical nature of spectral shifts and comparison with information content of broad bands. *Remote Sensing of Environment,* 41(2-3): 133-142.

Black, S.C., and Guo, X. 2007. Estimation of grassland CO2 exchange rates using hyperspectral remote sensing techniques. *International Journal of Remote Sensing,* 29(1): 145-155.

Blackburn, G.A. 2007. Hyperspectral remote sensing of plant pigments. *Journal of Experimental Botany,* 58(4): 855-867.

Blackburn, G.A., and Ferwerda, J.G. 2008. Retrieval of chlorophyll concentration from leaf reflectance spectra using wavelet analysis. *Remote Sensing of Environment*, 112(4): 1614-1632.

Coupland, R.T. 1950. Ecology of mixed prairie in Canada. *Ecological Monographs*, 20(4): 271-315.

Csillag, F., Kertész, M., Davidson, A., and Mitchell, S. 2001. On the measurement of diversity-productivity relationships in a northern mixed grass prairie (Grasslands National Park, Saskatchewan, Canada). *Community Ecology*, 2(2): 145-159.

Dalgaard, T., Hutchings, N.J., and Porter, J.R. 2003. Agroecology, scaling and interdisciplinarity. *Agriculture Ecosystems and Environment*, 100(1): 39-51.

Daubenmire, R.F. 1959. A canopy-cover method of vegetational analysis. *Northwest Science*, 33: 43-46.

Davidson, A., and Csillag, F. 2001. The influence of vegetation index and spatial resolution on a two-date remote sensing-derived relation to C4 species coverage. *Remote Sensing of Environment*, 75(1): 138-151.

Davidson, A., Wang, S., and Wilmshurst, J. 2006. Remote sensing of grassland-shrubland vegetation water content in the shortwave domain. *International Journal of Applied Earth Observation and Geoinformation*, 8(4): 225-236.

Deng, Y., Chen, X., Chuvieco, E., Warner, T., and Wilson, J. 2007. Multi-scale linkages between topographic attributes and vegetation indices in a mountainous landscape. *Remote Sensing of Environment*, 111(1): 122-134.

Denny, M.W., Helmuth, B., Leonard, G.H., Harley, C.D.G., Hunt, L.J.H., and Nelson, E.K. 2004. Quantifying scale in ecology: Lessons from a wave-swept shore. *Ecological Monographs*, 74(33): 513-532.

Dungan, J.L., Perry, J.N., Dale, M.R.T., Legendre, P., Citron-Pousty, S. Fortin, M.-J., Jakomulska, A., Miriti, M., and Rosenberg, M.S. 2002. A balanced view of scale in spatial statistical analysis. *Ecography*, 25(5): 626-640.

Flanagan, L.B. and Johnson, B.G. 2005. Interacting effects of temperature, soil moisture and plant biomass production on ecosystem respiration in a northern temperate grassland. *Agricultural and Forest Meteorology*, 130(3-4): 237-253.

Gao, B.C. 1996. NDWI - A normalized difference water index for remote sensing of vegetation liquid water from space. *Remote Sensing of Environment*, 58(3): 257-266.Goodchild, M.F. 1986. Spatial Autocorrelation. Catmog 47, Geo Books.

Goodchild, M.F., and Quattrochi, D.A. 1997. Scale, multiscaling, remote sensing, and GIS. In *Scale in Remote Sensing and GIS*, Quattrochi, D.A. and M.F. Goodchild, eds., pp. 1-11.

Haboudane, D., Miller, J.R., Pattery, E., Zarco-Tejad, P.J., and Strachan, I.B. 2004. Hyperspectral vegetation indices and novel algorithms for predicting green LAI of crop canopies: modeling and validation in the context of precision agriculture. *Remote Sensing of Environment*, 90(3): 337-352.

Harms, V.L. 2006. *Annotated catalogue of Saskatchewan vascular plants*. 116 pp.

Hattfield, J.L., Gitelson, A.A., Schepers, J.S., and Walthall, C.L. 2008. Application of spectral remote sensing for agronomic decisions. *Agronomy Journal*, 100(3): S-117-S-131.

He, Y., Guo, X., and Wilmshurst, J.F. 2006. Studying mixed grassland ecosystems I: suitable hyperspectral vegetation indices. *Canadian Journal of Remote Sensing*, 32(2): 98-107.

He, Y., Guo, X., and Si, B.C. 2007. Detecting grassland spatial variation by a wavelet approach. *International Journal of Remote Sensing*, 28(7): 1527-1545.

He, Y., Guo, X., and Wilmshurst, J.F. 2007. Comparison of different methods for measuring leaf area index in a mixed grassland. *Canadian Journal of Plant Science*, 87(4): 803-813.

He, Y., Guo, X., and Wilmshurst, J.F. 2009. Reflectance measures of grassland biophysical structure. *International Journal of Remote Sensing*, 30(10): 2509-2521.

Hyer, E.F. and Goetz, S.J. 2005. Comparison and sensitivity analysis of instruments and radiometric methods for LAI estimation: assessments from a boreal forest site. *Agricultural and Forest Meteorology*, 122(3-4): 157-174.

Legendre, P., and Fortin, M.J. 1989. Spatial pattern and ecological analysis. *Vegetatio*, 80(2): 107-138.

Levin, S.A. 1992. The problem of pattern and scale in ecology. *Ecology*, 73, 1943-1967.

Marceau, D.J. 1999. The scale issue in social and natural sciences. *Canadian Journal of Remote Sensing*, 25(4): 357-366.

Li, M., and Guo, X. 2014. Long term effect of major disturbances on the northern mixed grassland – A review. *Open Journal of Ecology*, 4(4): 214-233.

Li, Z., and Guo, X. 2010. A suitable vegetation index for quantifying temporal variations of LAI in semi-arid mixed grassland. *Canadian Journal of Remote Sensing*. 36(6): 709-721.

Meisel, J.E., and Turner, M.G. 1998. Scale detection in real and artificial landscapes using semivariance analysis. *Landscape Ecology*, 13(6): 347-362.

Michalsky, S.J., and Ellis, R.A. 1994. *Vegetation of Grasslands National Park*. DA Westworth and Associates, Calgary.

Miller, J., Franklin, J., and Aspinall, R. 2007. Incorporating spatial dependence in predictive vegetation models. *Ecological Modelling*, 202(3-4): 225-242.

Milne, B.T. 1989. Heterogeneity as a multi-scale characteristic of landscapes. *In Ecological Heterogeneity.* Edited by Kolasa J. and Pickett S.T.A. Springer-Verlag, New York.

Milne, B.T., Johnston, K.M., and Forman, R.T.T. 1989. Scale dependent proximity of wildlife habitat in a spatially-neutral Bayesian model. *Landscape Ecology*, 2(2): 101-110.

Ollinger, S.V. 2011. Sources of variability in canopy reflectance and the convergent properties of plants. *New Phytologist*, 189(2): 375-394.

Parsons, M., Thoms, M.C., and Norris, R.H. 2004. Using hierarchy to select scales of measurement in multiscale studies of stream macroinvertebrate assemblages. *Journal of the North American Benthological Society*, 23(2): 157-170.

Rahman, A.F., Gamon, J.A., Sims, D.A., and Schmidts, M. 2003. Optimum pixel size for hyperspectral studies of ecosystem function in southern California chaparral and grassland. *Remote Sensing of Environment*, 84(2): 192-207.

Rouse, J.W., Haas, R.H., Schell, J.A., and Deering, D.W. 1974. *Monitoring vegetation systems in the great plains with ERTS.* Proceedings, Third Earth Resources Technology Satellite-1 Symposium, Greenbelt: NASA SP-351, 301-317.

Royer, T.V., and Minshall, G.W. 2003. Controls on leaf processing in streams from spatial-scaling and hierarchical perspectives. *Journal of the North American Benthological Society* 22(3): 352-358.

Ross, J. 1981. The Radiation Regime and Architecture of Plant Stands. Junk, The Hague, 391 pp.

Saskatchewan Institute of Pedology. 1992. Grasslands National Park Soil Survey, University of Saskatchewan, Saskatoon.

Thenkabail, P.S., Smith, R.B., and Pauw, E.D. 2000. Hyperspectral vegetation indices and their relationships with agricultural crop characteristics. *Remote Sensing of Environment*, 71(2): 158-182.

Thorpe, J., Godwin, B., and McAdams, S. 2005. *Sage Grouse habitat in Southwestern Saskatchewan: Differences between active and abandoned leks.* Limited report, Saskatchewan Research Council. SRC Publication No. 11837-1E05. 40 pp.

Turner, M.G. 1989. Landscape Ecology: The Effect of Pattern on Process. *Annual Review of Ecology and Systematics*, 20: 171-197.

Turner, M.G., Dale, V.H., and Gardner, R.H. 1989. Predicting across scales: Theory development and testing. *Landscape Ecology*, 3(3-4): 245-252.

Urban, D.L., O'Neill, R.V., and Shugart, H.H., 1987. Landscape ecology. *Bioscience*, 37(2): 119-127.

Wiens, J.A., and Milne, B.T. 1989. Scaling of 'landscapes' in landscape ecology, or landscape ecology from a beetle's perspective. *Landscape Ecology*, 3(2): 87-96.

Yang, X., Wilmshurst, J., Fitzsimmons, M., and Guo. X. 2011. Can satellite imagery evaluate the pre-condition of a grazing experiment? *Prairie Perspectives*, 14: 45-50.

Yang, X., and Guo, X. 2011. Investigating vegetation biophysical and spectral parameters for detecting light to moderate grazing effects: a case study in mixed grass prairie. *Central European Journal of Geosciences*. 3(3): 336-348.

Yang, X., and Guo, X. 2014. Quantifying responses of spectral vegetation indices to dead materials in mixed grasslands. *Remote Sensing*. 6(5): 4289-4304.

Zhang, C., and Guo, X. 2006. Application of RADARSAT imagery to grassland biophysical heterogeneity assessment. *Canadian Journal of Remote Sensing.* 32(4): 281-287.

Zhang, C., and Guo, X. 2007. Measuring biological heterogeneity in the northern mixed prairie: a remote sensing approach. *The Canadian Geographer*, 51(4): 462–474.

Zhang, C. 2008. *Monitoring Biological Heterogeneity in a Northern Mixed Prairie Using Hierarchical Remote Sensing Methods.* Ph.D. Thesis, University of Saskatchewan, Saskatoon.

CHAPTER 3

REMOTE SENSING OF VEGETATION IN THE NORTHERN MIXED PRAIRIE: Spatial scale and effects of upscaling

ABSTRACT

With the availability of remotely sensed (RS) data at multiple spatial scales for ecological and earth-observation studies, it is critical to understand the limitations of scale and scaling as an arbitrary data scale selection can affect the patterns and predictions inferred from them.

In this study, RS data at spatial scales of 1 m (field spectroradiometer), 10 m (SPOT-5), 20 m (SPOT-4), and 30 m (Landsat-5) were acquired for a northern mixed prairie study area for June 2006 and July 2007. Spectroradiometer data was transformed to a set of narrowband vegetation indices (VI_n) and their corresponding broadband vegetation indices (VI_b) were derived from satellite imagery; both at original scales and at upscaled uniform scales of 40, 50, and 60 m. Multiple regression models were tested at original and upscaled scales using VI_b and terrain variables (elevation, slope, aspect, and wetness index) as the independent variables to predict VI_n and leaf area index (LAI).

Pearson's correlation analysis revealed that VI_n, VI_b, and LAI showed positive relationship with elevation and slope. Among the spatial scales tested, RS data at finer scales showed the strongest ability than coarser scales to estimate ground vegetation. VI_n were found to be better predictors than VI_b in estimating LAI, and upscaling at all spatial scales showed similar weakening trends for VI_b to predict LAI. Spatial autocorrelation was present in the data sets that violated the conditions of global regression models. However, the use of spatial regression models in-lieu of global regression models accounted for spatial- autocorrelation and dependency in the RS data and significantly improved the prediction results. Augmenting narrower field-based narrowband data with coarser space-borne broadband data is an ideal approach to understand vegetation heterogeneity in the northern mixed prairie. RS data scale selection based on convenience rather than relevance may lead to improper interpretations or conclusions.

3. 1 INTRODUCTION

Ecosystem processes and patterns in natural environments occur and function at different spatial and temporal scales, and are therefore ideally studied at their optimal scales or within their domains of scale. Ecological modeling exercises often require data to be scaled (upscaled or downscaled). Hence, a multi-scalar study approach is useful to identify the scaling trends, or the limitations with an arbitrary scale selection. A multi-scale study approach offers advantages to identify optimal study scale, understand the limitations of data sets for scaling, decide appropriate study scale, or design better sampling schemes.

The significance of vegetation data for ecosystem studies and analysis is well acknowledged and ecologists are interested in identifying rapid, reliable, and efficient ways of vegetation estimation. Traditional in-situ methods though efficient in terms of cost, time and equipment, however are destructive, laborious, and difficult to standardize with regard to scaling (Bonham et al., 2004, Kercher et al., 2003; Sykes et al., 1983). Field data are often collected at single, finer spatial scales (smaller areas) and therefore upscaling to coarser spatial scales (larger areas) can propagate error in the data. It is difficult to establish standard measurement or scaling protocols for multiple scales when using traditional field methods. Taking into account the scalar limitations, ecologists face challenges in identifying methods that are consistent, robust (repeatable), and yet efficient to adequately estimate vegetation at multiple spatial scales. Modern vegetation estimation methods such as digital photoplots, aerial photography, remote sensing (Kerr and Ostrovsky, 2003), and light detection and ranging (LiDAR; Lefsky et al., 2002) are becoming popular because of their ability to provide multi-scalar data.

3.1.1 Remote sensing of vegetation

Remote sensing (RS) is increasingly used by ecologists as it permits repeated monitoring of large areas in an instantaneous and non-destructive manner that is suitable for a variety of ecosystem- and landscape-analyses (Kerr and Ostrovsky, 2003; Turner et al., 2003). RS data from multiple sources (field, aerial, satellite) of varying spatial scales are now available: unmanned aerial vehicles (UAVs; 0.1 m), field spectroradiometer (~1 m), WorldView (0.5 m), RapidEye (5 m), DMC (22 m), SPOT (5-20 m), ASTER (15 m), Landsat (30 m), MODIS (250 m), and NOAA-AVHRR (1.1 km). RS has been successfully used in numerous studies for vegetation distribution

and mapping, estimating cover and plant biophysical parameters, and monitoring and predicting ecosystem change. RS data can be used to derive simple quantitative estimates such as vegetation indices (VI) using spectral reflectance along different bands of the electromagnetic spectrum. Several biophysical and biochemical VI have been developed that are used for vegetation analyses such as estimating structural, biophysical and biochemical parameters, assessing aboveground biomass, modeling biophysical and physiological states, and studying plant stresses (Haboudane, 2004).

3.1.2 Scale limitations in remote sensing

With RS data available from multiple sources at multiple spatial scales, ecologists are faced with the challenge of selecting appropriate RS data to answer specific research objectives. Often, the study scale is decided on the basis of the spatial (data) scale, the analysis scale, or by the coarsest data used in the analysis. For the sake of convenience, logistical or cost constraints, studies are frequently attempted with a single data scale.

Often, spatial scale is dependent on the capability of the image to resolve ground objects, i.e. spatial resolution (pixel size). Remote sensors record reflectance of land cover into one or many "georeferenced" pixels that may or may not adequately represent the optimal scales of boundaries of natural patterns and processes. Therefore, it is important to understand whether the RS dataset has adequately captured the ground information as it affects the types of patterns that can be observed, limits the scales within which the observations can occur (scale domains), or restricts the ability to allow for scaling information to other scales (scaling threshold).

Information may be masked if the scale of processes and patterns is finer than the scales of observation, and inferences might not be efficient if the data scale is finer than the scales of processes and patterns. Thus, observations made by the imposition of an arbitrary scale has a "smoothing or coarsening effect" on the patterns and processes being studied and their ability to give the ideal inference. Hence, it is difficult to compare results if studies employ different scales that have been selected based on convenience rather than relevance.

Information captured by a remote sensor is constrained by its spatial resolution or by the ground area imaged (instantaneous field of view; IFOV). A coarse resolution sensor images a larger ground area and records spectral reflectance from multiple land cover into a single pixel (a 'mixed pixel'). Hence, if the ground cover is heterogeneous, the full spectral variability on the

landscape may not be effectively captured by a pixel. When fine resolution sensors are used, it records the same land cover into multiple pixels (i.e. more noise and less variance). This introduces problems of spatial autocorrelation (SA; similarity in pairs of values of nearby locations) (Tobler, 1970) when data are collected for smaller areas and violates the conditions of the predictive global regression models. Statistical assumptions of correlation and regression (e.g. independence of observations) are not met when data shows SA (Ji and Peters, 2004) and therefore data requires 'corrections' adjusting for spatial effects when regression modeling.

3.1.3 Research questions

Given that RS of multiple scales (spatial and spectral resolutions) are currently available at multiple scales and cost advantages, how does the user choose a RS data set that performs best or is most advantageous (use- and cost-wise) while maintaining reliable ecosystem predictions? It is important understand the spatial dependence of vegetation surrogates with upscaling for effective incorporation into environmental modeling studies.

Therefore, this research explored the performance and compared the predictive capability of three satellite-based remote sensors (SPOT-5 HRG1, SPOT-4 HRVIR, and Landsat-5 TM) and a field remote sensor to estimate ground vegetation. We explored the implications of upscaling data from finer to coarser spatial scales, as well as how the predictive ability varied with upscaling (i.e. with coarsening of spatial scale). Specifically, we tested the following research questions:

(i) How do RS data sets of different spatial scales compare in estimating ground vegetation?
(ii) What are the effects of upscaling RS data from finer to coarser spatial scales?
(iii) What are the effects of SA and how can it be accounted while upscaling RS data sets?
(iv) How does the predictive ability of VI_b to estimate ground vegetation vary with upscaling?

3.2 DATA AND METHODS

3.2.1 Study area

The West Block of Grasslands National Park of Canada (GNPC, 49º12'N and 107º24'W) in Southern Saskatchewan was chosen for this study (Fig. 3.1). GNPC was established in 1984 to

conserve remnant mixed prairie in Canada and the park has since introduced management practices such as grazing to maintain vegetation heterogeneity in the region. The vegetation in the study area is primarily of native and mixed prairie grasses along with few shrubs, forbs, and invasive plants (Michalsky and Ellis, 1994). The main grasses include northern wheat grass (*Elymus lanceolatus*), and western wheat grass (*Pascopyrum smithii*), needle and thread (*Hesperostipa comata*), june grass (*Koeleria macrantha*), blue grama (*Bouteloua gracilis*), crested wheat grass (*Agropyron cristatum*), and smooth brome (*Bromus inermis*). Plant names are adapted from Harms (2006). Dense vegetation occurs along the Frenchman River valley lowlands, while short, sparse vegetation occurs in the uplands. GNPC has undulating topography characterized by knolls and valleys that control the movement and dynamics of surficial soil and water to ultimately determine the spatial patterns and variability of vegetation. The region has semi-continental arid climate with temperature extremes (monthly mean ranging from -12.4 to 18.3 ºC) and very low precipitation (~35 cm yr^{-1}).

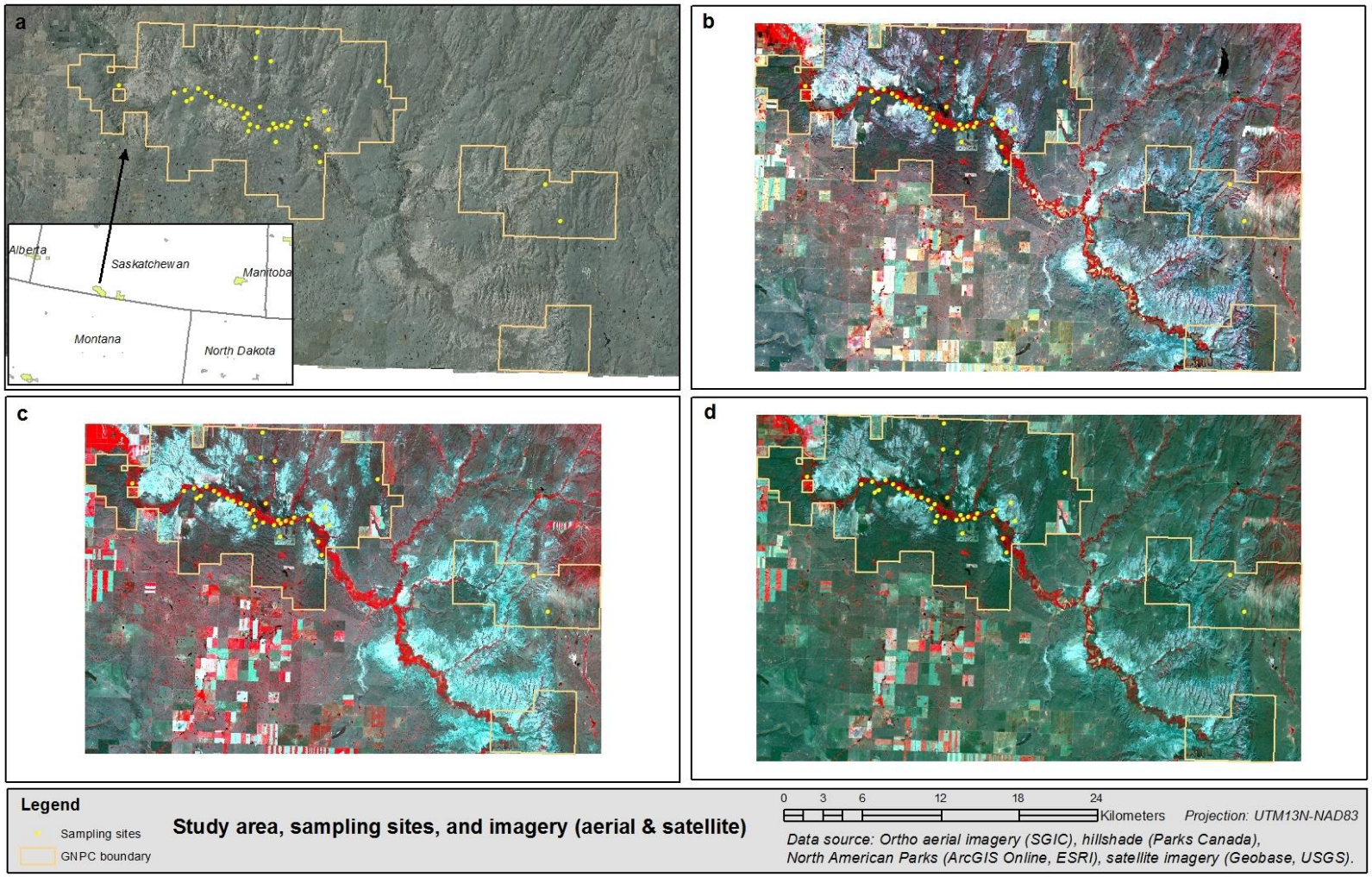

Fig. 3.1 Map showing the location of the study area (GNPC; Grasslands National Park of Canada), sampling sites, and topography of the region. Fig. 3.1a shows ortho aerial imagery (Source: SGIC; Saskatchewan Geospatial Imagery Collaborative) and North American Parks (Source: ArcGIS Online, ESRI), and Fig. 3.1b to 3.1c show SPOT-5 (27 July 2006), SPOT-4 (28 June 2006), and Landsat-5 (17 July 2006) image in standard false color, respectively.

3.2.2 Site design and sampling points

41 sites representing a variety of vegetation communities and three topographic positions (upland, sloped land, and lowland) were sampled in the summer of mid-June of 2006 and early July of 2007 corresponding to the peak vegetation growth period in the region (Fig. 3.1a). At each site, a cross-shaped design was established with transects of 100 m running in the cardinal N-S and E-W directions and intersecting at the site center. Sampling quadrats (50 cm*50 cm) were placed at 10 m intervals along each transect. Quadrat locations were converted to vector points (n = 686) in ESRI® ArcGIS 9.3 (ESRI, California) and used to extract reflectance values for the corresponding pixel co-ordinates from each satellite imagery at a specific spatial scale (Fig. 3.1b to 3.1d).

3.2.3 Field data and processing

At each sampling point, leaf area index (LAI) and canopy spectral measurements were collected as follows:

Leaf area index (LAI)

LAI, essentially plant area index, was collected using a LiCOR® LAI-2000 Plant Canopy Analyzer in 2006 and with a Decagon® Accupar (Lincoln, Nebraska) in 2007. LAI was measured with the LiCOR using the shadow method (He et al., 2007) and averaging four LAI values at each quadrat corner. These instruments measure the amount of photosynthetically active radiation (PAR) available above and below the canopy to estimate LAI. Note that the LAI measured is the amount of radiation intercepted by the canopy; it does not necessarily denote only the green component but also includes the standing dead component such as dead or senesced vegetation. Chapter 2 provides discussion on the concept of LAI, instruments and their working, and its measurement.

Narrowband vegetation indices (VI_n)

Canopy spectral reflectance measurements were collected above each quadrat using an ASD® FieldSpec FR Pro (Analytical Spectral Devices, Boulder, Colorado) spectroradiometer with a

spectral range of 350-2500 nm. Spectra were collected perpendicular to the canopy at a height of 1 m and with a 25^{o} field of view probe; corresponding to an IFOV of ~1 m^2 pixel size. Spectra were standardized to apparent reflectance using a Spectralon calibration panel (Labsphere Inc., New Hampshire). All spectral measurements were collected on clear days, within 2 hours of solar noon and under low wind conditions. Spectral reflectance (ρ) was transformed to three *narrowband* vegetation indices (VI_n): normalized difference vegetation index ($NDVI_n$), normalized difference wetness index ($NDWI_n$), and adjusted transformed soil adjusted vegetation index ($ATSAVI_n$) (Table 3.1).

Table 3.1 Spectral vegetation indices used in the study, formulae, references, and their major use.

Vegetation index		Formula	Reference	Usefulness
VI_n	$NDVI_n$	$\frac{\rho_{800} - \rho_{670}}{\rho_{800} + \rho_{670}}$	Rouse (1974)	Greenness, leaf area index, vegetation abundance
	$NDWI_n$	$\frac{\rho_{860} - \rho_{1240}}{\rho_{860} + \rho_{1240}}$	Gao (1996)	Canopy moisture content, wetness
	$ATSAVI_n$	$\frac{a(\rho_{800} - a\rho_{670} - b)}{a\rho_{800} + \rho_{670} - ab + X(1+a^2)}$	Baret & Guyot (1991)	Minimizes soil background effects
VI_b	$NDVI_b$	$\frac{\rho_{NIR} - \rho_R}{\rho_{NIR} + \rho_R}$	Rouse (1974)	Greenness, leaf area index, vegetation abundance
	$NDWI_b$	$\frac{\rho_{NIR} - \rho_{SWIR}}{\rho_{NIR} + \rho_{SWIR}}$	Gao (1996)	Canopy moisture content, wetness
	$ATSAVI_b$	$\frac{1.219 \times (\rho_{NIR} - 1.219 \times \rho_R - 0.029)}{1.219 \times \rho_{NIR} + \rho_R - 1.219 \times 0.029 + 0.08 \times (1 + 1.219^2)}$	Baret & Guyot (1992)	Minimizes soil background effects

Note: NDVI (Normalized Difference Vegetation Index), NDWI (Normalized Difference Vegetation Index), and ATSAVI (Adjusted Transformed Soil Adjusted Vegetation Index). The values for *a* (Gain) = 1.22, *b* (Offset) = 0.03, and *L* (Canopy background adjustment factor) = 0.5 were obtained from He et al. (2006). ρ (Spectral reflectance), and satellite bands: R (Red); NIR (Near infrared); and SWIR (Short wave infrared).

3.2.4 Satellite imagery and processing

Three cloud-free satellite images with spatial resolutions of 10 m (SPOT-5), 20 m (SPOT-4), and 30 m (Landsat-5) were acquired (Table 3.2) and processed using ENVI 4.7 (ITTVIS Inc.). The images were individually georeferenced using a high resolution SPOT-5 HRG1 PAN (5 m panchromatic) image (Source: *www.geobase.ca*) to UTM 13N-NAD83 projection, orthorectified and resampled using the nearest neighbor method to their native pixel sizes. The Landsat-5 and SPOT-4 images were further co-registered to the SPOT-5 image as this image had the highest location accuracy. Images were processed from raw digital numbers to surface reflectance following the Fast Line-of-Sight Atmospheric Analysis of Spectral Hypercubes (FLAASH; Anderson et al., 1999) atmospheric correction. To compare the three satellite images at common scales and to understand their trends with upscaling, the spatial scale of each image was resized using the pixel aggregation method from their native pixel sizes of 10, 20, 30 m to coarser spatial scales of 40, 50, and 60 m.

Broadband vegetation indices (VI_b)

Similar to the calculation of VI_n, using quadrat point vectors the ρ values of each image band were spatially extracted to calculate three comparable *broadband* vegetation indices (VI_b): $NDVI_b$, $NDWI_b$, and $ATSAVI_b$ (Table 3.1) at original (10, 20, 30 m) and upscaled (40, 50, 60 m) coarser spatial scales (Table 3.2).

Table 3.2 Satellite images used in the study along with their sensor details, date of acquisition, spatial scale (resolution/pixel size), scales tested and data source.

Satellite image	Date of acquisition	Native spatial scale (m)	Satellite bands used*	Tested spatial scales (m)	Data source
SPOT-5 HRG1	27 July 2006	10	G, R, NIR, MIR (1234)	10, 40, 50, 60	*www.geobase.ca*
SPOT-4 HRVIR1	28 June 2006	20	G, R, NIR, MIR (1234)	20, 40, 50, 60	*www.geobase.ca*
Landsat-5 TM	17 July 2006	30	B, G, R, NIR, MIR, MIR (123457)	30, 40, 50, 60	*www.usgs.gov*

* B - Blue, G - Green, R - Red, NIR - Near Infrared, MIR - Mid Infrared. Thermal band (6) of Landsat-5 TM image was excluded.

3.2.5 Additional data

Terrain variables

A digital elevation model (DEM) of 20 m spatial scale (Source: *www.geobase.ca*) for the study area was used to derive maps of percent slope, aspect, and wetness index (WI; Beven and Kirkby, 1979) using the ESRI® ArcGIS Spatial Analyst Tools. WI, as a surrogate for soil moisture, was calculated using the following equation:

$$WI = Ln\ (A_s/Tan\ B) \quad (3.1)$$

where *Ln* is natural logarithm, A_s is the contributing catchment area (m^2) and *B* is the slope (degrees).

Pixel values for the terrain variables (TVs) were spatially extracted from the terrain maps and appended to quadrat point vector. Note that the terrain maps were not upscaled as with satellite imagery since the study objective was to identify how RS data at different spatial scales would compare to predict ground vegetation.

3.2.6 Statistical and spatial analysis

Regression variables

Test of normality and outlier analysis were performed on the LAI data and the outliers (LAI <0.5 or >5) were removed from further analysis. Our previous study (Chapter 2) showed topography and soil moisture influence vegetation abundance and distribution through elevation, topographic position, and soil moisture availability; hence TVs were used along with VI_b or VI_n to predict ground vegetation. Multiple regression analysis was performed with the field-measured variables (LAI and VI_n) as the dependent variables, and the satellite-derived (VI_b) and terrain variables as the independent variables (Table 3.3). Five prediction models were tested on the three images at four different scales - a total of 60 prediction models (see Table 3.2).

Table 3.3 Regression prediction models tested on each image of specific spatial scale. Total of 60 prediction models were tested. Number of observations (n) = 686.

Model	Dependent variables	Independent variables
1	LAI	$NDVI_b$, WI, Elevation, Slope, Aspect
2	LAI	$ATSAVI_b$, WI, Elevation, Slope, Aspect
3	$NDVI_n$	$NDVI_b$, WI, Elevation, Slope, Aspect
4	$NDWI_n$	$NDWI_b$, WI, Elevation, Slope, Aspect
5	$ATSAVI_n$	$ATSAVI_b$, WI, Elevation, Slope, Aspect

It was also of interest to identify how effectively the VI_n could predict LAI at the finest scale (1 m), therefore the following regression models were additionally tested:

$$LAI = NDVI_n + WI + Elevation + Slope + Aspect \quad (3.2)$$

$$LAI = NDVI_b + WI + Elevation + Slope + Aspect \quad (3.3)$$

Regression analysis

The global regression model can be written as:

$$y = \beta_0 + \beta_1 x_1 + \beta_2 x_2 + \beta_3 x_3 + \varepsilon \quad (3.4)$$

where y is the dependent variable, β_0 the intercept, x_1 to x_3 are three independent variables, β_1 to β_3 the estimated coefficients, and ε is the random error term.

The global regression model assumes that the relationship under study is spatially constant, i.e. the observations are independent of one another and the estimated parameters remain constant over the study area. Another condition of the linear regression model is that the residuals are normally and independently distributed with a mean of zero and a constant variance, and such a model is usually fit using the ordinary least squares (OLS) regression. However, these assumptions of the global regression model are violated when the variables are spatially autocorrelated (i.e. similarity between any pair of observations at smaller distances than those farther away), spatially dependent (i.e. nearby locations having similar values), or with non-stationarity (i.e. relationship between the variables varies over the geographical space, and therefore prediction estimates become unreliable over the entire study area. Spatial regression

(SR) methods have been developed to overcome these limitations with OLS, especially with spatial data sets, by accounting for two types of spatial autocorrelation (SA): *spatial lag* and *spatial error* (Anselin, 1988). The *spatial error* model is appropriate when there is dependency structure in the residual term, and the *spatial lag* model is suitable when a spatial structure is present in the model variables.

Regression models

Our first objective was to identify the effective predictor variables to estimate ground vegetation through regression modeling; therefore all variables of interest were checked for multi-collinearity (i.e. high degree of correlation between the predictor variables) using the condition number and the variation inflation factor (VIF). Since SA is inherent in most ecological and RS data sets, the Moran's *I* statistic in ESRI® ArcGIS was used to identify if the data sets showed any significant SA. If the data sets were found to be spatially dependent, SR were used to incorporate the spatial component in the regression models. Stepwise regressions were performed in SPSS 17 on the variables of interest to identify the best prediction models (Table 3.3). The best predictor models identified from stepwise regression were further used in GeoDA 0.9.5-i (Anselin, 2005) to run OLS regressions with diagnostic tests for non-normality, heteroskedasticity, and spatial dependence, in addition to being used to assess whether or not the consideration of the incorporation of the spatial component would improve the modeling results. OLS was followed by selecting the appropriate SR model: spatial lag or spatial error, suggested by the OLS diagnostic tests.

Spatial weight files were created at 100 m threshold distances following Anselin (2002). GeoDA provides spatial diagnostics tests (Lagrange Multiplier (LM) test statistics: LM Lag or LM Error, and Robust LM Lag or Robust LM Error) to check if the data sets were spatially dependent and were further used to decide which exact SR model to be run, i.e. spatial lag or spatial error. For each satellite image, OLS and SR were run at the original spatial scale (10, 20, 30 m) and also at the resized coarser spatial scales (40, 50, 60 m). The regression prediction models at various spatial scales, including original and upscaled scales, were compared using the R^2 value ($R^2_{adj.}$) and the *corrected* Akaike Information Criterion (AIC_c; see Fotheringham (2002)) for further details) values. *AIC* (Hurvich et al., 1998) is a measure of goodness of fit that can be used to compare different regression models. As a general rule, the lower the AIC_c value the closer the

approximation of the model to reality. Fotheringham (2002) recommends that the best model is the one with the lowest AIC_c and a real difference exists between the two regression models only if the AIC_c values differ by at least 3. Note that the same type and number of predictor variables (Table 3.3) and number of observations (n = 686) were used in each model and across its different image scales.

3.3. RESULTS AND DISCUSSION

3.3.1 Topographic variability of biophysical variables

Descriptive statistics for LAI, green plant cover, and VI_n (Table 3.4) showed that the average value for all the variables differed significantly in the lowland, the sloped land, and the upland prairie, indicating the effect of topography in affecting vegetation distribution and abundance. Topography affects the dynamics of water and run-off and ultimately influences the spatial patterns and variability of vegetation by effecting the availability of water and nutrients for plant growth. The effect of slope and aspect on vegetation patterns has been demonstrated in several ecological and remote sensing studies.

Table 3.4 Mean values for plant cover, LAI, and VI_n at three topographic groups. LAI, $NDVI_n$, $NDWI_n$, and $ATSAVI_n$ are unitless.

Topographic group	**Elevation (m)**	**Green plant cover (%)**	**LAI**	**$NDVI_n$**	**$NDWI_n$**	**$ATSAVI_n$**
Upland	913.2	49.50	0.695	0.39235	-0.13808	0.19678
Sloped	818.7	65.67	1.291	0.55150	-0.07384	0.32831
Lowland	773.5	60.12	2.263	0.67648	-0.04691	0.41774
Mean	785.5	60.79	2.050	0.64634	-0.05427	0.39565
S.D.	31.3	23.56	1.210	0.19973	+0.08083	0.16711

3.3.2 Comparison of biophysical variables

Studies have demonstrated a strong relationship between LAI and VI (Thenkabail et al, 2000). Similarly, Pearson's correlation analysis showed that LAI and all VI_n or VI_b were positively correlated (Table 3.5); though NDVI and ATSAVI showed stronger relationship when compared

to NDWI. VI_n were positively correlated to VI_b (R = 0.47-0.61) demonstrating that both data sets, even though acquired at different spatial scales (canopy- or satellite-level) are comparable and represent similar vegetation properties of greenness and wetness. VI_n (R = 0.60-0.69) showed stronger positive relationship to LAI when compared to VI_b (R = 0.46-0.48). This is to be expected as spectral reflectance collected directly over the plant canopy has less interference due to atmospheric effects and minimal spectral contamination from background materials. Vegetation in the uplands and sloped lands have sparse cover, shorter with larger gaps in the canopy, and with relatively higher amount of standing dead or non-photosynthetic vegetation (NPV) component. Therefore, VI_b derived from satellite spectral reflectance is likely contaminated by background materials that add higher amount of reflectance to the red spectral region and thereby reducing the efficiency of VI. Zhang and Guo (2007) have reported weak relationships between green biomass and VI_b for the northern mixed prairie.

Negative correlation was observed for elevation (R = - 0.18 to -0.31) and slope (R = -0.17 to -0.24) to both VI_n and VI_b, thereby further supporting the fact that topography controls the dynamics of surface water run-off and soil moisture variation to determine spatial patterns of vegetation. This trend was evident in our field observations as vegetation cover decreased with increase in elevation (Table 3.4). Pearson's correlation analysis revealed that VI showed similar trend to LAI, elevation, slope, aspect, and WI. VI and LAI showed positive relationship to elevation and slope, i.e. higher VI and LAI at lower elevation and slope.

Table 3.5 Matrix showing the relationship between LAI, VI_n, VI_b, and the terrain variables. Nature of the relationship (positive or negative), Pearson's correlation coefficients, and their level of significance are shown. Note that variables suffixed with a [b] were significant only at the 0.01 level.

Variable	$NDVI_n$	$NDWI_n$	$ATSAVI_n$	LAI	$NDVI_b$	$NDWI_b$	$ATSAVI_b$	Elevation	Slope	Aspect	WI
$NDVI_n$	1										
$NDWI_n$	0.843[a]	1									
$ATSAVI_n$	0.970[a]	0.852[a]	1								
LAI	0.691[a]	0.602[a]	0.689[a]	1							
$NDVI_b$	0.613[a]	0.480[a]	0.609[a]	0.481[a]	1						
$NDWI_b$	0.569[a]	0.474[a]	0.569[a]	0.462[a]	0.953[a]	1					
$ATSAVI_b$	0.611[a]	0.478[a]	0.607[a]	0.478[a]	1.000[a]	0.957[a]	1				
Elevation	-0.263[a]	-0.176[a]	-0.240[a]	-0.308[a]	-0.257[a]	-0.203[a]	-0.246[a]	1			
Slope	-0.170[a]	-0.180[a]	-0.180[a]	-0.170[a]	-0.229[a]	-0.241[a]	-0.234[a]	0.338[a]	1		
Aspect	0.001	-0.005	0.008	0.003	-0.083	-0.072	-0.083	0.156[a]	0.300[a]	1	
WI	0.028	0.029	0.047	0.101[b]	0.085	0.116[b]	0.087	0.039	0.034	0.386[a]	1

[a]Significant at the 0.001 level (2-tailed).

[b]Significant only at the 0.01 level (2-tailed).

3.3.3 Predictive abilities of RS data at various scales

He et al. (2006) found that ATSAVI or its modified version, L-ATSAVI (litter-corrected ATSAVI), improved estimation of LAI in the northern mixed prairie due to their usefulness in minimizing background (soil or litter) effects. However, our comparison of three VI_b: $NDVI_b$, $NDWI_b$ and $ATSAVI_b$ used in this study did not show ATSAVI to be more useful than NDVI or NDWI (Table 3.6b). Similar results were obtained when VI_n were used to estimate LAI to further supporting this conclusion (Table 3.6a). Li and Guo (2010) also report NDVI to be performing better than L-ATSAVI for LAI estimation. However, majority of our sampling sites were in the lowland prairie, therefore ATSAVI or L-ATSAVI might be more useful in upland prairie or in sites with high soil or litter. Yet, Davidson and Csillag (2001) in upland prairie sites, compared broadband ratio-based and soil-adjusted VI calculated from plot-level spectroradiometer-derived spectral reflectance and upscaled to 0.5, 2.5, 10, and 50 m, and found that NDVI was comparable or only slightly less inferior to SAVI for predicting aboveground live biomass.

Table 3.6 Predictive abilities of remotely sensed data at four spatial data scales (1, 10, 20, 30 m) to estimate LAI and VI_n. Dependent variables are given in the first column, and r^2 *adjusted* values are given. All relationships were significant at $p < 0.01$.

(a) Field remote sensing (1 m):

Data scale	**Spectroradiometer (1 m)**		
	$NDVI_n$	$NDWI_n$	$ATSAVI_n$
LAI	0.48	0.36	0.47

(b) Satellite remote sensing (10, 20, 30 m):

Data scale	**SPOT-5 (10 m)**			**SPOT-4 (20 m)**			**Landsat-5 (30 m)**		
	$NDVI_b$	$NDWI_b$	$ATSAVI_b$	$NDVI_b$	$NDWI_b$	$ATSAVI_b$	$NDVI_b$	$NDWI_b$	$ATSAVI_b$
LAI	0.23	0.21	0.23	0.25	0.25	0.25	0.25	0.25	0.25
$NDVI_n$	0.38			0.38			0.36		
$NDWI_n$		0.22			0.19			0.21	
$ATSAVI_n$			0.37			0.35			0.34

Moran's *I* statistics revealed that the data sets were spatially autocorrelated and thereby violated the conditions of the global regression model, making the OLS modeling results unreliable. The OLS diagnostic tests confirmed this and further suggested which SR model to be selected: spatial lag or spatial error. Results from OLS and SR modeling and their R^2 and AIC_c values are shown in Table 3.7 and Table 3.8, respectively. The selection of the SR model over the OLS model was evident by significant reduction in AIC_c and improvement in R^2 values. Note that the OLS results are shown only to compare with the SR and to demonstrate their inferiority over SR. Also, often the spatial error regression model was selected over the spatial lag, therefore only the results from the spatial error regressions are discussed.

Table 3.7 Results of OLS (ordinary least squares) models for the SPOT-5 (S5), SPOT-4 (S4), Landsat-5 (L5) images. Shown are R^2 (top cell) and its AIC_c (bottom cell) values for each image scale for a specific model. TVs (Terrain variables). Note that OLS results are given only for comparing with SR (spatial regression) and to highlight their inferiority compared to SR. n = 686.

Scale (m)	Model 1 (LAI = $NDVI_b$ + TVs)			Model 2 (LAI = $ATSAVI_b$ + TVs)		
	S5	**S4**	**L5**	**S5**	**S4**	**L5**
10	0.275	0.279	0.285	0.275	0.280	0.283
	1999.20	1996.14	1990.05	1999.92	1995.45	1992.27
40	0.309	0.277	0.294	0.308	0.277	0.292
	1966.61	1997.91	1981.12	1968.04	1997.43	1982.98
50	0.274	0.275	0.276	0.274	0.276	0.275
	2000.31	1999.82	1998.75	2000.77	1998.46	1999.27
60	0.281	0.273	0.276	0.279	0.274	0.275
	1993.83	2001.60	1998.34	1995.52	2000.92	1999.97

Scale (m)	Model 3 ($NDVI_n$ = $NDVI_b$ + TVs)			Model 4 ($NDWI_n$ = $NDWI_b$ + TVs)			Model 5 ($ATSAVI_n$ = $ATSAVI_b$ + TVs)		
	S5	**S4**	**L5**	**S5**	**S4**	**L5**	**S5**	**S4**	**L5**
10	0.395	0.393	0.378	0.238	0.203	0.221	0.384	0.371	0.362
	-597	-595	-578	-1680	-1649	-1664	-830	-815	-805
40	0.417	0.399	0.401	0.235	0.206	0.232	0.400	0.381	0.385
	-622	-602	-604	-1677	-1652	-1675	-847	-826	-830
50	0.386	0.402	0.385	0.211	0.207	0.218	0.378	0.384	0.376
	-587	-605	-586	-1656	-1652	-1662	-822	-829	-820
60	0.361	0.380	0.354	0.181	0.176	0.187	0.347	0.365	0.342
	-559	-580	-552	-1630	-1626	-1635	-789	-809	-783

Table 3.8 Results of SR (spatial regression) models for the SPOT-5 (S5), SPOT-4 (S4), Landsat-5 (L5) images. Shown are R^2 (top cell) and its AIC_c (bottom cell) values for each image scale for a specific model. TVs (Terrain variables). n = 686.

Scale (m)	Model 1 (LAI = $NDVI_b$ + TVs)			Model 2 (LAI = $ATSAVI_b$ + TVs)		
	S5	**S4**	**L5**	**S5**	**S4**	**L5**
10	0.444	0.447	0.450	0.443	0.447	0.450
	1848.73	1843.75	1839.67	1849.22	1844.00	1840.16
40	0.452	0.440	0.442	0.452	0.440	0.442
	1834.48	1851.00	1846.85	1835.34	1851.56	1847.53
50	0.424	0.430	0.428	0.424	0.430	0.428
	1869.76	1862.68	1864.59	1869.65	1862.25	1864.2
60	0.431	0.436	0.436	0.431	0.436	0.436
	1861.01	1855.98	1855.87	1861.01	1856.11	1855.86

Scale (m)	Model 3 ($NDVI_n$ = $NDVI_b$ + TVs)			Model 4 ($NDWI_n$ = $NDWI_b$ + TVs)			Model 5 ($ATSAVI_n$ = $ATSAVI_b$ + TVs)		
	S5	**S4**	**L5**	**S5**	**S4**	**L5**	**S5**	**S4**	**L5**
10	0.471	0.460	0.460	0.290	0.274	0.283	0.448	0.434	0.439
	-669	-657	-656	-1717	-1699	-1709	-887	-871	-875
40	0.469	0.456	0.458	0.286	0.272	0.281	0.444	0.432	0.435
	-673	-655	-657	-1713	-1699	-1709	-887	-871	-876
50	0.443	0.453	0.448	0.266	0.265	0.267	0.421	0.427	0.425
	-639	-652	-644	-1694	-1693	-1696	-860	-867	-864
60	0.418	0.436	0.423	0.238	0.251	0.249	0.399	0.413	0.404
	-609	-630	-613	-1668	-1678	-1678	-832	-850	-836

Fig. 3.2 shows the trends for R^2 (Fig. 3.2) and AIC_c (Fig. 3.3) values from SR modeling for the three satellite images at original and upscaled scales. Comparison of R^2 and AIC_c values for imagery showed that RS data at finer scales had the highest predictive ability to estimate ground vegetation (LAI or any of $NDVI_n$, $NDWI_n$, $ATSAVI_n$) than upscaled coarser scales. At the original spatial scale (10, 20, 30 m), all three imagery were comparable in modeling ground estimates (Table 3.7 and Fig. 3.2); with Landsat being slightly better in the LAI prediction. E.g. for LAI-$NDVI_b$, SPOT-5 (R^2 = 0.44, AIC_c = 1848) and Landsat-5 (R^2 = 0.45, AIC_c = 1839) performed similarly. A similar trend was observed in the case of LAI-$ATSAVI_b$, SPOT-5 (R^2 = 0.44, AIC_c = 1849) and Landsat-5 (R^2 = 0.45, AIC_c = 1840); considered significant as the AIC_c difference between the models is >3 (Fotheringham, 2002). However, SPOT-5 was better in the modeling of VI_n with higher R^2 and significant reduction in AIC_c for the models, e.g. for $NDVI_n$-$NDVI_b$, SPOT-5 (R^2 = 0.47, AIC_c = -597) and Landsat-5 (R^2 = 0.46, AIC_c = -578), and in the case of $ATSAVI_n$-$ATSAVI_b$, SPOT-5 (R^2 = 0.44, AIC_c = -830) and Landsat-5 (R^2 = 0.43, AIC_c = -805).

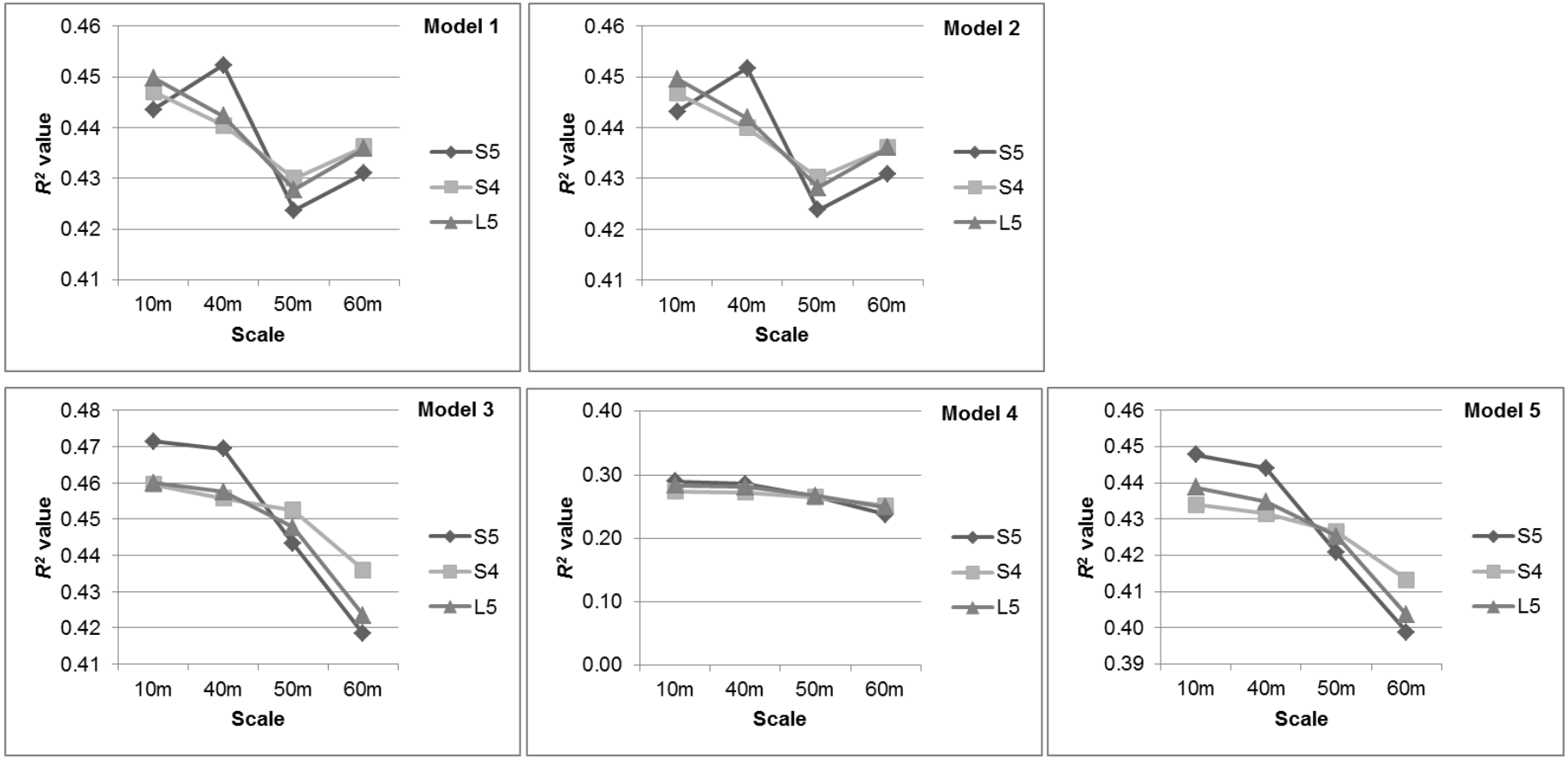

Fig. 3.2 Graphs showing the trends for R^2 values for the SPOT-5 (S5), SPOT-4 (S4), Landsat-5 (L5) images at original scale (10, 20 or 30 m) and upscaled common scales (40, 50 and 60 m). Graphs are arranged in the order of **Model 1** (LAI = $NDVI_b$ + TVs), **Model 2** (LAI = $ATSAVI_b$ + TVs), **Model 3** ($NDVI_n$ = $NDVI_b$ + TVs), **Model 4** ($NDWI_n$ = $NDWI_b$ + TVs), and **Model 5** ($ATSAVI_n$ = $ATSAVI_b$ + TVs), respectively. TVs (WI, Elevation, Slope, Aspect). Number of observations (n) = 686.

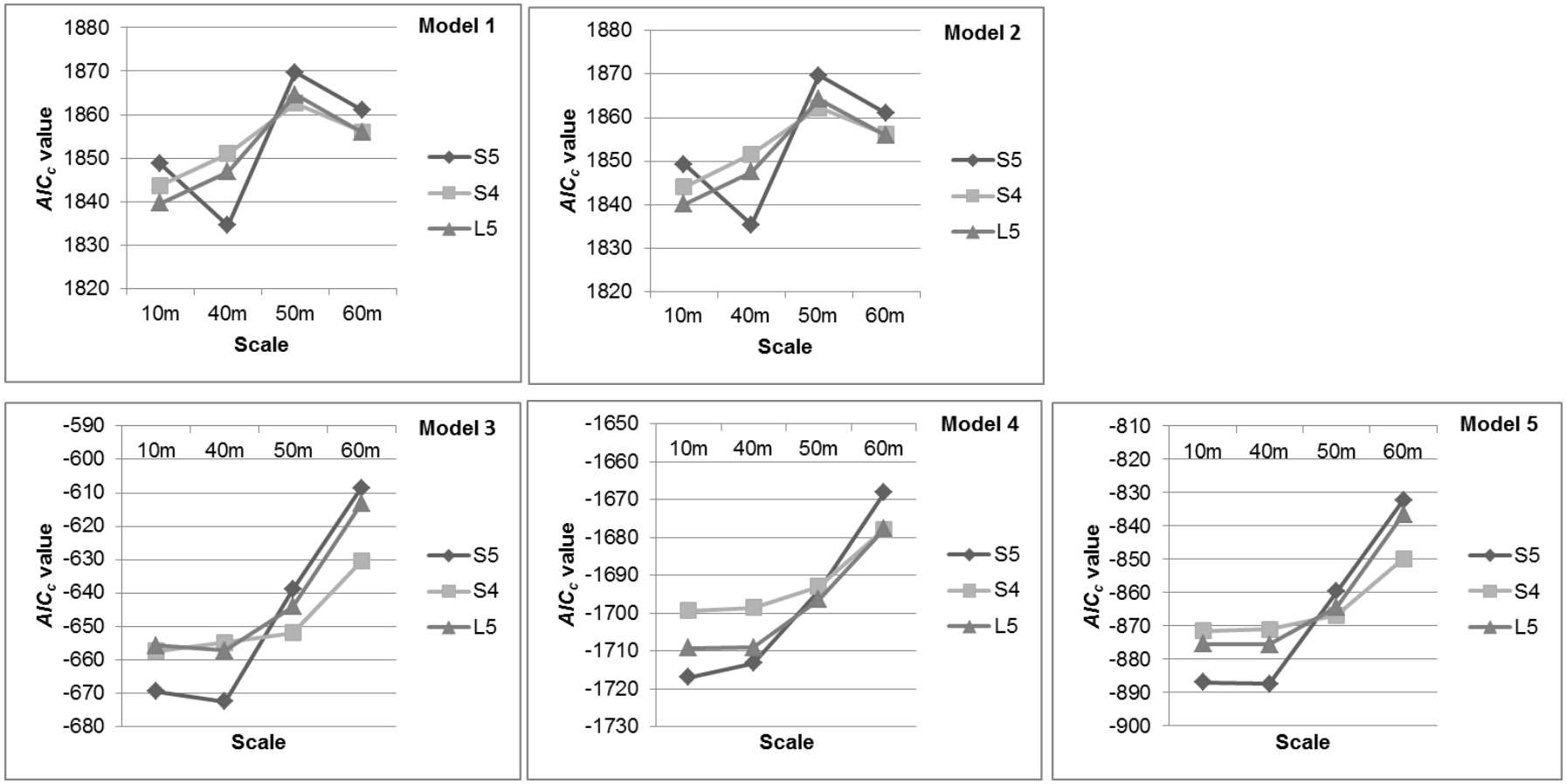

Fig. 3.3 Graphs showing the trends for AIC_c values for the SPOT-5 (S5), SPOT-4 (S4), Landsat-5 (L5) images at original scale (10, 20 or 30 m) and upscaled common scales (40, 50 and 60 m). Graphs are arranged in the order of **Model 1** (LAI = $NDVI_b$ + TVs), **Model 2** (LAI = $ATSAVI_b$ + TVs), **Model 3** ($NDVI_n$ = $NDVI_b$ + TVs), **Model 4** ($NDWI_n$ = $NDWI_b$ + TVs), and **Model 5** ($ATSAVI_n$ = $ATSAVI_b$ + TVs), respectively. TVs (WI, Elevation, Slope, Aspect). Number of observations (n) = 686.

In Fig. 3.2 and Fig. 3.3, it is seen that all three images show a similar weakening trend with upscaling, i.e. decreasing R^2 values or increasing AIC_c values as the images are upscaled from finer to coarser resolutions. This indicates the lack of correspondence of imagery-derived data to field data with successive upscaling. Further supporting this result, a better relationship was estimated through SR models than with OLS: LAI-NDVI$_n$ (R^2 = 0.61, AIC_c = 1609) and LAI-ATSAVI$_n$ (R^2 = 0.61, AIC_c = 1606) than for LAI-NDVI$_b$ (R^2= 0.44, AIC_c = 1849) and LAI-ATSAVI$_b$ (R^2 = 0.44, AIC_c = 1849). In both cases of prediction of LAI or VI$_n$ from VI$_b$ showed that at image scales beyond 50 m, there is a sudden change in the trend indicating that 50 m might be the threshold scale in these type of natural ecosystems. Consistent to this, our findings in the same study area showed spatial scale of plant biophysical variables to be between 35 and 200 m (Chapter 2).

VI$_n$ were found to be better predictors than VI$_b$ in estimating LAI. The comparison of data from four sensors at different spatial scales revealed that finer-resolution remote sensor had the best predictive ability to estimate ground vegetation. The superiority of finer spatial scales over coarser spatial scales suggests that the coarser remote sensors are disadvantaged when imaging heterogeneous land cover such as the mixed prairie. As the sensor resolution become coarser, spectral reflectance from different surface cover within the IFOV of the remote sensor are mixed into a single pixel and thereby weakening the relationship between VI$_n$ and VI$_b$. This highlights the issues of spectral mixing and the problem of 'mixed pixels' in these types of ecosystems. Small (2004) has discussed the effects of mixing of spectral signals, dimensionality of the spectral mixing space, and their consequence for spectral analysis with regard to Landsat ETM+ imagery.

Studies in the northern mixed prairie have estimated the spatial scale of variation of NDVI as: 35 m (Govind), 55 m (Zhang and Guo, 2007), 70 m (He et al., 2006), and that of LAI from 62 m, 70 m, 76 m, respectively. Govind also found that the comparison of the range values of NDVI estimated from finer spatial scales had a lower range (35 m, VI$_n$) than those estimated from coarser spatial scales (66 m, VI$_b$). These range values for NDVI and LAI suggest that the spatial dependency of these biophysical variables is within 80 m. The spatial scale of RS data is sensitive to the heterogeneity of the land cover, and as the spatial scale of the sensor becomes coarser it tends to average the spectral reflectance of different surface materials and produce a

mixed (composite) spectra and thereby weakening the relationship between satellite- and ground-estimates.

Nevertheless, Landsat imagery performed only slightly less better when compared to the SPOT imagery suggesting that Landsat can be safely used to study vegetation and ecosystem processes in the northern mixed prairie despite its at coarser spatial resolution. Compared to the SPOT sensor, the Landsat sensor offers finer spectral resolution, larger image footprint, and significantly reduced costs. Note that the Landsat-7 ETM+ and Landsat-5 TM sensor have now failed and are out of operation, however USGS launched Landsat-8 in 2013 and continue to provide low-cost earth observation data as a part of the Landsat Data Continuity Mission (LDCM).

3.4 CONCLUSIONS

This study tested the effectiveness of RS data at various spatial scales to predict field estimates and how they compare at their original scales and when upscaled to coarser scales. In general, we found finer spatial scales to be more effective than coarser scales in estimating ground vegetation in the northern mixed prairie. As the spatial scale of the remote sensor became coarser, their ability to estimate ground vegetation decreased. This can be attributed to the fact the northern mixed prairie is heterogeneous, both spatially and spectrally. As the spatial scale becomes coarser, the IFOV of the remote sensor is imaging a larger ground area and therefore if the surface cover is heterogeneous, spectral reflectance from different materials are non-linearly mixed to create the problem of mixed pixels. Further, reflectance from non-green components such as dead plant material, litter, and soil add to the vegetation spectrum, thereby reducing the efficiency of VI which are based on the amount of reflectance in the red (R) and infrared (IR) region.

With the increasing application of remote sensing in ecological applications, it is critical to choose remote sensors at the optimum scale for any ecosystem analysis. Rahman et al. (2003) estimated the spatial scale of variation of NDVI using semivariogram analysis and recommended that the optimum pixel size to study ecosystem processes should be roughly within half of the range value. Similarly, with the range values for the plant biophysical variables estimated through our study at <80 m (see Chapter 2), pixel sizes of 30 m or finer are recommended as

ideal for studying the northern mixed prairie. Vegetation in the northern mixed prairie is also spectrally unique showing spectral diversity, spatially and temporally. Therefore, the choice of spatial resolution over spectral resolution should not be the default choice as the identification and mapping of land cover may be affected by using imagery with high spatial resolution but of poor spectral resolution.

The effects of SA in ecological and spatial data sets including RS data sets have been acknowledged in the past, however only recently have statistical or geostatistical methods to incorporate these spatial effects become prevalent. Spatial regression (SR) and geographically weighted regression (GWR) are now available in software packages such as ArcGIS, GeoDA, GWR (Geographically Weighted Regression), Surfer, SAGA (System for Automated Geoscientific Analyses), SpaceStat, R, SAM (Spatial Analysis for Macroecology; Rangel et al., 2010) and PASSAGE (Pattern Analysis, Spatial Statistics and Geographic Exegesis; Rosenberg and Anderson, 2011) to incorporate the effects of spatial- autocorrelation and dependency. In this study, SA was present in the data sets at finer resolution and the use of SR methods in-lieu for global regression methods accounted for the spatial dependency in the vegetation data sets. Considering the violations to the conditions of the global regression model and significant improvement in prediction results, researchers are encouraged to consider adopting SR methods for modeling vegetation parameters. Much of the previous studies have ignored these spatial effects, and some researchers (Dale and Fortin, 2002) suggest that majority of the past research and their findings may be re-examined for effects of SA and how ecological predictions would differ if SA effects were accounted in the data sets. We believe that augmenting ground-based hyperspectral data with coarser space-borne satellite data is an ideal approach to understand the spatial heterogeneity of the northern mixed prairie vegetation.

3.5 ACKNOWLEDGEMENT

Randy Bonin, Jesse Nielsen, Chunhua Zhang, and Yuhong He assisted with field work. Financial support for this research was provided by the University of Saskatchewan, Saskatchewan Ministry of Environment, and Nature Saskatchewan. Xulin Guo, Joseph Piwowar, and Greg McDermid provided instruments. Geoff Bohling and Eric Lamb provided statistical consultation. Satellite imagery were the courtesy of USGS and GeoBase.

3.6 REFERENCES

Anderson, G.P., Pukall, B., Allred, C.L., Jeong, L.S., Hoke, M., Chetwynd, J.H., Adler-Golden, S.M., Berk, A., Bernstein, L.S., Richtsmeier, S.C., Acharya, P.K., and Matthew, M.W. 1999. FLAASH and MODTRAN4: state-of-the-art atmospheric correction for hyperspectral data. *IEEE Proceedings of Aerospace Conference*, pp. 177-181, Snowmass at Aspen, CO, USA.

Anselin, L. 1988. *Spatial econometrics: Methods and models*, Dordrecht: Kluwer Academic Publishers.

Anselin, L., Syabri, I., and Kho, Y. 2005. GeoDa: An Introduction to Spatial Data Analysis. *Geographical Analysis*, 38(1): 5-22.

Asner, G. 1998. Biophysical and biochemical sources of variability in canopy reflectance. *Remote Sensing of Environment*, 64(3): 234-253.

Asner, G., Wessman, C., and Archer, S. 1998. Scale dependence of absorption of photosynthetically active radiation in terrestrial ecosystems. *Ecological Applications,* 8(4): 1003-1021.

Baret, F., and Guyot, G. 1991. Potentials and limits of vegetation indices for LAI and APAR assessment. *Remote Sensing of Environment*, 35(2-3): 161-173.

Baret, F., Jacquemoud, S., Guyot, G., and Leprieur, C. 1992. Modeled analysis of the biophysical nature of spectral shifts and comparison with information content of broad bands. *Remote Sensing of Environment*, 41(2-3): 133-142.

Beven, K.J., and Kirkby, M.J. 1979. A physically based, variable contributing area model of basin hydrology. *Hydrological Sciences Bulletin*, 24(1): 43-69.

Bonham, C.D., Mergen, D.E., and Montoya, S. 2004. Plant Cover Estimation: A contiguous Daubenmire frame. *Rangelands*, 26(1): 17-22.

Coupland, R.T. 1950. Ecology of mixed prairie in Canada. *Ecological Monographs*, 20(4): 271-315.

Coupland, R.T. 1961. A reconsideration of grassland classification in the Northern Great Plains of North America. *Journal of Ecology*, 49(1): 135-167.

Dale, M.R.T., and Fortin, M-J. 2002. Spatial autocorrelation and statistical tests in ecology. *Ecoscience*, 9(2): 162-167.

Daubenmire, R.F. 1959. A canopy-cover method of vegetational analysis. *Northwest Science*, 33: 43-46.

Davidson, A., and Csillag, F. 2001. The influence of vegetation index and spatial resolution on a two-date remote sensing-derived relation to C4 species coverage. *Remote Sensing of Environment*, 75(1): 138-151.

Fotheringham, A.S., Brunsdon, C., and Charlton, M.E. 2002. Geographically Weighted Regression: The Analysis of Spatially Varying Relationships, Chichester: Wiley.

Gao, B.C. 1996. NDWI - A normalized difference water index for remote sensing of vegetation liquid water from space. *Remote Sensing of Environment*, 58(3): 257-266.

Haboudane, D., Miller, J.R., Pattery, E., Zarco-Tejad, P.J., and Strachan, I.B. 2004. Hyperspectral vegetation indices and novel algorithms for predicting green LAI of crop canopies: modeling and validation in the context of precision agriculture. *Remote Sensing of Environment*, 90(3): 337-352.

Harms, V.L. 2006. *Annotated catalogue of Saskatchewan vascular plants*. 116 pp.

He, Y., Guo, X., and Wilmshurst, J.F. 2006. Studying mixed grassland ecosystems I: suitable hyperspectral vegetation indices. *Canadian Journal of Remote Sensing*, 32(2): 98-107.

Hurvich, C.M., Simonoff, J.S., and Tsai, C.L. 1998. Smoothing parameter selection in nonparametric regression using an improved Akaike information criterion, *Journal of Royal Statistical Society, Series B*, 60, 271-293.

Ji, L., and Peters, J.A. 2004. A spatial regression procedure for evaluating the relationship between AVHRR-NDVI and climate in the northern Great Plains. *Canadian Journal of Remote Sensing*, 25(2): 297-311.

Li, Z., and Guo, X. 2010. A suitable vegetation index for quantifying temporal variations of LAI in semi-arid mixed grassland. *Canadian Journal of Remote Sensing*. 36(6): 709-721.

Kerr, J., and Ostrovsky, M. 2003. From space to species: ecological applications for remote sensing. *Trends in Ecology & Evolution*, 18(6): 299-305.

Kercher, S.M., Frieswyk, C.B., and Zedler, J.B. 2003. Effects of sampling teams and estimation methods on the assessment of plant cover. *Journal of Vegetation Science*, 14(6): 899-906.

Klimeš, L. 2003. Scale-dependent variation in visual estimates of grassland plant cover. *Journal of Vegetation Science*, 14(6): 815-821.

Lefsky, M.A., Cohen, W.B., Parker, G.G., and Harding, D.J. 2002. Lidar remote sensing for ecosystem studies. *Bioscience*, 52(1): 19-30.

Michalsky, S.J., and Ellis, R.A. 1994. *Vegetation of Grasslands National Park*. DA Westworth and Associates, Calgary.

Rahman, A.F., Gamon, J.A., Sims, D.A., and Schmidts, M. 2003. Optimum pixel size for hyperspectral studies of ecosystem function in southern California chaparral and grassland. *Remote Sensing of Environment*, 84(2): 192-207.

Rangel, T.F., Diniz-Filho, J.A.F., and Bini, L.M. 2010. SAM: A comprehensive application for spatial analysis in Macroecology. *Ecography*, 33(1): 46-50.

Rosenberg, M.S., and Anderson, C.D. 2011. PASSaGE: Pattern Analysis, Spatial Statistics and Geographic Exegesis. *Methods in Ecology and Evolution*, 2(3): 229-232.

Rouse, J.W., Haas, R.H., Schell, J.A., and Deering, D.W. 1974. *Monitoring vegetation systems in the great plains with ERTS.* Proceedings, Third Earth Resources Technology Satellite-1 Symposium, Greenbelt: NASA SP-351: 301-317.

Small, C. 2004. The Landsat ETM+ spectral mixing space. *Remote Sensing of Environment*, 93(1-2): 1-17.

Sykes, J.M., Horrill, A.D., and Mountford, M.D. 1983. Use of visual cover assessments as quantitative estimators of some British woodland taxa. *Journal of Ecology*, 71: 437-450.

Tobler, W.R. 1970. A computer movie simulating urban growth in the Detroit region. *Economic Geography*, 46(2): 234-24.

Turner, W., Spector, S., Gardiner, N., Fladeland, M., Sterling, E., and Steininger, M. 2003. Remote sensing for biodiversity science and conservation. *Trends in Ecology and Evolution*, 18(6): 306-314.

Ustin, S.L., Roberts, D.A., Gamon, J.A., Asner, G.P., and Green, R.O. 2004. Using imaging spectroscopy to study ecosystem processes and properties. *Bioscience*, 54(6): 523-534.

Zhang, C., and Guo, X. 2007. Measuring biological heterogeneity in the northern mixed prairie: a remote sensing approach. *The Canadian Geographer*, 51(4): 462–474.

CHAPTER 4

VEGETATION MAPPING IN THE NORTHERN MIXED PRAIRIE USING SPECTRAL UNMIXING APPROACHES

ABSTRACT

Landscape-level vegetation mapping in semi-arid regions with sparse vegetative cover and high heterogeneity (spatial and spectral) pose challenges with 'mixed pixels' and non-linear mixing when traditional whole pixel-based image classification approaches are used on medium-resolution imagery. Spectral unmixing approaches such as the multiple endmember spectral mixture analysis (MESMA) have been suggested to overcome these limitations to a certain extent by improved modeling of sub-pixel variability.

In this study, MESMA was used for vegetation mapping with three multispectral satellite images: SPOT-5 (10 m), SPOT-4 (20 m), and Landsat-5 (30 m) using 97 optimal endmembers (em) representing green vegetation (GV), non-photosynthetic vegetation (NPV), and soil identified for the West Block of Grasslands National Park of Canada.

Results showed MESMA to be more effective than the simple SMA and produced improved vegetation maps compared to the whole pixel-based or object-oriented classifiers. MESMA successfully captured the spatial heterogeneity of vegetation and incorporated the spectral variability of land cover within the study area. By developing a comprehensive region-specific endmember library and identifying optimal endmembers, MESMA was useful in mapping the dominant vegetation types and estimating sub-pixel fractions of GV, NPV, and soil for the study area. The efficiency of spectral unmixing was found to be highly dependent on the identification of optimal endmembers, however not all endmembers were successfully modeled. Comparison of MESMA on the three images showed spectral resolution to be important over spatial resolution. 3-em models were found to be better suited than the 2-em models for modeling vegetation types in the study area, however the availability of only multispectral imagery limited the full unmixing capability. The methodology presented is more effectively used on hyperspectral imagery if it becomes available for the northern mixed prairie. Nevertheless, map

products derived from spectral unmixing are useful for monitoring and management of native and invasive vegetation, habitat- and fire-modeling, and effective park management.

4.1 INTRODUCTION

4.1.1 Northern mixed prairie

The northern mixed prairie is ecologically significant and represents one of the most endangered habitats on Earth (Gauthier et al., 2003). In addition to the land use-land cover changes due to human activities such as agriculture, grazing, and oil and mineral exploration, studies have pointed that the effects of climate change in these ecosystems can be significant (Li and Guo, 2014). Ecological and biodiversity conservation efforts in this ecoregion have suggested that the conservation and maintaining heterogeneity of the native prairie vegetation are the best ways to manage the population of the endangered fauna and to maintain the ecological integrity. Therefore, continued monitoring of these ecosystems is critical, and efficient monitoring warrants methods which are small-scale, long-term, continuous, and cost-effective (Fraser et al., 2009; Wulder et al., 2008, 2012).

Remote sensing (RS) has become increasingly popular in ecosystem studies due to its ability to provide multi-scalar, multi-spectral, and multi-temporal datasets at reasonable costs (Kerr and Ostrovsky, 2003; Cohen and Goward , 2004). Some popular methods of vegetation monitoring using RS are through image classification and mapping, change-detection, and image transformation (i.e. spectral vegetation indices (SVI). Among the vegetation mapping methods include field GPS-based mapping (Michalsky and Ellis, 1994), interpretation and mapping from aerial photographs (Penniket et al., 2004; Thorpe et al., 2005), and image classification of remotely sensed datasets using pixel-based, object-oriented, or neural network classifiers (He, 2009; Zhou, 2007). However, many challenges exist for the efficient RS and vegetation mapping of semi-arid ecosystems such as the northern mixed prairie (Davidson, 2001; Okin et al., 2001). The northern mixed prairie is characterized by sparse vegetative cover, high surface heterogeneity, and high spatial and spectral variability at relatively small spatial and temporal scales (Zhang, 2008). High amounts of standing dead vegetation (Yang and Guo, 2014; Xu et al., 2014) and bare soil add linear mixing to the reflected vegetation spectrum. Therefore, spectral mixture of endmembers due to multiple scattering by plant canopies and soil surfaces makes it

non-linear (Roberts et al., 1993; Ray and Murray, 1996). Similar to other arid environments, poor performance of SVI due to non-linear mixing and background noise from soil and litter has been reported in the northern mixed prairie.

4.1.2 Spectral unmixing approaches, background, and relevance

Traditional image classification methods (unsupervised, supervised, or object-oriented) are whole pixel-based and treat each image pixel as a homogenous land cover or as a single feature class (a 'pure pixel'). However, as the spatial heterogeneity of the land cover becomes complex (i.e. more spatially heterogeneous) or as the instantaneous field of view (IFOV) of the remote sensor becomes larger (i.e. towards coarser spatial scales), the surface reflectance spectra recorded by the remote sensor becomes 'non-linearly mixed' (see Somers et al., 2011) with the individual reflectance spectra of several land cover combined into a single image pixel (a 'mixed pixel'). Thus, the whole-pixel approaches become less efficient and classification methods such as the spectral mixture analysis (SMA) that can effectively incorporate sub-pixel spectral variability become more relevant.

The basic assumptions of SMA are: i) the landscape is composed of few endmembers that are distinctly spectrally variable; ii) the spectral signature of each endmember is constant and the entire remotely sensed scene (within the IFOV) can be modeled by using few spectrally-constant endmembers; and iii) the spectral signal of a pixel can be modeled as linear fractions of endmembers within the pixel. In SMA, the reflectance spectrum of a 'mixed pixel' is modeled as the sum of pure ground component endmember spectra, each weighted by the fraction of an endmember required to produce the mixture and multiplied by their fractional cover (Adams et al., 1993; Roberts et al., 1993; Somers et al., 2011). Hence, the reflectance of an image pixel (ρ'_λ) can be written as:

$$\rho'_\lambda = \sum_{i=1}^{N} f_i * \rho_{i\lambda} + \varepsilon_\lambda \qquad (4.1)$$

where $\rho_{i\lambda}$ is the spectral reflectance of an endmember (i) for a specific band (λ), N is the number of endmembers, endmember fraction (f_i), and ε_λ is the residual error (Dennison and Roberts, 2003). The fit of an endmember model to an image pixel for M bands can be estimated using

model residuals (ε_λ) or the root mean square error (RMSE; Roberts et al., 1998). RMSE is calculated as:

$$RMSE = \sqrt{\frac{\sum_{\lambda=1}^{M} (\varepsilon_\lambda)^2}{M}} \quad (4.2)$$

SMA has advantage over the whole pixel-based approaches as it provides physically meaningful measures of land cover by accounting for sub-pixel mixing. Yet, SMA fails to account for the pixel-scale variability in spectral dimensionality, spectral degeneracy between materials and the variation in the natural spectral response of most materials (VIPER 1.5 Manual). SMA is limited as it models every image pixel using only a fixed number of endmembers and cannot fully account for the spectral variability of endmembers. As a result, simple SMA under-utilizes the potential of most RS datasets for discriminating surface materials while at the same time producing fractional errors due to the incorrect type or number of endmembers used to unmix a specific image pixel (VIPER 1.5 Manual, 2007). Inability to account for non-linear mixing is another acknowledged limitation of SMA (Adams et al., 1993). Non-linear mixing is significant in semi-arid environments, however in most cases the effects of multiple scattering are assumed to be negligible.

Multiple endmember spectral mixture analysis (MESMA) is an improvement over simple SMA and allows the number and types of endmembers to vary on a per-pixel basis (Roberts et al., 1998). MESMA overcomes the limitations of SMA by testing multiple unmixing models for each image pixel that provide the best-fit by requiring the model to meet specified minimum fit, fraction and residual constraints. MESMA is typically implemented by developing spectral libraries (field-collected or image-derived) which are used to unmix an image using every possible combination of endmembers. Using MESMA, materials can be mapped across an image while minimizing pixel-scale fraction errors by selecting the best-fit model for each pixel. The endmember fractions from SMA are typically interpreted as ground component fractions, and studies have shown that the quantitative comparisons of ground cover to unmixed fractions to be highly accurate over a diverse number of surfaces (Elmore et al., 2000; Painter et al., 2003; Powell et al., 2007). Further, SMA fractions have been suggested to be more robust than the traditional SVI and also strongly linked to the plant biophysical parameters (Dennison and

Roberts, 2003a). Applications of MESMA include improved LAI estimation in boreal forests (Sonnentag et al., 2007) and mapping of plant species (Roberts et al., 1998; Dennison and Roberts 2003a,b; Roberts et al., 2003), invasive plant species (Ustin, 2010), soil in arid environments (Okin et al., 2001), landforms (Ballantine et al., 2005), fire temperature (Dennison et al., 2006), snow cover (Painter et al., 1998; 2003), and urban environments (Rashed et al., 2003; Powell et al., 2007; Franke, 2010).

4.1.3 Research objectives

SMA is usually performed using satellite or airborne hyperspectral imagery, and majority of the previous research have employed MESMA on hyperspectral imagery such as AVIRIS or HyMap. These data sets are often difficult to acquire due to financial or logistical constraints or simply unavailable for many study sites, including the northern mixed prairie. New and archived multispectral satellite imagery such as Landsat and SPOT are readily available at lower costs and at good temporal resolutions and therefore present opportunities for ecologists and decision-makers to utilize them for small-scale, long-term, continuous, and cost-effective mapping and monitoring purposes. Few studies (Song, 2005; Powell, 2006, 2007; Quintano et al., 2013) have tested the feasibility of MESMA on medium-resolution multispectral satellite imagery. Hence, this study was interested in identifying the feasibility of applying MESMA for vegetation mapping in the northern mixed prairie. Also, comparison of spatial scale of RS data and its effect on efficiency of spectral unmixing have not been explored in any of the previous studies. Therefore, the objectives of this study were:

(i) To explore the potential of spectral unmixing strategies for identifying and mapping the dominant vegetation types in the northern mixed prairie and for estimating their fractional endmember abundances;

(ii) To identify and select the optimum endmembers for landscape-level vegetation mapping;

(iii)To investigate the role of spatial scale of RS data in the performance of spectral unmxing for vegetation mapping.

4.2 MATERIALS AND METHODS

4.2.1 Study area

Field data for this study was collected from the West Block of Grasslands National Park of Canada (GNPC; +49º12' and -107º24') in Southern Saskatchewan (Fig. 4.1). GNPC, situated in the northern mixed prairie region, was established in 1984 to conserve the remnant native mixed prairie in Canada and with a mandate for long-term ecological monitoring and research. The GNPC has been protected from human disturbances for over 25 years, however grazing by bison (introduced) and cattle and prescribed burning are practiced in the region to maintain the vegetation heterogeneity. The region experiences a semi-arid climate with mean monthly temperature ranging from -12.4˚C to 18.3˚C and low precipitation of 150 to 325 mm (Environment Canada, 2003). The region has an average elevation of ~860 m, high landscape diversity, with chernozem as the dominant soil order (Saskatchewan Institute of Pedology, 1992).

Two types of vegetation, cool- and warm-season, occur in the northern mixed prairie. The proportion of the cool-season type is higher, however this is dependent on climate, topography, and soil factors (Singh et al., 1983). The West Block of GNPC is mainly dominated by upland, sloped, and lowland grasslands in addition to the shrub, eroded, and disturbed range types (Blood and Ledingham, 1986). The major plant communities include *Stipa-Bouteloua, Bouteloua-Stipa,* and *Stipa-Agropyron* (Coupland, 1950). Shrubs are mostly seen along the Frenchman River valley areas with higher soil moisture (Looman and Best, 1987) and coarse textured soils (Coupland, 1950). Plant growing season is relatively short (~170 days) (Csillag et al., 2001) and the peak plant growth occurs between June and July (Zhang and Guo, 2007; Zhang, 2008).

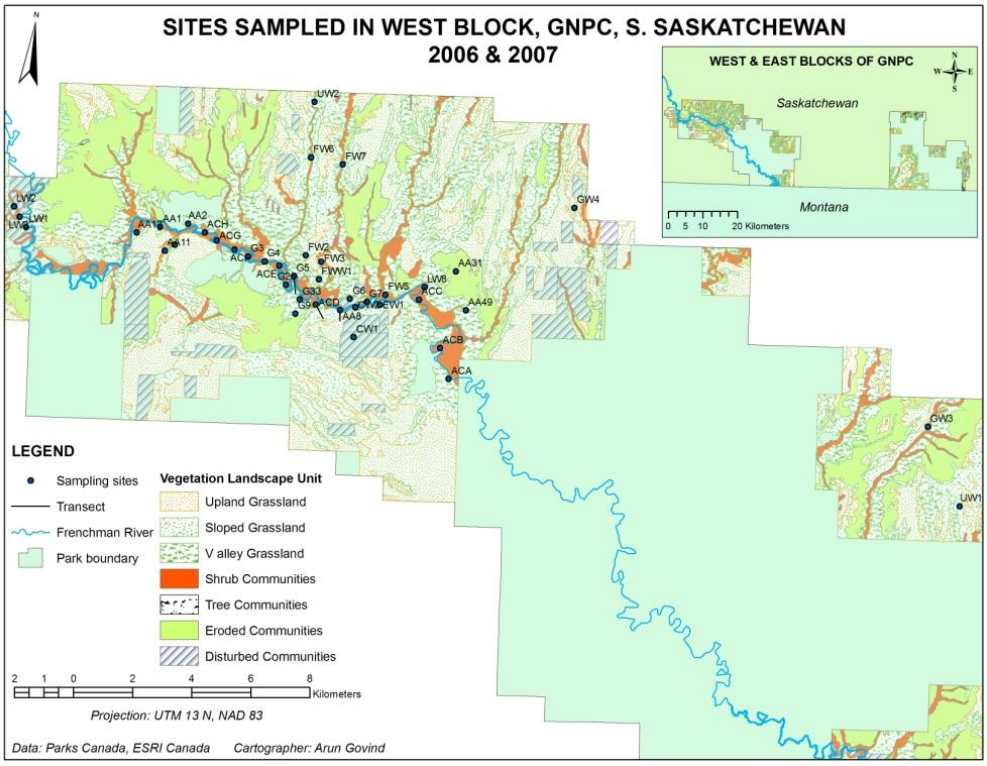

Fig. 4.1 Map showing the study area: West Block of Grasslands National Park of Canada, sampling locations and the vegetation landscape units (VLU; Michalsky and Ellis, 1994).

4.2.2 Sampling locations and methods

The field sampling scheme was based on the vegetation inventory data sets of Michalsky and Ellis (1994), Thorpe et al. (2005), Penniket et al. (2005), and a soil cover map (Saskatchewan Institute of Pedology, 1992). 41 sites were sampled in the West Block of GNPC (Fig. 4.1) in June 2006 and July 2007 corresponding to the peak vegetative growth period in the region. These sites represented a variety of vegetation landscape units (VLU) and topographic groups (Michalsky and Ellis, 1994). At each site, one cross-shaped plot (1 ha size) was randomly set up by running transects of 100 m each in the north-south and east-west directions. Vegetation data and plant biophysical data were collected at 10 m sampling intervals along each of the 100 m plot-transect using the methods described below. Additionally, geographic coordinates and elevation information were collected using a GPS at each sampling point.

Ground estimates of vegetation

Vegetation cover was estimated at each sampling plot using a visual method where surface cover within a quadrat of 50 cm*50 cm was classified into seven groups: graminoids, shrubs, forbs, cacti, lichen and moss, standing dead, rock, and bare ground. The individual cover values were estimated in percentages and summed to obtain the total cover estimate for a single vegetation layer (maximum 100% cover). The total cover was further separated into green cover and standing dead. Plants and their species composition occuring dominantly within a quadrat were visually identified and recorded.

Leaf area index (LAI) was estimated using a LiCOR LAI-2000 Plant Canopy Analyzer in 2006 and an Accupar® (Decagon, Lincoln, Nebraska) in 2007. Both these instruments work on the same principle and measure the amount of photosynthetically active radiation (PAR) available above and below the canopy to estimate LAI. LAI was measured with the LAI-2000 by averaging four LAI values at each quadrat corner and using the shadow method (He et al., 2007). Aboveground fresh biomass was estimated by clipping the aboveground vegetation at the ground-level within a quadrat of size 50 cm*20 cm (a GNPC stipulation). The clipped vegetation was placed in air-sealed bags and weighed in the field to estimate the weight of fresh (wet) biomass.

Field spectral measurements and processing

Spectral reflectance measurements were collected at 10 m sampling intervals using a full range ASD® FieldSpec FR Pro spectroradiometer (Analytical Spectral Devices Inc., Boulder, Colorado) at a spectral resolution of 3 nm in the 350-1000 nm and 10 nm in the 1000-2500 nm region. Spectra were collected perpendicular to the target (quadrat or plant canopy) at a height of 1 m and with a 25^{o} field of view. All spectral measurements were calibrated to apparent reflectance using a Spectralon reference panel (Labsphere, New Hampshire). Spectra were collected within ±2 hours of solar noon and under low wind and stable atmospheric conditions. Additionally, reference (field) endmembers for green vegetation (GV), non-photosynthetic vegetation (NPV), and soil classes were collected at all possible site locations to be used for developing spectral libraries to use in the spectral unmixing (see section 4.2.3). As the purpose of the study was primarily for mapping vegetation, GV endmember spectra were collected

specifically for the major vegetation communities in the study area. It was ensured for reference GV endmembers that their dominant cover was >80% within the quadrat (see Fig. 4.2). In addition, photoplots for the quadrats were taken vertically that ensured that the post-processed spectra were allotted to the correct endmember spectral library group. Few vegetation endmembers (viz. lichens, cacti, moss) were excluded as the collection of their pure spectra is impossible in the field because they appear in sparse cover, multiple layers, or inter-mixed with other vegetation or soil or litter and produce mixed spectra. Nevertheless, these vegetation types are significant to the ecology of the area and provide significant challenges to their endmember collection in the field. Non-linear mixing and mixed pixels are an issue with these endmembers.

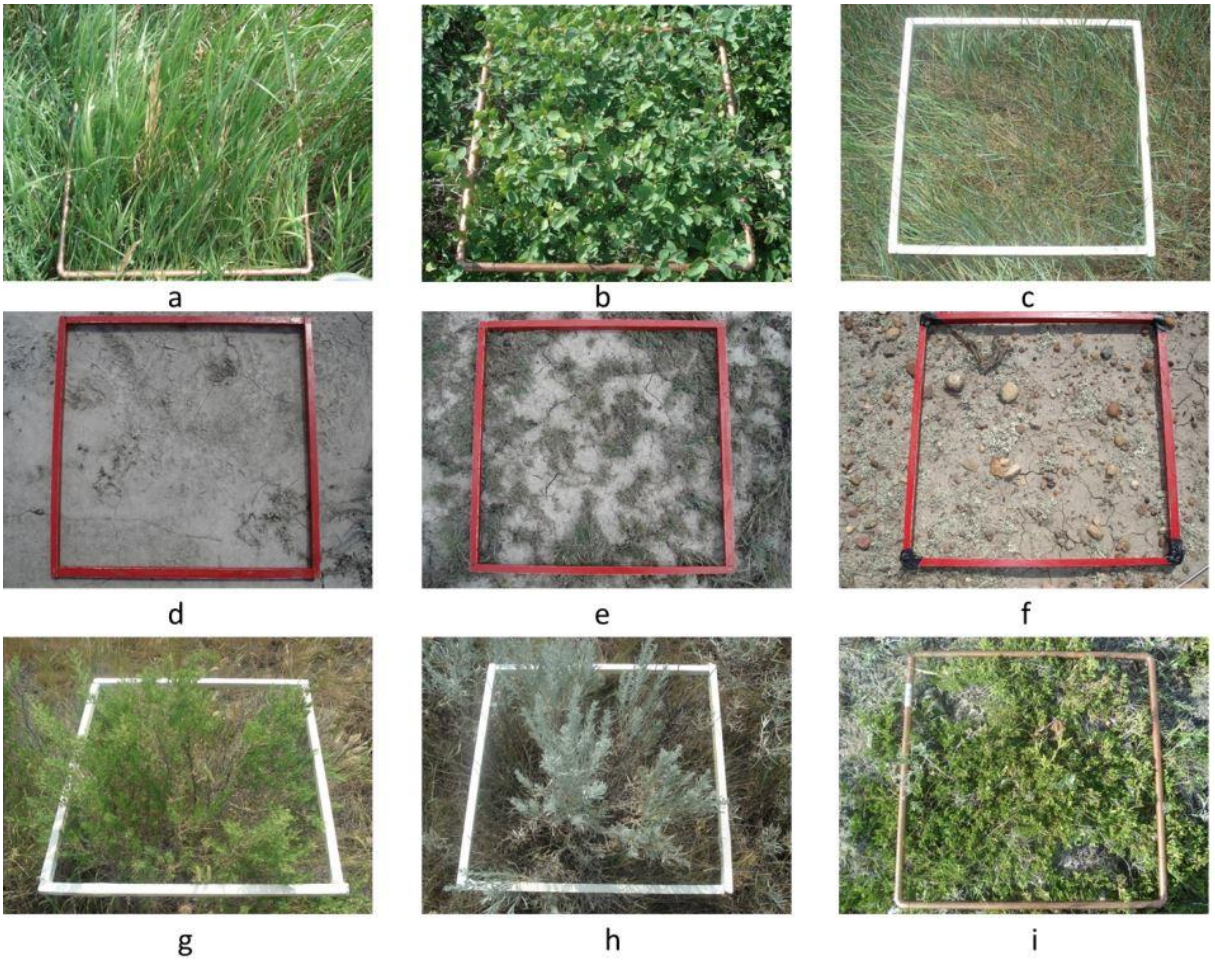

Fig. 4.2 Examples of locations from where reference endmembers were collected: green vegetation endmembers (a-c, g-i), soil endmembers (d-f). Note that the quadrats were placed subsequent to spectra collection.

To understand the spectral differences among the land cover classes, spectral reflectance curves were plotted and analyzed in SAMS© (Spectra Analysis and Management System, Univ. of California, Davis, *http://sams.projects.atlas.ca.gov/*) and ViewSpec Pro (Analytical Spectral Devices, Boulder, CO, USA) software. The primary water absorption regions ~1400 and ~1900 nm were removed from the spectra before spectral analysis.

4.2.3 Satellite imagery and pre-processing

Three cloud-free satellite images of spatial scales of 10, 20 and 30 m (Table 4.1) and corresponding with the peak vegetative growth period were acquired for the GNPC area. The images were individually georeferenced using a high-resolution SPOT-5 HRG1 PAN image (5 m panchromatic; *www.geobase.ca*), orthorectified (UTM 13N-NAD83) and resampled using the nearest neighbor scheme to their native pixel sizes. Further the images were co-registered and transformed from raw digital numbers to surface reflectance values using the Moderate Resolution Transmittance (MODTRAN4) based Fast Line-of-sight Atmospheric Analysis of Spectral Hypercubes (FLAASH; Anderson et al., 1999) atmospheric correction method. All image bands except the Landsat thermal band were used in the atmospheric correction and subsequent image processing. Finally, the images were clipped to the park holding boundary of the West Block of the GNPC (Fig. 4.1). All satellite image processing was completed in ENVI 4.8 (ITTVIS, Boulder, CO, USA).

Table 4.1 Details of the satellite images used in the study.

Satellite & sensor	**Date of acquisition**	**Pixel size (m)**	**Bands used *(names and numbers)****	**Data source**
SPOT-5 HRG1	27 July 2006	10	G,R,NIR,SWIR (1234)	*www.geobase.ca*
SPOT-4 HRVIR1	28 June 2006	20	G,R,NIR,SWIR (1234)	*www.geobase.ca*
Landsat-5 TM	17 July 2006	30	B,G,R,NIR,MIR,MIR (123457)	*www.usgs.gov*

* B - Blue, G - Green, R - Red, NIR - Near Infrared, SWIR – Shortwave Infrared, MIR - Mid Infrared. Band 6 (Thermal) of Landsat-5 TM image was excluded.

The images were individually unmixed to estimate fractions of GV, NPV, and soil in the study area. The images of varying scales were used to understand the effect of spatial scale of RS data on the efficiency of spectral unmixing. MESMA was implemented using VIPER Tools

(*www.vipertools.org*), an open-source add-on for ENVI, which permits the creation and management of spectral libraries and their metadata, selection and optimization of endmembers, building unmixing models, and provides methods and constraints for spectral unmixing (VIPER 1.5 Manual).

4.2.4 Development of region-specific spectral libraries

To unmix the satellite images, region-specific spectral libraries were developed that are comprehensive and yet elaborate enough to effectively capture the spectral variability of the land cover (surface materials) in the study area. Reference (field) endmember spectra were imported to ENVI and organized using a hierarchical scheme into three spectral libraries: GV, NPV and soil (Table 4.2). Acronyms used for the GV land cover classes are a combination of the first two letters of their generic and species name of the vegetation, except for NPV and soil. The source of plant scientific names is Harms (2006). The GV library included spectral reflectance of major species of native prairie grasses, shrubs, forbs, and exotic grasses (smooth brome and crested wheat). NPV included dead grass, senesced grass, and dead branches or burnt stems of shrubs. The soil library consisted of spectra for bare soil, out-wash plains, and exposed rock or gravel. Therefore, the spectral libraries compiled were representative of the surface materials (cover) seen at the sampling sites.

As the field endmembers do not scale-up to the reflectance spectra collected by the satellite sensor (Powell, 2006) or contain the same systematic errors from atmospheric correction as the image (Settle and Drake, 1993), a few image endmembers were additionally identified from the Landsat-5 TM image using the Pixel Purity Index (PPI; Boardman et al., 1995) algorithm. To reduce the spectral data dimensionality and to estimate the inherent noise in the satellite image, a minimum noise fraction (MNF; Green et al., 1998) procedure was performed which resulted in only the first three MNF fractions showing high eigenvalues and high spatial coherency. These first three MNF fractions were subsequently used for PPI mapping using a threshold level of 0.02 and 35,000 iterations to identify the pure endmembers. The PPI threshold level was estimated by gradually increasing the numbers of iterations until no more spectrally pure pixels (those with the highest PPI values) were obtained. Using the n-D Visualizer tool in ENVI, the MNF data was rotated interactively and the image endmembers were identified in the feature space. The image endmembers were developed by exporting mean spectra from the regions of interest (ROI) and

compared with the reference endmembers in the spectral library. Finally, all spectral libraries (field-collected or image-derived) were separately convolved to the spectral regions of the SPOT-5 HRG, SPOT-4 HRVIR, and Landsat-5 TM sensors.

Table 4.2 97 optimal endmembers identified to represent the land cover classes in the study area.

No.	Class	Sub-class	Land cover class	Scientific name	Acronym	No. of spectra
1	GV	Grass	Needle and thread	*Hesperostipa comata*	stco	3
2			Blue grama	*Bouteloua gracilis*	bogr	1
3			Slender wheat grass	*Agropyron trachycaulum*	agtr	2
4			Western wheat grass	*Pascopyrum smithii*	agsm	4
5			Northern wheat grass	*Elymus lanceolatus*	agda	3
6			June grass	*Koeleria macrantha*	kocr	0
7			Kentucky blue grass	*Poa pratensis*	popr	1
8			Sand drop seed	*Sporobolus cryptandrus*	spcr	2
9			Nuttal's alkali grass	*Puccinellia nuttalliana*	punu	2
10			Bluberg's sand grass	*Poa sandbergii*	posa	0
11			Prairie muhly	*Muhlenbergia cuspidata*	mucu	4
12			Smooth brome*	*Bromus inermis*	brin	3
13			Crested wheat grass*	*Agropyron cristatum*	agcr	3
14		Shrub	Buckbrush	*Symphoricarpos occidentalis*	syoc	6
15			Sagebrush	*Artemisia cana*	arca	4
16			Willow	*Salix canadensis*	saca	4
17			Broad willow	*Salix* sp.	sasp	3
18			Rabbit brush	*Chrysothamnus nauseosus*	chna	3
19			Winter fat	*Krascheninnikovia lanata*	eula	2
20			Thorny buffaloberry	*Shepherdia argentea*	shar	6
21			Canada buffaloberry	*Sheperdia canadensis*	cash	2
22			Goose berry	*Ribes oxycanthoides*	riox	3
23			Wood rose	*Rosa woodsii*	rowo	5
24			Creeping juniper	*Juniperus horizontalis*	juho	2
25		Forb	Pasture sage	*Artemisia frigida*	arfr	4
26			Prairie sage	*Artemisia ludoviciana*	arlu	3
29			Forb	Types of minor forbs	forb	7
35		Sedge	Sedge	*Carex* sp.	sedge	2
37	NPV	Grass	Senesced/dead grass	Standing dead (grass)	dgrass	1
38		Shrub	Dead stem	Standing dead (shrub)	dshrub	3
39		Shrub	Burnt stem	Result of natural/prescribed fire	burnt	1
40	Soil		Bare soil	Bad lands	bsoil	2
41			Exposed soil	Result of soil erosion	esoil	3
42			Soil mixture	Gravel, rock, soil mixture	msoil	2

4.2.5 Endmember selection and optimization

The identification and selection of optimal (type and number) endmembers is a critical step for successful and efficient unmixing (Tompkins et al., 1997; Somers et al., 2011). The use of a high number of endmembers for image unmixing makes MESMA computationally demanding (Halligan, 2002) and also increases the confusion among the land cover types. VIPER Tools provides three endmember selection metrics: Count Based Endmember Selection (CoB; Roberts et al., 2003), Endmember Average RMSE (EAR; Dennison and Roberts, 2003), and Minimum Average Spectral Angle (MASA; Dennison et al., 2004) for identifying and selecting the optimum or representative endmembers within each class. For CoB metric, the selected optimal endmember is the one that models the highest number of endmembers within their class. CoB is used to rank endmembers based on maximizing the models selected within the correct class while minimizing confusion with other classes (Clark, 2005). For EAR, endmembers are selected that produce the lowest RMSE within a class (Dennison and Roberts, 2003), and with MASA those endmembers are selected that have the lowest intra-class average spectral angle (Dennison et al., 2004).

Though initially a total of 1150 endmember spectra were compiled, the number of optimal endmembers was subsequently reduced to 85 GV, 5 NPV, and 7 soil endmembers (Table 4.2) by using a combination of EAR, MASA, and CoB metrics to make MESMA computationally viable and yet attain physically meaningful results. The optimal GV, NPV, and soil endmembers with the best desirable selection metric value were further used in VIPER Tools for creating 2- and 3-endmember models (Table 4.3) and for unmixing each satellite image.

4.2.6 Endmember models and spectral unmixing

Powell et al. (2006) suggested that 2-endmember (2-em) models are best for modeling natural ecosystems, 3-em models for disturbed landscapes, and 4-em models for urban areas. 2-em models were created as combinations of a bright endmember (GV, NPV or soil) and shade, and are limited as they model only a single class within a pixel. Considering the large amount of NPV (dead or senesced vegetation and litter) and exposed soil in the study area, 3-em models (Table 4.3) were developed that would permit modeling more than one class (GV or NPV or soil) within a pixel (Okin, 2001).Therefore, MESMA was initially run with the simpler (2-em) models to understand the spatial distribution and trends of GV, NPV and soil classes in the study

area, and subsequently the successful endmembers were used to develop more complex (3-em) models.

Table 4.3 Endmember models tested (type, combination, number, and spectra used). GV indicates green vegetation endmembers for grass, shrubs, forbs, and sedges. NV indicates non-vegetation endmembers (dead or senesced plants, exposed or bare soil). Note: Only the endmembers found successful from the 2-em unmixing were further used for the 3-em model development and 3-em unmixing.

Model type	**Model combination tested**	**No. of models created (SPOT-5, SPOT-4, Landsat-5)**	**No. of spectra used (GV, NPV, soil)**
2-em	GV, NPV, soil + shade	97, 97, 97	85, 5, 7
3-em	GV + NV + shade	360, 517, 266	Depends on successful 2-em

VIPER Tools provides options to constrain the unmixing based on fractions, RMSE, or residuals. Thus a partially constrained fit metric was adopted with a minimum allowable fraction of -0.5, maximum allowable fraction of 1.05, and maximum RMSE of 0.025 (Halligan, 2002; Roberts et al., 2003). From all the endmember models created, VIPER Tools selects the single best endmember model with the lowest RMSE for each image pixel and assigns the pixel class to the endmember with the highest fraction. The image pixel was unmodeled if the specified model constraints were not met. The outputs of MESMA are a spectral unmixing image which contains endmember fractions, shade fraction, RMSE of the unmixing model, and a metadata with the list of possible models, the endmembers comprising each model, and the proportion of the image modeled by each successful unmixing model.

4.3 RESULTS AND DISCUSSION

The field sampling plots (n = 686) were grouped on the basis of their elevation into three topographic groups: upland, sloped land, and lowland. Detailed description of the vegetation characteristics and the spatial variability of the plant biophysical properties observed at the sampling sites can be found in Chapter 2. The mean total plant cover, green-and standing dead cover, aboveground biomass, and LAI for the three topographic groups are summarized in Table 4.4.

Table 4.4 Average total cover, LAI, and aboveground biomas at three topographic groups.

Topographic group	Elevation (m)	Green cover (%)	Standing dead cover (%)	Aboveground biomass (g/m^2)	LAI
Upland	913.2	49.50	7.25	119.80	0.695
Sloped land	818.7	65.67	6.92	158.96	1.291
Lowland	773.5	60.12	9.74	177.95	2.263

Generally, higher plant cover, LAI, and aboveground biomass were seen in areas of lower elevation and higher soil moisture content (Table 4.4), i.e. along the Frenchman River Valley (Fig. 4.1). This indicates the presence of the spatial variability of vegetation characteristics and plant biophysical properties along topographic and moisture gradients. The major vegetation in the uplands included grasses such as blue grama (*Bouteloua gracilis*), needle and thread (*Stipa comata*), june grass (*Koeleria macrantha*), western wheat grass (*Pascopyrum smithii*), and northern wheat grass (*Elymus lanceolatus*). The lowland riparian sites were dominated by tall- and low-shrubs such as buckbrush (*Symphoricarpos occidentalis*), buffaloberry (*Shepherdia argentea*), sagebrush (*Artemisia cana*), and willows (Salix sp.), and high cover of exotic grasses such as crested wheat grass (*Agropyron cristatum*) and smooth brome (*Bromus inermis*). Plant names adapted from Harms (2006). Uplands were characterized by low cover of native prairie grasses such as western wheat, blue grama, needle and thread. Similar vegetation distribution trends were observed in the standard false color composite (FCC) image where bright red tones of dense vegetation are along the river valley, light red tones of sparser vegetation appear in the uplands, and very bright tones of soil appear in the badlands.

4.3.1 Spectral characteristics of reference endmembers (GV, NPV, and soil)

This is the first study in the northern mixed prairie to explore the spectral reflectance characteristics of the major vegetation types, especially the lowland types. Reference (field) endmember spectra compiled for GV, NPV, and soil (Table 4.2) were averaged (except cases where only one spectra was available) to obtain mean spectral reflectance for a particular land cover class (Table 4.2). The mean spectra were visually analyzed for differences in their spectral reflectance across the 350-2500 nm region (Fig. 4.3). The different GV, NPV, and soil endmembers show varying spectral response in the visible (400-700 nm) and the near-infrared (NIR; 800-1400 nm) region corresponding to differences in plant pigment and water content.

Generally, the shrubs showed higher reflectance than the grasses (inter-specific variability), which may be attributed to the higher content of green chlorophyll pigments or higher amount of moisture in the canopy (Ollinger, 2010). Spectral responses were different even for the same plant species (intra-specific variability) growing at different locations, and this might be due to the influence of background materials, edaphic factors (soil: moisture, nutrients, or type), canopy architecture, or varying illumination conditions. Similar spectral reflectance trends were seen for the native prairie grasses: *Pascopyrum smithii* (agsm), *Elymus lanceolatus* (agda), *Bouteloua gracilis* (bogr), and *Hesperostipa comata* (stco). The spectral response for *Agropyron trachycaulum* was very similar to these grasses, but overall showed higher reflectance across all the spectral regions. These similarities in spectral trends might be a reason for the confusion among these cover types during image modeling and unmixing. These plants are of low cover and therefore the background noise from soil and litter materials might be adding to the spectral reflectance and preventing their spectral discrimination.

Lichens or moss are often seen inter-mixed with native prairie grasses or do not appear in homogeneous stands to permit *in-situ* collection of spectrally-pure reference endmembers. Therefore, even if endmember spectra were obtained from other sources (viz. laboratory-based spectroscopy or publically available spectral libraries such as the USGS, JPL), these may not be adequately captured and will appear mixed with other materials in image pixels of 10, 20, or 30 m. Some of the sub-dominant vegetation types such as forbs and sedges were not effective in the spectral unmixing.

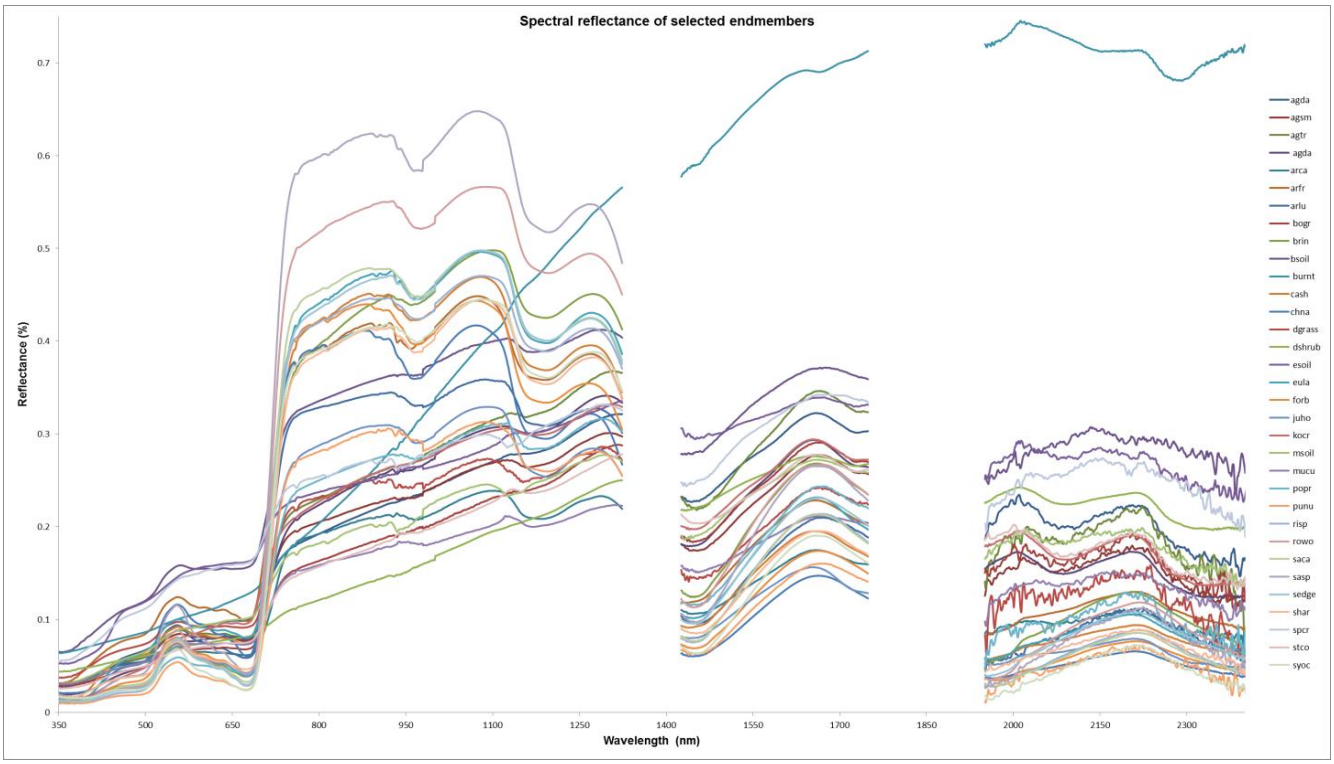

Fig. 4.3 Average spectral reflectance of optimal GV, NPV, and soil endmembers (Table 4.2) used for image unmixing. Water absorption regions (~1400 and ~1900 nm) were removed from the full range (350-2500 nm) spectra. Acronyms of land cover classes: agcr (*Agropyron cristatum*), agda (*Elymus lanceolatus*), agsm (*Pascopyrum smithii*), agtr (*Agropyron trachycaulum*), arca (*Artemisia cana*), arfr (*Artemisia frigida*), arlu (*Artemisia ludoviciana*), bogr (*Bouteloua gracilis*), brin (*Bromus inermis*), bsoil (bare soil), burnt (fire burnt plant), cash (*Sheperdia canadensis*), chna (*Chrysothamnus nauseosus*), dgrass (dead grass), dshrub (dead shrub), esoil (eroded soil), eula (*Krascheninnikovia lanata*), forb (types of minor forbs), juho (Juniperus horizontalis), kocr (*Koeleria macrantha*), msoil (soil-rock mix), mucu (*Muhlenbergia cuspidata*), popr (*Poa pratensis*), posa (*Poa sandbergii*), punu (*Puccinellia nuttalliana*), riox (*Ribes oxycanthoides*), rowo (*Rosa woodsii*), saca (*Salix canadensis*), sasp (*Salix* sp.), sedge (*Carex* sp.), shar (*Shepherdia argentea*), spcr (*Sporobolus cryptandrus*), stco (*Hesperostipa comata*), syoc (Symphoricarpos *occidentalis*).

4.3.2 Estimation of endmember fractions and mapping of vegetation types

MESMA was successful in identifying and mapping the dominant vegetation types and estimating the endmember fractions of GV, NPV, and soil in the study area in contrast to the very broad land covers mapped by Zhou (2007) and He (2009). Fig. 4.4 shows the MESMA classification maps using 2-em unmixing on the SPOT-5 (4.4a), SPOT-4 (4.4b), and Landsat-5 (4.4c) images. Note that classification maps from 3-em unmixing are not shown. The classification images, even with 2-em models, showed that the extent and the spatial variability

of the vegetation types clearly follows the distribution trends suggested by Michalsky and Ellis (1994) and He (2008). Visual comparison of the MESMA classification images with the vegetation maps from Michalsky and Ellis (1994) show that Michalsky and Ellis (1994) over-estimated some of the vegetation types, especially the lowland riparian vegetation. This might be due to observer bias or over-estimation due to human error. It might also be due to the temporal change to these vegetation types; however this needs to be explored further. Generally the lowland grassland, shrubs and soil were mapped well using MESMA, however the upland and sloped grasslands were mapped with some confusion or misclassification. It might be that vegetation cover is very sparse in the uplands and the sloped lands, i.e. the dominant graminoid vegetation in these areas account for an average cover of only <30%. There was also high cover of standing dead, lichens, litter or bare ground (>15%). Therefore, the specific GV reference endmember spectra collected for these upland or sloped vegetation types are possibly contaminated by the reflectance from background soil and litter.

Table 4.5 shows the model type and model combination tested for the three images using 2- and 3-em models, number of successful endmember models, and the number of unmixing models required to model 99.9% of the image.

Table 4.5 Number of successful endmember models and the number of unmixing models required to model 99.9% of the image using 2- and 3-em models.

Model type	**Model combination tested**	**No. of successful models**			**No. of models required to model 99.9% of the image**		
		SPOT-5	**SPOT-4**	**Landsat-5**	**SPOT-5**	**SPOT-4**	**Landsat-5**
2-em	GV, NPV, soil + shade	69	76	70	42	58	45
3-em	GV + NV + shade	289	512	262	189	458	221

Unmixing with 2-endmember models

In Table 4.5, it is seen that of the 97 2-em unmixing models tested (Table 3), the number of successful models on each of the three images were: 69 (SPOT-5), 76 (SPOT-4), and 70 (Landsat-5), respectively. However, it is seen that lower numbers of models were required to model 99.9% of the images: 42 (SPOT-5), 58 (SPOT-4), and 45 (Landsat-5). The images were modeled with reasonable accuracy and the vegetation types were identified along the

topographical and moisture gradients; the riparian shrubs and invasive grasses were mapped along the Frenchman River Valley and the sparser native grasses were identified in the uplands. Thus, the optimal endmembers included in the spectral library were effective in capturing the spectral diversity of the surface materials in the study area. Few of the unmodeled pixels were water (the Frenchman River). High residuals were seen for the very bright pixels, i.e. the bad lands and areas with very dense vegetation.

Unmixing with the 2-em models showed that the native prairie grasses (*Elymus lanceolatus*, *Pascopyrum smithii*, *Agropyron trachycaulum*, and *Stipa comata*), shrubs (*Artemisia cana*) and forbs (*Artemisia frigida*) as the dominant land cover (>80 % of the images); however this is slightly over-estimated (Fig. 5). This result agrees with Okin et al. (2001) who found that MESMA overestimates vegetation in semi-arid environments with sparse vegetative cover. Also taking into consideration that the soil or NPV classes are often seen mixed with GV, these estimates from 2-em unmixing are reasonable. Soil (esoil) was mapped as a dominant class only in the Landsat-5 image (5.5%), however the SPOT images did not successfully map them. However, analysis of the SPOT images showed that the badlands were actually classified (<1%, hence not shown) as exposed soil (esoil), bare soil (bsoil), or soil mixture (msoil). Sagebrush and smooth brome were the other types of vegetation that were identified. Shrubs commonly seen at field sites such as thorny buffalo berry and buckbrush were not modeled and this might be because these plants are often seen as isolated stands or occur in patches less than 10 m size and hence not resolved within an image pixel.

As the same set of endmembers were used to model the three satellite images, the difference in the number of successful 2-em models between the three images (Table 4.5) may be attributed to the spectral variability arising due to plant phenology in the study area (Li and Guo, 2012) or due to the spectral resolution of the remote sensors. The Landsat-5 image was acquired in mid-July and the SPOT-5 image in late-July by which time most of the native grasses (except the invasive species which are perennial) should have begun their senescence stage. The Landsat-5 image, even with coarser spatial resolution, used slightly higher number of 2-em models, and this might be due to the better spectral resolution of the Landsat sensor when compared to that of the SPOT. The effect of plant phenology on endmember selection and its impact on vegetation mapping has been discussed by Dennison and Roberts (2003b).

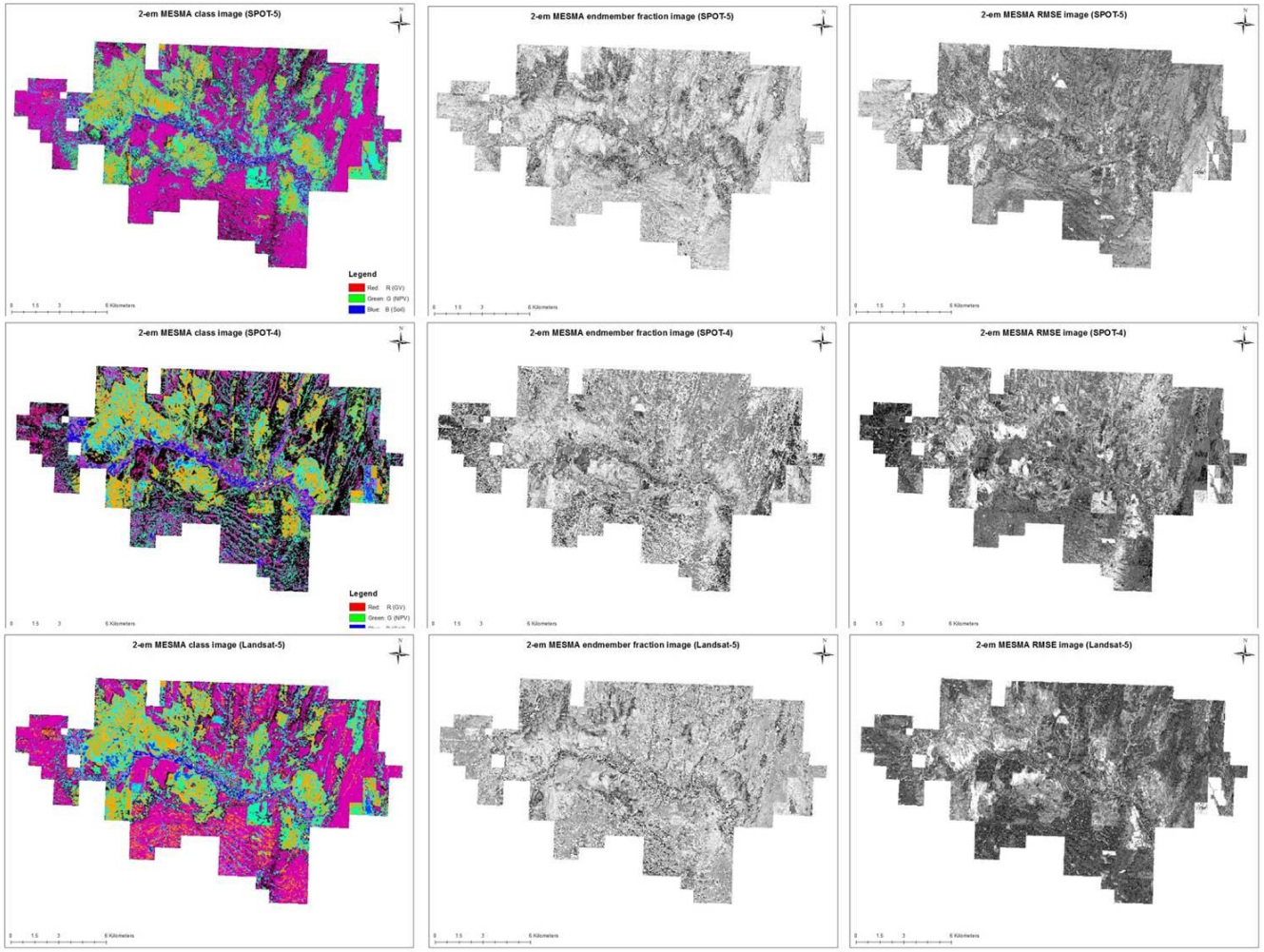

Fig. 4.4 Image outputs from MESMA: Class image (left column), endmember fraction (middle column), RMSE (right column) from 2-em unmixing of SPOT-5 (4.4a), SPOT-4 (4.4b), and Landsat-5 (4.4c) images. In the RMSE image, darker pixels mean lower errors and brighter pixels mean higher error.

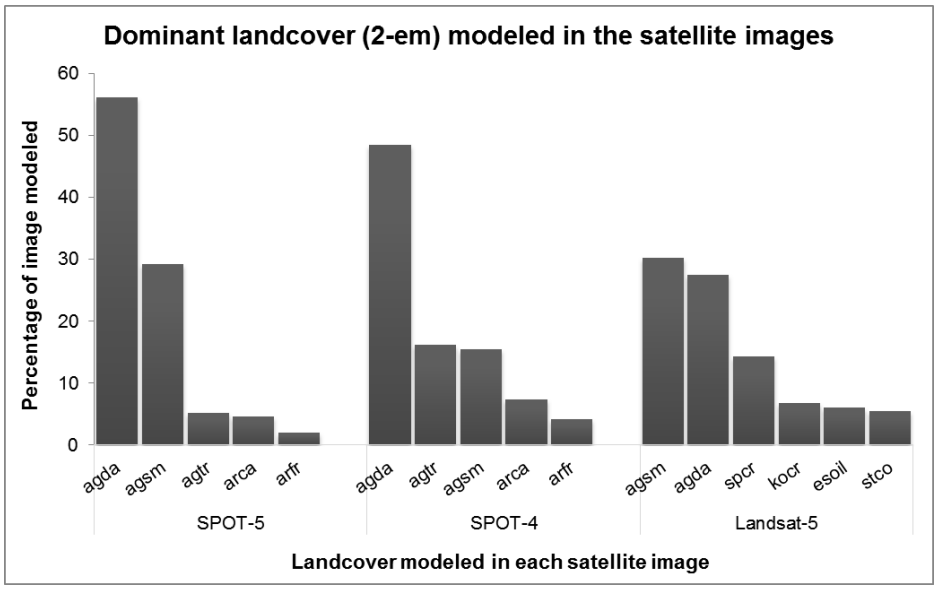

Fig. 4.5 Percentage of the image SPOT-5, SPOT-4, or Landsat-5 modeled by 2-em models (1 bright endmember+shade). Note: Only the dominant land cover that modeled >90% of each image is shown. Table 4.2 lists the acronyms for the land cover classes.

Unmixing with 3-endmember models

More than one plant species occur in most locations in the study area, therefore it is not appropriate to model an image pixel with a single bright endmember, and 3-em models were further tested. 3-em models should be preferable because in the majority of the study area GV is often seen mixed with NPV or soil, and also no single GV endmember completely dominates any pixel.

It should be noted that unlike the unmixing using the 2-em models, different numbers of 3-em models (Table 4.3) were tested on the three images. Of the 360 models tested for the SPOT-5 image, only 289 were found successful. Similarly for the SPOT-4 image, only 512 were successful out of 517 models tested. Only 262 were successful out of the 266 models tested for the Landsat-5 image. The number of 3-em models required to model 99.9% of the image were: 189 (SPOT-5), 458 (SPOT-4) and 221 (Landsat-5), respectively. The high number of successful models gives an idea about the spectral variability of surface classes in the study area (Table 4.5) and points to the usefulness of hyperspectral data sets for these ecosystems.

Grasses were mapped as the dominant land cover in all three images (Fig. 4.7a, 4.7b, 4.7c), and the dominant vegetation types identified were: grasses (*Elymus lanceolatus*, *Agropyron cristatum, Pascopyrum smithii*, *Agropyron trachycaulum*, *Hesperostipa comata*, *Bouteloua gracilis*, *Muhlenbergia cuspidata*, *Bromus inermis*), shrubs (*Artemisia cana* and *Juniperus horizontalis*) and forbs (*Artemisia frigida* and *Artemisia ludovicianus*). An advantage of using 3-em models is that they help to understand the association of different land covers. In Fig. 4.5, it is seen that the native grasses are associated with the soil (bsoil, esoil, msoil) or NPV (dshrub, dgrass) classes, and this is indicative of the type of land cover association commonly seen in the study area. Unmixing with the SPOT-4 image resulted in smaller percentage of land covers (<3%) when compared to the SPOT-5 or Landsat-5 images (Fig. 4.6). This is difficult to explain other than the effect of spectral variability arising due to vegetation phenology; further research will be needed to confirm this. Compared to the grasses, shrubs especially buckbrush and thorny buffaloberry were not effectively modeled in any of the images even though higher number of reference endmembers were used in the model building (Table 4.2). This indicates the incapability of multispectral RS datasets to successfully identify the shrub vegetation types within coarse and mixed image pixels. Future research may explore whether the shrub vegetation types can be effectively identified and mapped from hyperspectral imagery.

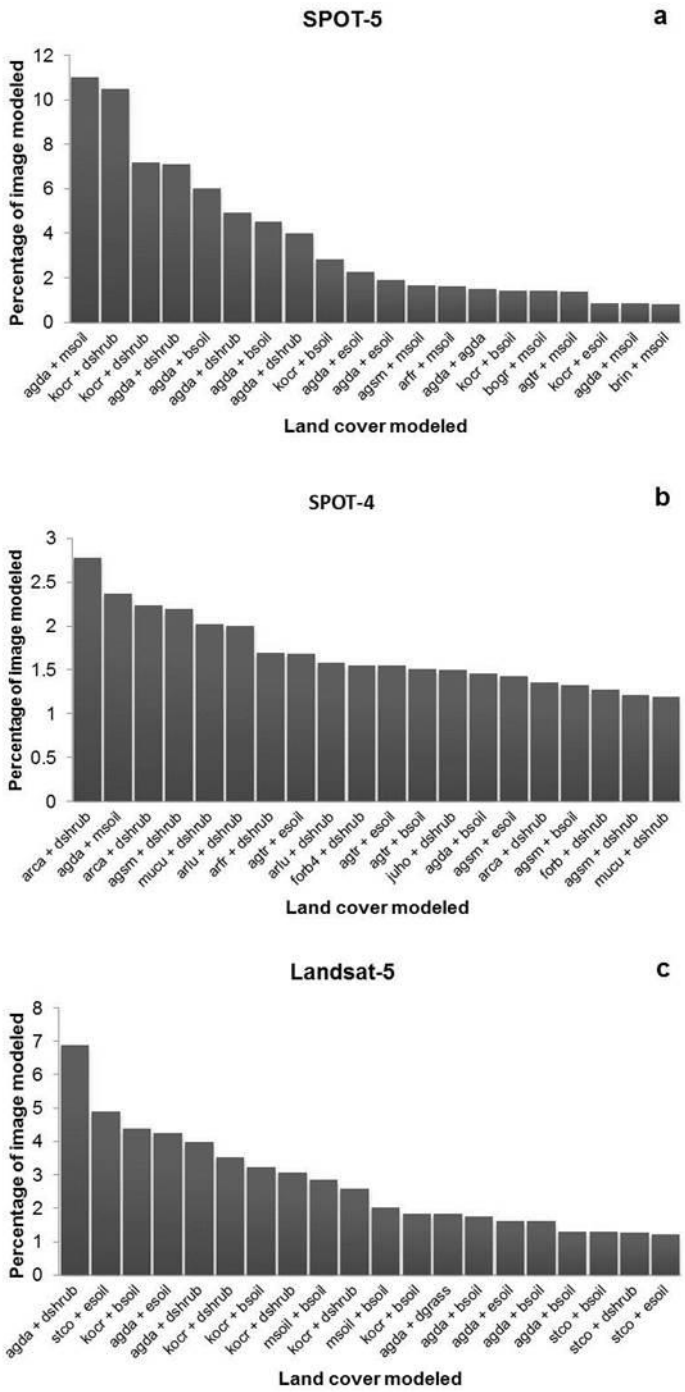

Fig. 4.6 Percentage of the image SPOT-5 (5a), SPOT-4 (5b), or Landsat-5 (5c) modeled by 3-em models (2 bright endmembers+shade). The top 20 dominant land covers modeled 74%, 34%, and 56% of each image. Table 4.2 lists the acronyms for the land cover classes.

Overall, MESMA successfully identified and mapped vegetation in the study area (Fig. 4.7a, 4.7b, 4.7c). However, there was confusion in successfully delineating the exotic grass types. This

is mostly because in the lowlands the exotic grasses (except crested wheat grass) are often seen intermixed with shrubs such as buckbrush, buffaloberry or willows. In the uplands, the grass cover is often very sparse and mostly dominated by the native prairie grasses such as blue grama and northern wheat. Also, the high cover of soil adds linear mixing to the vegetation reflectance spectra and causing confusion. Peak vegetation growth in the northern mixed prairie is between June and July (Zhang, 2008), therefore plant phenology may have created some difficulty as the Landsat-5 and SPOT-5 images were acquired for mid- and late-July, respectively. Zhang (2008) and Li and Guo (2012) discuss vegetation phenology in the same study area.

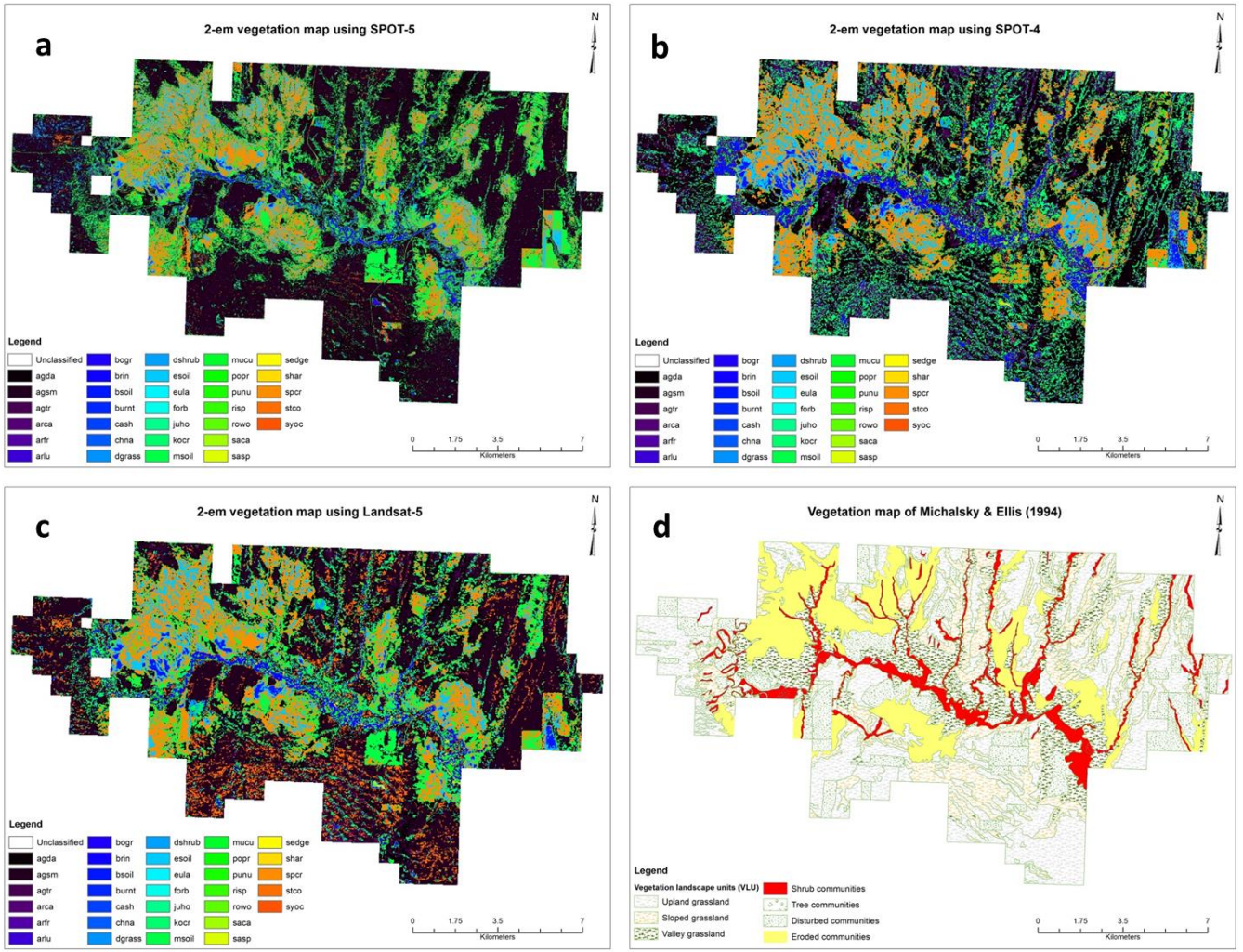

Fig. 4.7 Vegetation maps for the study area derived from MESMA for SPOT-5 (4.7a), SPOT-4 (4.7b), Landsat-5 (4.7c). Map of Michalsky and Ellis (1994) is given for comparison (4.7d).

In general, the success of spectral unmixing was found to be dependent on the number and type of endmembers. Also prior knowledge of the vegetation communities and their associations from Michalsky and Ellis (1994) greatly helped to create and build comprehensive region-specific endmember spectral libraries (Roberts et al., 1997) for the study area.

Vegetation in the three images, especially the native grasses, is in varying stages of phenology (maturity or senescence), except the shrubs and smooth brome which are perennial. The SPOT-5 image (10 m) was acquired in late July which is in the later part of the peak vegetative growth, therefore the native prairie grasses were beginning senescence. For SPOT-4 and Landsat-5 images, even though they were acquired during the peak vegetative growth period, the coarser spatial resolution (20 and 30 m, respectively) could have caused higher linear mixing when compared to the finer spatial resolution of the SPOT-5 image (10 m).

Previous studies have tested maximum likelihood classifier (MLC) and object-oriented (He, 2009), and artificial neural network (ANN) and MLC (Zhou, 2007) methods to classify land covers in the same study region in the context of modeling vegetation productivity or for crop insurance programs. Though they report overall classification accuracies of >80%, their image classification could map only six to eight very broad land cover / land use classes, therefore those classified map products are suitable only for small-scale (wider area) applications.

4.3.3 Effect of spatial scale of RS data on the efficiency of spectral unmixing

In Table 4.5, it is seen that the number of models required to model each image increased with decrease in the spatial scale of the image: the SPOT-5 image (10 m) only required 42 models (out of 69) to classify 99.9% of the image while Landsat-5 (30 m) required 58 models (out of 70). This leads to conclude that as the spatial scale of the remotely sensed data becomes coarser, their image pixels are likely becoming more mixed (spatially aggregated), thus requiring higher numbers of unmixing models to effectively model them. However, the number of successful models selected for the three images were comparable: 69, 76, and 70 for SPOT-5, SPOT-4, and Landsat-5, respectively. The slightly higher number of successful models for the SPOT-4 image can be attributed to the vegetation phenology trends seen in the study area whereby the native prairie grasses complete most of their vegetative growth between June and July. The SPOT-4 image was acquired in late June which coincides with the ‘green-up’ period of most graminoids.

Though not very explicit, Landsat-5 image showed slightly higher number of successful models compared to the SPOT-5 image, and this is likely due to the higher spectral resolution of Landsat to that of SPOT.

Even though higher numbers of shrub endmembers were used in the model-building (Table 4.2), all three satellite images failed to effectively identify them in their unmixing, both with 2- and 3-em models. This concludes that RS imagery of higher spectral resolution is needed to identify them; SPOT only has 4 bands compared to the 6 bands of Landsat (thermal band excluded). However as the pixel size becomes coarser there is more aggregation as spectral reflectance from multiple surface materials at the landscape-level, or their ground cover are too sparse to be resolved at the 30 m pixel size of the Landsat image.

4.4 CONCLUSIONS

MESMA was successfully used in this study on medium-resolution images to identify and map the dominant vegetation types in the northern mixed prairie. In comparison to the pixel- or object-based or artificial neural network classifiers used in the previous studies, MESMA was more effective in identifying the dominant vegetation and their sub-pixel fractions. The success of MESMA also highlights the fact that simple SMA or traditional whole-pixel classification approaches are less effective for vegetation mapping in ecosystems with high spatial- and spectral-variability.

Consistent to previous field-based (GPS) mapping (Michalsky and Ellis, 1994), MESMA correctly mapped the native prairie grasses as the dominant vegetation types. MESMA was more successful in mapping the vegetation in the uplands than in the lowlands, which indicates the limitations of multispectral datasets for spectral unmixing. Previous research has demonstrated that vegetation cover in the northern mixed prairie is dependent on topography and soil moisture conditions. Contrary to the recommendation of Powell (2006) that 2-em models are better suited for natural ecosystems, our study found that 3-em models are better suited for the northern mixed prairie. Even though 2-em models identified the spatial distribution and variability of the vegetation types, 3-em models were found to be more appropriate than the 2-em models in representing the association of land cover classes (i.e. GV mixed with NPV or soil).

Few vegetation types were not successfully mapped. This may be because these plant types are not dominant at the landscape-level, are seen inter-mixed with other vegetation types or litter or soil, or are too sparse in ground cover to be resolved at the satellite pixel-level. Future studies may try to include these types in the unmixing algorithms by expanding the spectral library database compiled in this study. This study also did not consider the vegetation phenology, especially of the native prairie grasses, the SPOT-5 image was acquired towards the end of July by which time most native grasses have begun senescence. However, this limitation was overcome to a certain extent in the current study by using reference endmembers collected throughout the peak vegetative growing period (June through July). One reason for the success of MESMA was that spectra of dominant vegetation types were acquired during their peak vegetative growth and this might have helped capture the intra-species spectral variability. Another reason for the success of this study was the dominant use of field endmember spectra and few image spectra. Image spectra have the disadvantage that they are already 'mixed' with few or several surface materials within the IFOV combined into a single pixel. Nevertheless, the results from this study are promising in that even with multispectral datasets, vegetation types and their spatial distribution could be identified at the landscape-level and indicating that future research will benefit by using hyperspectral imagery to an even greater level of success.

4.4.1 Research significance and challenges

Significance

Hyperspectral data sets are currently unavailable for the northern mixed prairie, nonetheless this study has shown that spectral unmixing methods may be effectively used even on multispectral data sets to reveal valuable information about the spatial variability and distribution of vegetation types and soil in semi-arid ecosystems such as the northern mixed prairie. A variety of useful map products can be derived that help to understand the spatial patterns and variability of vegetation and further the knowledge of habitat and forage availability to the fauna in the park. This study has proved that vegetation mapping in semi-arid regions can benefit from spectral unmixing approaches to reveal valuable information about the surface materials, map their abundances, and estimate their fractions. It is anticipated that this study will aid in developing

better spectral unmixing algorithms, specifically for semi-arid ecosystems. The performance of SPOT (10 m, 4 band) imagery suggests that imagery such as WorldView (0.5 m, 8 band) and RapidEye (5 m, 5 band) may be more effective for vegetation mapping in this ecosystem due to their finer spatial and spectral resolutions and also both having a vegetation-specific red-edge band.

Challenges

Spectral unmixing and MESAM are typically implemented using hyperspectral data sets such as AVIRIS, Hyperion, and HyMap with very high spectral resolution (hundreds of narrower spectral bands) and medium spatial resolution (< 30 m). Hyperspectral imageryare lacking for the northern mixed prairie, and therefore the coarser spatial and spectral resolution of multispectral images (4-7 bands) used in this study did have an effect on the efficiency ofvegetation mapping. Nevertheless, this study was successful in mapping the dominant vegetation for most of the study area. The three satellite images used in this study differ in their spatial and spectral resolution and also with respect to their dates of acquisition. Future research can explore how different imagery obtained at even closer phenological time points may perform for spectral unmixing.

Reference endmembers collected for grasses were often mixed with other vegetation types, soil, standing dead or litter, thus making it difficult to collect their reference endmembers in the field. This limitation was critical with endmembers such as moss, cacti, and lichen which are ecological significant in this region, however they are seen in sparse cover and inter-mixed with other vegetation, soil, or litter and making it difficult to collect their reflectance in the field. This mixed nature of materials causes non-linear mixing. Publically available spectral libraries (i.e. USGS, JPL, ASTER) lack spectra for the mixed prairie vegetation, and therefore there are opportunities with sharing of spectral databases among researchers.

4.5 ACKNOWLEDGEMENTS

University of Saskatchewan, Saskatchewan Environment, and Nature Saskatchewan provided financial support. Randy Bonin, Jesse Nielsen, Chunhua Zhang, and Yuhong He assisted with field work. Xulin Guo, Joseph Piwowar, and Greg McDermid shared field instruments. Imagery

was sourced from GeoBase and USGS. ISC provided ortho aerial imagery at subsidized costs. Alberto Meroni (ITTVIS) coded custom scripts.

4.6 REFERENCES

Adams, J.B., Smith, M.O., and Gillespie, A.R. 1993. Imaging spectrometry: interpretation based on spectral mixture analysis, In Pieters CM, Englert P, editors. Remote geochemical analysis: elemental and mineralogical composition. New York: Cambridge Univ. Press, 7: 145-166.

Anderson, G.P., Pukall, B., Allred, C.L., Jeong, L.S., Hoke, M., Chetwynd, J.H., Adler-Golden, S.M., Berk, A., Bernstein, L.S., Richtsmeier, S.C., Acharya, P.K., and Matthew, M.W. 1999. FLAASH and MODTRAN4: state-of-the-art atmospheric correction for hyperspectral data. *IEEE Proceedings of Aerospace Conference,* pp. 177-181, Snowmass at Aspen, CO, USA.

Ballantine, J-A C., Okin, G.S., Prentiss, D.E., and Roberts, D.A. 2005. Mapping African landforms using continental scale unmixing of MODIS imagery. *Remote Sensing of Environment,* 97(4): 470-483.

Beyer, H.L. 2010. Geospatial Modelling Environment (version 0.5.2 Beta). (software). URL: http://www.spatialecology.com/gme.

Blood, D.A., and Ledingham, G.F. 1986. *An evaluation of interim range management options on lands acquired for the purpose of establishing Grasslands National Park.* Prepared for Parks Canada by D.A. Blood and Associates Ltd. 189 pp.

Boardman, J.W., Kruse, F.A., and Green, R.O. 1995. Mapping target signatures via partial unmixing of AVIRIS data in Summaries of the 5th JPL Airborne Earth Science Workshop, JPL Publication, 95-1(1): 23-26.

Cohen, W.B., and Goward, S.N. 2004. Landsat's role in ecological applications of remote sensing. *BioScience*, 54(6): 535-545.

Davidson, A., and Csillag, F. 2001. The influence of vegetation index and spatial resolution on a two-date remote sensing-derived relation to C4 species coverage. *Remote Sensing of Environment,* 75(1): 138-151.

Dennison, P.E., Charoensiri, K., Roberts, D.A., Peterson, S.H., and Green, R.O. 2006. Wildfire temperature and land cover modeling using hyperspectral data. *Remote Sensing of Environment*, 100(2): 212-222.

Dennison, P.E., Halligan, K.Q., and Roberts, D.A. 2004. A comparison of error metrics and constraints for multiple endmember spectral mixture analysis and spectral angle mapper. *Remote Sensing of Environment*, 93(3): 359-367.

Dennison, P.E., and Roberts, D.A. 2003a. Endmember selection for multiple endmember spectral mixture analysis using endmember average RMSE. *Remote Sensing of Environment*, 87(2-3): 123-135.

Dennison, P.E., and Roberts, D.A. 2003b. The effects of vegetation phenology on endmember selection and species mapping in Southern California chaparral. *Remote Sensing of Environment*, 87(2-3): 295-309.

Dennison, P.E., Roberts, D.A., and Peterson, S.H. 2007. Spectral shape-based temporal compositing algorithms for MODIS surface reflectance data. *Remote Sensing of Environment*, 109(4): 510-522.

Elmore, A.J., Mustard, J.F., Manning, S.J., and Lobell, D.B. 2000. Quantifying vegetation change in semiarid environments: precision and accuracy of spectral mixture analysis and the normalized difference vegetation index. *Remote Sensing of Environment*, 73: 87-102.

Franke, J., Roberts, D.A., Halligan, K., and Menz, G. 2009. Hierarchical Multiple Endmember Spectral Mixture Analysis (MESMA) of hyperspectral imagery for urban environments. *Remote Sensing of Environment*, 113(8): 1712-1723.

Fraser, R.H., Olthof, I., and Pouliot, D. 2009. Monitoring land cover change and ecological integrity in Canada's national parks. *Remote Sensing of Environment*, 113(7): 1397-1409.

Gardner, M. 1997. *Mapping chaparral with AVIRIS using advanced remote sensing techniques*, M.Sc. Thesis, University of California, Santa Barbara.

Gauthier, D.A., Lafon, A., Toombs, T., Hoth, J., and Wiken, E. 2003. Grasslands: Toward a North American Conservation Strategy. Canadian Plains Research Center, University of Regina, Regina, Saskatchewan, and Commission for Environmental Co-operation, Montreal, Quebec, Canada.

Halligan, K.Q. 2002. *Multiple endmember spectral mixture analysis of vegetation in the northwest corner of Yellowstone National Park*. M.Sc. Thesis, University of California, Santa Barbara.

Harms, V.L. 2006. *Annotated catalogue of Saskatchewan vascular plants*. 116 pp.

He, Y., Guo, X., and Wilmshurst, J.F. 2006. Studying mixed grassland ecosystems I: suitable hyperspectral vegetation indices. *Canadian Journal of Remote Sensing*, 32(2): 98-107.

He, Y., Guo, X., and Si, B.C. 2007. Detecting grassland spatial variation by a wavelet approach. *International Journal of Remote Sensing*, 28(7): 1527-1545.

He, Y., Guo, X., and Wilmshurst, J.F. 2007. Comparison of different methods for measuring leaf area index in a mixed grassland. *Canadian Journal of Plant Science*, 87(4): 803-813.

He, Y. 2008. *Modeling grassland productivity through remote sensing products.* Ph.D. Thesis, University of Saskatchewan, Saskatoon.

Kerr, J., and Ostrovsky, M. 2003. From space to species: ecological applications for remote sensing. *Trends in Ecology & Evolution*, 18(6): 299-305.

Li, M., and Guo, X. 2014. Long term effect of major disturbances on the northern mixed grassland – A review. *Open Journal of Ecology*, 4(4): 214-233.

Li, Z., and Guo, X. 2012. Detecting climate effects on vegetation in northern mixed prairie using NOAA AVHRR 1-km time-series NDVI data. *Remote Sensing*. 4(1): 120-134.

Looman, J. and K.F. Best. 1987. *Budd's flora of the Canadian Prairie Provinces.* Research branch, Agriculture Canada, Publication 1662. 863 pp.

Michalsky, S.J., and Ellis, R.A. 1994. Vegetation of Grasslands National Park. DA Westworth and Associates, Calgary.

Okin, G.S., Roberts, D.A., Murray, B., and Okin, W.J. 2001. Practical limits on hyperspectral vegetation discrimination in arid and semiarid environments. *Remote Sensing of Environment*, 77(2): 212-225.

Ollinger, S.V. 2011. Sources of variability in canopy reflectance and the convergent properties of plants. *New Phytologist*, 189(2): 375-394.

Painter, T.H., Dozier, J., Roberts, D.A., Davis, R.E., and Green, R.O. 2003. Retrieval of subpixel snow-covered area and grain size from imaging spectrometer data. *Remote Sensing of Environment*, 85: 64-77.

Painter, T.H., Roberts, D.A., Green, R.O., and Dozier, J. 1998. The effect of grain size on spectral mixture analysis of snow-covered area from AVIRIS data. *Remote Sensing of Environment*, 65(3): 320-332.

Powell, R. 2006. *Long-Term monitoring of urbanization in the Brazilian Amazon using remote sensing*. Ph.D. Thesis, University of California, Santa Barbara.

Powell, R., Roberts, D.A., Dennison, P.E., and Hess, L.L. 2007. Sub-pixel mapping of urban land cover using multiple endmember spectral mixture analysis: Manaus, Brazil. *Remote Sensing of Environment*, 106(2): 253-267.

Quintano, C., Fernández-Manso, A., and Roberts, D.A. 2013. Multiple endmember spectral mixture analysis (MESMA) to map burn severity levels from Landsat images in Mediterranean countries. *Remote Sensing of Environment*, 136: 76-88.

Rashed, T., Weeks, J.R., Roberts, D., Rogan, J., and Powell, R. 2003. Measuring the physical composition of urban morphology using multiple endmember spectral mixture models. *Photogramm. Eng. Remote Sens.* 69(9): 1011-1020.

Ray, T.W., and Murray, B.C. 1996. Nonlinear spectral mixing in desert vegetation. *Remote Sensing of Environment*, 55(1): 59-64.

Roberts, D.A., Adams, J.B., and Smith, M.O. 1993. Discriminating green vegetation, non-photosynthetic vegetation and soils in AVIRIS data. *Remote Sensing of Environment*, 44: 1-25.

Roberts, D.A., Batista, G., Pereira, J., Waller, E., and Nelson, B. 1998. Change identification using multitemporal spectral mixture analysis: Applications in Eastern Amazonia, Chapter 9 in Remote Sensing Change Detection: Environmental Monitoring Applications and Methods, (Elvidge, C. and Lunetta R., Eds.), Ann Arbor Press, Ann Arbor, MI, pp. 137-161.

Roberts, D.A., Brown, K.J., Green, R., Ustin, S., and Hinckley, T. 1998. Investigating the relationship between liquid water and leaf area in clonal Populus, Proc. 7th AVIRIS Earth Science Workshop JPL 97-21, Pasadena, CA 91109, 335-344.

Roberts, D.A., Dennison, P.E., Gardner, M., Hetzel, Y., Ustin, S.L., and Lee, C. 2003. Evaluation of the potential of Hyperion for fire danger assessment by comparison to the Airborne Visible/Infrared Imaging Spectrometer. *IEEE Transactions on Geoscience and Remote Sensing*, 41(6): 1297-1310.

Roberts, D.A., Gardner, M., Church, R., Ustin, S.L., and Green, R.O. 1997. Optimum strategies for mapping vegetation using multiple endmember spectral mixture models, in SPIE Conf. Vol 3118, Imaging Spectrometry III, 108-119., San Diego, CA July 27-Aug 1, 1997.

Roberts, D.A., Gardner, M., Church, R., Ustin, S., Scheer, G., and Green, R.O. 1998. Mapping chaparral in the Santa Monica mountains using multiple endmember spectral mixture models. *Remote Sensing of Environment*, 65: 267-279.

Roberts, D.A., Green, R.O., and Adams, J.B. 1997. Temporal and spatial patterns in vegetation and atmospheric properties from AVIRIS. *Remote Sensing of Environment*, 62(3): 223-240.

Roberts, D.A., and Herold, M. 2004. Imaging Spectrometry of Urban Materials, in Molecules to Planets: Infrared Spectroscopy in Geochemistry, Exploration Geochemistry and Remote Sensing (P. King, M. Ramsey and G. Swayze, Ed.), Mineral Association of Canada, 155-183.

Roberts, D.A., Numata, I., Holmes, K.W., Batista, G., Krug, T., Monteiro, A., Powell, B., and Chadwick, O. 2002. Large area mapping of land-cover change in Rondônia using multitemporal spectral mixture analysis and decision tree classifiers. *Journal of Geophysical Research: Atmospheres*, 107(D20): LBA 40-1–LBA 40-18.

Roberts, D.A., Ustin, S.L., Ogunjemiyo, S., Greenberg, J., Dobrowski, S.Z., Chen, J. and Hinckley, T.M., 2004. Spectral and structural measures of Northwest forest vegetation at leaf to landscape scales. *Ecosystems*, 7(5): 545-562.

Sonnetag, O., Chen, J.M., Roberts, D.A., Talbot, J., Halligan, K.Q., and Govind, A. 2007. Mapping tree and shrub leaf area indices in an ombrotrophic peatland through multiple endmember spectral unmixing. *Remote Sensing of Environment*, 109(3): 342-360.

Saskatchewan Institute of Pedology, 1992. Grasslands National Park Soil Survey, University of Saskatchewan, Saskatoon.

Settle, J.J., and Drake, N.A., 1993. Linear mixing and the estimation of ground cover proportions, *International Journal of Remote Sensing*, 14(6): 1159-1177.

Somers, B., Asner, G.P., Tits, L., and Coppin, P. 2011. Endmember variability in spectral mixture analysis: A review. *Remote Sensing of Environment*, 115(7): 1603-1616.

Song, C.H. 2005. Spectral mixture analysis for subpixel vegetation fractions in the

urban environment: How to incorporate endmember variability? *Remote Sensing of Environment*, 95(2): 248-263.

Tompkins, S., Mustard, J.F., Pieters, C.M., and Forsyth, D.W., 1997, Optimization of endmembers for spectral mixture analysis. *Remote Sensing of Environment*, 59(3): 472-489.

Ustin, S.L., Roberts, D.A., Gamon, J.A., Asner, G.P., and Green, R.O. 2004. Using imaging spectroscopy to study ecosystem processes and properties. *Bioscience*, 54(6): 523-534.

Ustin, S.L., and Gamon, J.A. 2010. Remote sensing of plant functional types. *New Phytologist*, 186(4): 795-816.

Wulder, M.A., White, J.C., Goward, S.N., Masek, J.G., Irons, J.R., Herold, M., Cohen, W.B., Loveland, T.R., and Woodcock, C.E. 2008. Landsat continuity: Issues and opportunities related to Landsat continuity. *Remote Sensing of Environment*, 112(3): 955-969.

Wulder, M.A., Masek, J.G., Cohen, W.B., Loveland, T.R., and Woodcock, C.E. 2012. Opening the archive: How free data has enabled the science and monitoring promise of Landsat. *Remote Sensing of Environment*, 122: 2-10.

Roberts, R., Halligan, K., and Dennison, P. 2007. VIPER Tools User Manual. 91p.

Xu, D., Guo, X., Li, Z., Yang, X., and Yin, H. 2014. Measuring the dead component of mixed grassland with Landsat imagery. *Remote Sensing of Environment*, 142: 33-43.

Yang, X., and Guo, X. 2014. Quantifying responses of spectral vegetation indices to dead materials in mixed grasslands. *Remote Sensing*. 6(5): 4289-4304.

Zhang, C., and Guo, X. 2007. Measuring biological heterogeneity in the northern mixed prairie: a remote sensing approach. *The Canadian Geographer*, 51(4): 462-474.

Zhang, C. 2008. *Monitoring biological heterogeneity in a northern mixed prairie using hierarchical remote sensing methods.* Ph.D. Thesis, University of Saskatchewan, Saskatoon.

Zhou, W. 2007. *Assessing remote sensing application on rangeland insurance in Canadian Prairies.* M.Sc. Thesis, University of Saskatchewan, Saskatoon.

CHAPTER 5

DETECTING SPATIO-TEMPORAL CHANGES TO THE NORTHERN MIXED PRAIRIE VEGETATION USING MULTIPLE ENDMEMBER SPECTRAL MIXTURE ANALYSIS

ABSTRACT

Spatio-temporal change-detection in terrestrial ecosystems has become readily possible with open access to time-series Landsat imagery, thereby permitting researchers to utilize historical imagery for studies on ecosystem monitoring and environmental change.

This study used multiple endmember spectral mixture analysis (MESMA) and NDVI image differencing on seven time-series Landsat-5 TM imagery for a 27-year period (1984-2011) to identify the spatio-temporal changes to the northern mixed prairie vegetation. A comprehensive region-specific endmember spectral library comprising 1150 reference endmember spectra of green vegetation, non-photosynthetic vegetation, and soils was collected through intensive field sampling at 41 sites in the West Block of the Grasslands National Park of Canada (GNPC). 97 optimal endmembers were identified using endmember selection metrics to create 2-endmember models and used in image unmixing to map the dominant vegetation types and estimate sub-pixel fractions of land cover in each historical image. Spatio-temporal change-detection was performed by image-differencing each image in the time-series from the base (1984) image. Results showed that MESMA can be used as a standard tool for identifying spatio-temporal changes on time-series imagery. MESMA was effective in mapping the dominant vegetation types and produced comparable mapping results for each image in the time-series. Climatic variables of temperature and precipitation were found to affect the number of successful image unmixing models, with lesser number of models for years of climatic extremes. Change-detection showed the effectiveness of biodiversity conservation practices of GNPC since establishment and suggests that its conservation strategies are effective in maintaining heterogeneityin the park region. The methodology presented can be continued to be used to monitor spatio-temporal changes in the northern mixed prairie, and may be tested in other ecosystems to gain valuable insight into their dynamics.

5.1 INTRODUCTION

5.1.1 Significance of the northern mixed prairie and need for monitoring

The North American grasslands are among the world's most productive and diverse terrestrial ecosystems. These grasslands have been subjected to over 500 years of human settlement, intensive agriculture, ranching, and livestock activities (Gauthier et al., 2003). Only a very small portion of the native prairie vegetation is remnant (Samson and Knopf, 1994; 1996), making the grasslands one of the most endangered habitats in the world. Grasslands provide critical habitats for many endangered fauna or species at-risk, hence it is important to effectively manage and conserve their endangered habitats to sustain diminishing populations (Fraser et al., 2009). Factors for land use-land cover change in the northern mixed prairie include agriculture, grazing by livestock, oil and mineral exploration, invasion by exotic plant species. Apart from human pressures, climate change is projected to have significant effects on the grasslands. There is lack of understanding regarding how the mixed prairie will react to climate change and its effects. Vegetation growth in the northern mixed prairie is limited primarily by the availability of moisture, and therefore any fluctuations in temperature and precipitation will have direct and pronounced impact on the vegetation productivity and plant phenology in the region. Researchers predict that the effects of climate change in the grasslands may include ecological succession, changes to vegetation zones and their conversion to shrublands, or even shift of the dominant photosynthetic types to the sub-dominant type (Davidson and Csillag, 2001). Therefore, it is of utmost priority for long-term ecological- or ecosystem-monitoring to conserve the native prairie and maintain their vegetation heterogeneity. The northern mixed prairie warrants high conservation priority both in Canada and the United States. Parks Canada has envisioned a long-term mandate for preserving ecological integrity (Fraser et al., 2009) and for restoring and conserving the native prairie vegetation by establishing its first and only national park solely devoted to grassland conservation, the Grasslands National Park of Canada (GNPC), and adopting an adaptive management strategy for maintaining vegetation heterogeneity by introducing natural disturbances such as burning and grazing. Long-term ecological monitoring and research (LTER) remains the primary goal for GNPC as they are helpful to measure the success of any biodiversity conservation efforts or restoration programs. Michalsky and Ellis

(1994) suggest that systematic vegetation inventory and mapping in this region is important for: a) management of native vegetation communities; b) management of rare plant species and communities; c) maintenance of non-native plant species; d) restoration of modified or disturbed lands; and e) proper vegetation and ecosystem management.

5.1.2 Review of change-detection methods

Ecosystems are dynamic and ecologists are often interested in identifying and monitoring ecosystem changes due to land use-land cover modifications, changes to vegetation type, and impacts of natural- or human-induced disturbances. Remote sensing (RS), using aerial photography or with satellites, provides invaluable primary data sets for ecosystem studies due to their ability to detect, identify, and monitor ecosystem- or environmental dynamics in non-destructive and cost-effective ways. Change-detection involves the quantification of any phenomena or process over space and time (spatio-temporal) using multi-date RS imagery (Coppin et al., 2004; Fraser et al., 2009). Aerial photography and air photo interpretation were widely used in the past, however their main drawbacks include one-time acquisition, high costs, problems related to data acquisition (optimum flying conditions), data issues (shadows, limited spectral range), and most importantly being large scale (covering smaller area). In contrast, satellite RS offers repetitive, small-scale (larger area), and cost-effective way of monitoring ecosystems and their dynamics using a multi-scalar (multi- spatial, spectral, and temporal) approach. In addition, variety of maps of land cover, vegetation indices (VI), and biomass can be derived from RS data sets. Due to these advantages, ecologists are increasingly using satellite imagery or information or products derived from them for ecosystem monitoring.

Several change-detection methods using RS data exist, and these can be grouped into three main categories: algebra, transformation, and classification and post-classification (Lu et al., 2004), though a few other types also exist. These three categories include methods such as VI differencing, principal component analysis (PCA), minimum noise fraction (MNF), and spectral mixture analysis (SMA) as examples. Coppin et al. (2004), Lu et al. (2004), and Singh (1989) provide comprehensive reviews on the change-detection methods used in ecosystem monitoring along with their strengths and weaknesses.

RS data sets used for change-detection analysis require special considerations (refer to Coppin et al., 2004; Lu et al., 2004). Change-detection is usually performed at the pixel-level with time-

series RS imager, and therefore the images must be co-registered. Ideally, the RS data sets used for change-detection should ideally be acquired by the same remote sensor (for similar image characteristics) and also maintain consistency in their resolution (spectral range and spatial scale). Importantly, results from change-detection may be affected if the phenological time points of dominant vegetation are not comparable as even the same vegetation type can have different spectral response at various phenological stages. Further, the data sets used for change-detection should be processed and corrected for variations in atmospheric conditions and solar position during image acquisition. This is typically achieved by using robust atmospheric correction models, radiometric calibration, and processing images to surface reflectance values for 'spectral similarity' and 'phenological stability' as suggested by Coppin et al. (2004). Archived time-series Landsat imagery from sensors Multi Spectral Scanner (MSS; available since 1972), Thematic Mapper (TM; from 1984), and Enhanced Thematic Mapper (ETM+; since 1999) from the United States Geological Survey (USGS) are ideal for change-detection analysis since they are already geometrically- and radiometrically-corrected and at suitable spatial (30 m) and temporal (16 days) resolutions.

Change-detection has its limitations. Studies suggest that currently no single standard methodology exists for change-detection analysis, and often based on the study area or the RS data sets. Therefore, researchers report different results and success by using various change-detection techniques and making the comparison challenging. Changes between spectrally-similar land covers are difficult to detect if their spectral reflectance are comparable; this is a common problem in semi-arid regions such as the northern mixed prairie where several grass types have similar reflectance patterns (Chapter 4).

Past studies such as Zhang (2006), He (2008), and Li and Guo (2012) have employed normalized difference vegetation index (NDVI) time-series or maximum value composites (MVC) to identify the short- and long-term changes to the northern mixed prairie vegetation. Successfully used at smaller (regional- or biome-level) scales, the main limitation with time-series NDVI is that they only provide trends of NDVI-change, however there is no information about the actual change (modification or conversion) of the vegetation type or of any ecological succession, which is often of main interest to ecologists and Park managers. Further, VI such as NDVI have been shown to have relatively low correlation to vegetation properties in the mixed prairie due to high background noise and non-linear mixing from litter and exposed soil (He et al., 2006; Li

and Guo, 2010). Additionally, high vegetation heterogeneity has also been reported for the northern mixed prairie (Zhang, 2008), therefore the reflectance signal recorded by the remote sensor or the NDVI calculated for an image pixel is a spatial aggregate of the reflectance from dissimilar ground cover. Hence, image classifiers based on the homogeneous whole (pure) pixel concept do not perform efficiently, and therefore spectral unmixing approaches become more appropriate as they can account for the spectral variability of surface materials and also extract sub-pixel cover fractions.

5.1.3 Research questions

The hypothesis used in the study was that a comprehensive (spatial and temporal) endmember spectral library can be effectively used for classifying time-series imagery. The objectives of the study were:

(i) To test the performance and robustness of multiple endmember spectral mixture analysis (MESMA) on time-series satellite imagery;

(ii) To identify spatio-temporal change to vegetation in a representative area in the northern mixed prairie over a 27-year period (1984-2011);

(iii) To detect areas of significant change, if any, in the study area and identify the vegetation types that might have changed in their extent.

5.2 MATERIALS AND METHODS

5.2.1 Study area

The Grasslands National Park of Canada (GNPC), located at the Saskatchewan-Montana border (Fig. 5.1), was selected as a representative area to identify and detect any significant vegetation changes to the northern mixed prairie. GNPC is comprised of the West Block and the East Block and covers ~900 km^2. GNPC was established by Parks Canada in 1981 to conserve remaining native mixed prairie in Canada. Since its establishment, the park has been protected from agriculture, ranching, and livestock grazing (excluding cattle introduced for grazing experiments), however plains bison were re-introduced to the West Block in 2006 as an ecosystem management strategy to restore the native prairie vegetation through natural grazing.

In addition, GNPC follows its own research activities of prescribed-burning and re-seeding of native prairie grasses for prairie restoration. Crop and forage cultivation, livestock grazing, oil and mineral exploration are still practiced around the park and pose threats to the biodiversity conservation in the region (Fraser et al., 2009; Gauthier et al., 2003).

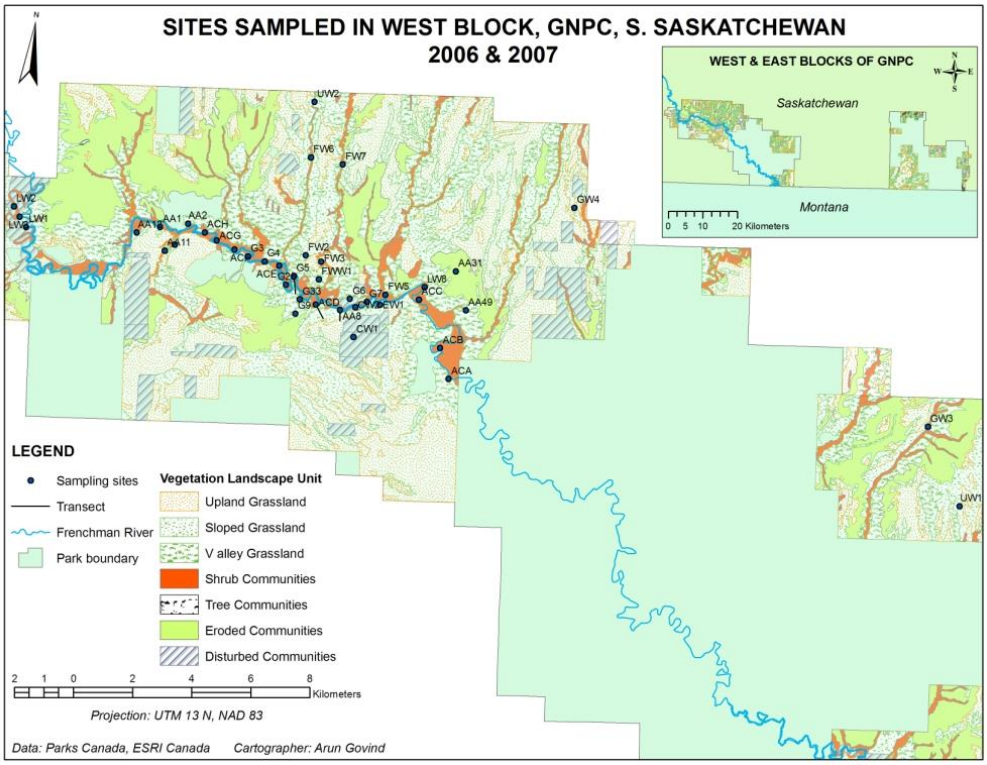

Fig. 5.1 Location map showing the East and West Block of the Grasslands National Park of Canada (GNPC) and GNPC's context in the North American grasslands ecoregion.

The region experiences a continental semi-arid climate with wide variation in mean monthly temperature (-12.4˚C to 18.3˚C) and low precipitation (150 to 325 mm) (Environment Canada, 2003). The region has an average elevation of ~860 m and high landscape diversity. This creates a moisture-limited environment for plant growth with a very short plant growing season of ~170 days and peak vegetative growth occurring between June and July. Chernozems is the dominant soil order, and the other important soils include regosols and solonetzs (Saskatchewan Institute of Pedology, 1992). The vegetation in the northern mixed prairie is highly heterogeneous (Zhang, 2006; Zhang, 2008) and the GNPC vegetation can be broadly classed into upland, sloped land, and lowland grasslands. The dominant vegetation types include native prairie grasses such

as western wheat grass (*Agropyron smithii*), northern wheat grass (*Elymus lanceolatus*), blue grama (*Bouteloua gracilis*), needle and thread (*Hesperostipa comata*), and june grass (*Koeleria macrantha*). In addition, forbs such as prairie sage (*Artemisia ludovicianus*) and pasture sage (*Artemisia frigida*), and shrubs such as sagebrush (*Artemisia cana*), willow (*Salix* sp.), thorny buffaloberry (*Shepherdia argentea*), buckbrush (*Symphoricarpos occidentalis*), rabbitbrush (*Chrysothamnus nauseosus*), and creeping juniper (*Juniperus horizontalis*) also occur. Eroded and exposed surfaces (badlands) from soil and water erosion are also widely seen in the study area along with microphytic communities of lichen (*Xanthoparmelia* sp.) and moss (*Phlox hoodii, Selaginella densa*). Plant names are adapted from Harms (2006).

5.2.2 Data and processing

Satellite imagery and processing

Processed Landsat data since 1974 have become freely and publically available and therefore provide tremendous opportunities for researchers to exploit time-series imagery to identify and monitor environmental- or ecosystem-changes in terrestrial ecosystems. Archived multispectral Landsat-5 TM imagery (L1T; standard terrain corrected product) from the USGS were obtained for the study area (path: 37, row: 26) for a 27-year period (1984-2011) at approximately 5-year intervals (Table 5.1). Even though other Landsat sensor (MSS and ETM+) data were available, only Landsat-5 images were considered in this study as previous research (Chapter 4) showed that both spatial- and spectral-resolution of RS data have positive effect on the efficiency of unmixing and in the estimation of the type or class of land cover fractions and Landsat-5 imagery at 30 m is within the suitable spatial resolution. Regarding the timeframe used in this study, 1984 was chosen as the starting point as it will give insight into the land use-land cover patterns due to disturbance events (or activities) immediately prior to the acquisition of the park in 1984. Also, the timeframe selected should give a good idea about the effectiveness of the biodiversity conservation or management practices since the establishment of the park.
Seven cloud-free Landsat-5 TM images were identified that corresponded with the peak vegetative growth period (June to July) in the study area. The images were reprojected to UTM 13N-NAD83 using the nearest neighbor resampling method and checked for co-registration. Further, the images were individually processed for radiometric calibration (Chander et al.,

2009) and atmospheric correction using the Fast Line-of-sight Atmospheric Analysis of Spectral Hypercubes (FLAASH; Anderson et al., 1999) using the image metadata and scene parameters to convert radiance units to surface reflectance values for spectral unmixing. Additionally, all processed scenes were transformed to NDVI images (Fig. 5.2) using the surface reflectance values in the near-infrared (NIR) and red (R) bands. All images were subset to the Park boundary and image processing was completed using ENVI 4.8 (ITTVIS, Boulder, CO, USA) and VIPER Tools 1.5 (UCSB, Santa Barbara).

Table 5.1 Time-series Landsat-5 TM imagery (L1T product) used in the study along with their scene ID, date of acquisition, and percent cloud cover (Source: United States Geological Survey; USGS). Only the imagery corresponding with the peak vegetative growth period and with <1% cloud cover were used in the study.

Scene ID	**Date of acquisition**	**Cloud cover**	**Sun azimuth**	**Sun elevation**	**Acquisition time**
LT50370261984202PAC00	20 July 1984	0	133.31	54.47	17:28:31
LT50370261989183XXX02	02 July 1989	0	131.28	56.65	17:27:17
LT50370261994181PAC03	30 June 1994	1	128.13	55.67	17:18:11
LT50370261999195PAC01	14 July 1999	0	135.58	56.53	17:37:20
LT50370262005195PAC01	14 July 2005	0	139.44	57.57	17:47:23
LT50370262006198PAC01	17 July 2006	0	148.82	57.72	17:52:43
LT50370262011196PAC01	15 July 2011	0	139.99	57.63	17:48:45

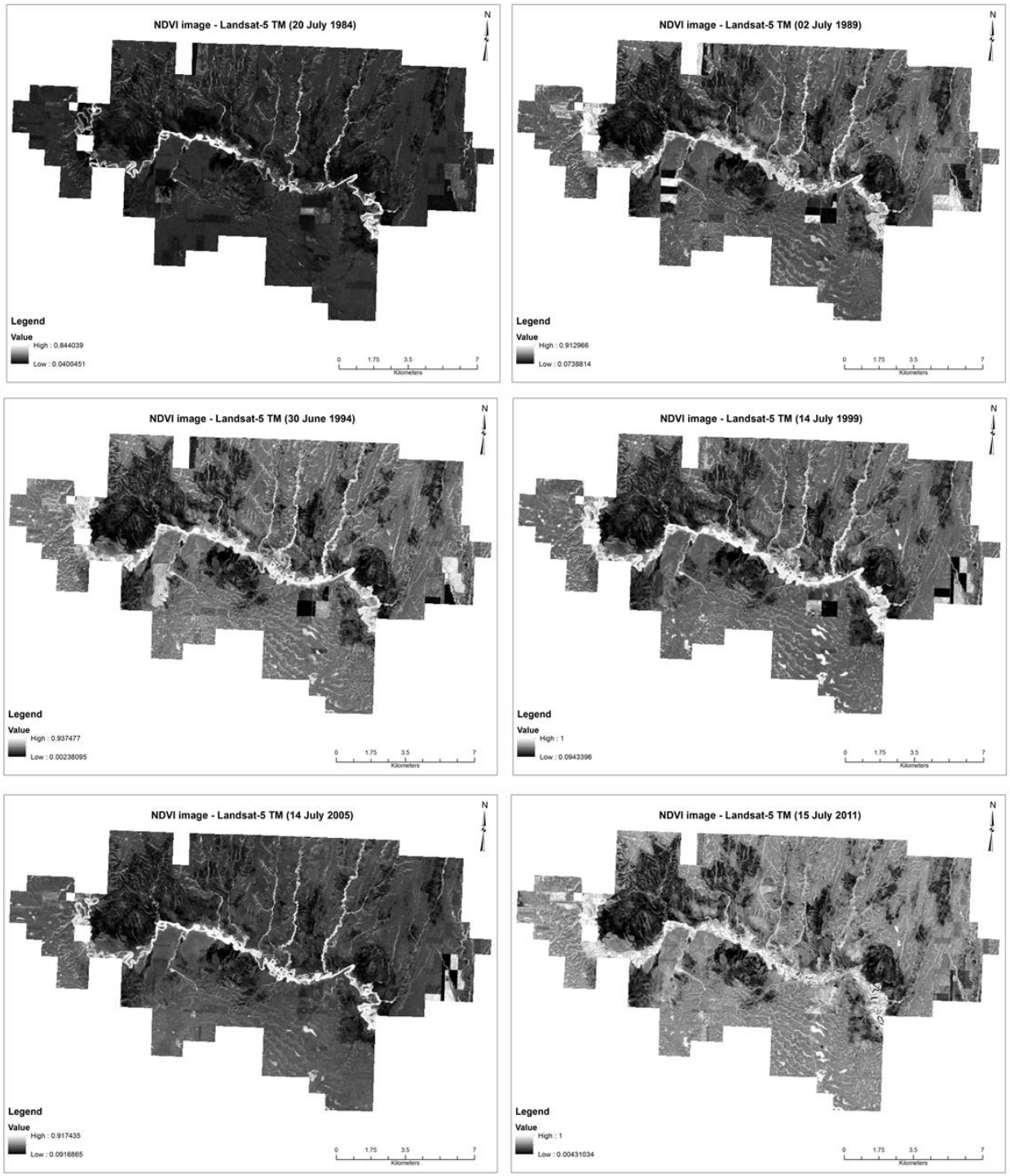

Fig. 5.2 NDVI images for the Landsat time-series (1984, 1989, 1994, 1999, 2005, 2011). Bright tones indicate higher NDVI values (higher vegetation), and darker tones indicate lower NDVI values (lower vegetation).

Field spectral measurements and processing

In-situ spectral reflectance for green vegetation (GV; grasses, shrubs, and forbs) and non-photosynthetic vegetation (NPV; dead or senesced plants, exposed or bare soil) were collected at 10 m sampling interval from 41 random sites (each site 100 m*100 m) in the West Block of GNPC in the summer of 2006 and 2007.

Spectra were collected using an ASD® FieldSpec FR Pro spectroradiometer (Analytical Spectral Devices Inc., Boulder, Colorado) at a spectral resolution of 3 nm in the 350-1000 nm and 10 nm in the 1000-2500 nm region. The spectroradiometer was held at a height of 1 m perpendicular to the target and fitted with a sensor of 25^{o} field of view. The spectral measurements were standardized to apparent reflectance using a Spectralon reference panel (Labsphere, New Hampshire). All spectral measurements were completed between 10:00 to 14:00 hours and under low wind conditions.

Additionally, reference (field) endmembers for GV, NPV and soil classes were collected at all possible site locations for developing spectral libraries to use in the spectral unmixing. As the purpose of the study was primarily for mapping dominant vegetation types, GV reference endmember spectra were also collected specifically for the major vegetation communities in the study area. While collecting GV endmembers, it was ensured that the dominant cover of the particular endmember was >80% on the ground. In addition, photoplots (vertical photos of quadrats) ensured that the post-processed spectra were allotted to the correct endmember spectral library group. A few non-dominant vegetation endmembers such as forbs, lichens, cacti, and moss were excluded as they would not be relevant at the landscape-level or are too sparse of cover to be resolved within the Landsat 30 m pixel.

Multiple endmember spectral mixture analysis (MESMA)

Multiple endmember spectral mixture analysis (MESMA), a modified form of spectral mixture analysis (SMA; Adams, 1993), permits endmembers to vary on a per-pixel basis and tests multiple unmixing models (combinations of endmembers) for each image pixel to estimate sub-pixel endmember fractions (Roberts et al., 1998; Somers et al., 2011). MESMA is used to unmix a remotely-sensed image by developing and using region-specific spectral libraries comprising of reference (field-collected) or image (image-derived) endmembers and their every possible

combination. MESMA identifies the best-fit model by requiring an unmixing model to meet minimum fit, fraction, and residual constraints for any image pixel. Types of SMA include multiple endmember SMA (Roberts, 1998), variable endmember SMA (Garcia-Haro, 1998), relative SMA (Okin, 2001), hierarchical SMA (Franke, 2009), and Bayesian SMA (Song, 2005). However, MESMA was chosen for this study due to its ability to incorporate spectral diversity of specific endmember and due to the availability of VIPER Tools.

Chapter 4 showed that MESMA is a successful and useful approach to identify and map the dominant vegetation types and their sub-pixel fractions in the northern mixed prairie. In that study, a total of 1150 endmembers representing GV (native prairie grasses, exotic grasses, shrubs and forbs), NPV (dead or senesced plants, burnt stems), and soil (exposed or bare soil) were obtained. Using a set of endmember selection metrics (Dennison et al., 2003a; 2003b), a comprehensive spectral library of 97 optimal endmembers representing 85 GV, 5 NPV, and 7 soil classes were identified for the study area. This comprehensive spectral library was convolved to the spectral bands of the Landsat-5 TM sensor and used to create 97 2-em models (combinations of a bright endmember and photometric shade). These 2-em models were used in the MESMA to unmix the image pixels into endmember fractions in each of the time-series imagery to identify and map the major vegetation types. Only 2-em models were used for the unmixing as the study objective was to identify and map the dominant vegetation types, even though in a previous study 3-em models (GV, non-vegetation (NPV, soil) and shade) were found to be more appropriate for this study area. Detailed description of the endmembers, their selection and optimization using selection metrics, MESMA and its set-up, and unmixing parameters are provided in the previous study. The same set of endmembers, 2-em unmixing models, and endmember model-fit constraints were used on all seven Landsat imagery. Note that since the seven TM images have the same georeferencing procedure and similar registration accuracy, the pixel locations and their values (fractions or NDVI) are assumed to be spatially comparable if no change has occurred. To ensure that the selected historical time points were spectrally comparable, Landsat imagery were chosen for phenologically-similar periods, i.e. for the peak vegetative growth period in the study area (Table 5.1, column 2).

Change-detection analysis

Change-detection analysis was performed on the MESMA fraction images and the NDVI images using a bi-temporal image-differencing approach, i.e. by subtracting each historical image from the 1984 image (base year) to produce change images, as our intent was to identify any areas showing consistent change over the 27-year period rather than to identify any small year-to-year change. The goal of bi-temporal image differencing was to identify the spatio-temporal changes to the land cover in the study area. Nine threshold classes (no change, < -0.75, -0.75 to -0.5, -0.5 to -0.25, -0.25 to 0, 0 to +0.25, +0.25 to +0.5, +0.5 to +0.75, > +0.75) were created for the NDVI change-difference image and nine threshold classes (no change, <0.125, 0.125 to 0.25, 0.25 to 0.375, 0.375 to 0.50, 0.50 to 0.625, 0.625 to 0.75, 0.75 to 0.875, > 0.875) created for the MESMA fraction change-difference image. These threshold classes were to identify areas of positive, no, or negative change and decided based on the descriptive statistics calculated for the seven TM images for the study area (Table 5.3). Areas of positive and negative change permitted us to identify the vegetation types that either increased or decreased in spatial extent over the 27-year timeframe. The threshold classes in the change-difference images were converted to vector polygons and geoprocessing analysis was done to simplify the interpretation.

Analysis of climate data

As climatic events would be the main factor controlling vegetation dynamics in the study area, climatic data of mean temperature and total precipitation (snow and rain combined) were obtained (Fig. 5.3) for the closest weather station: Val Marie (+49.37° N, -107.85° W), Saskatchewan.

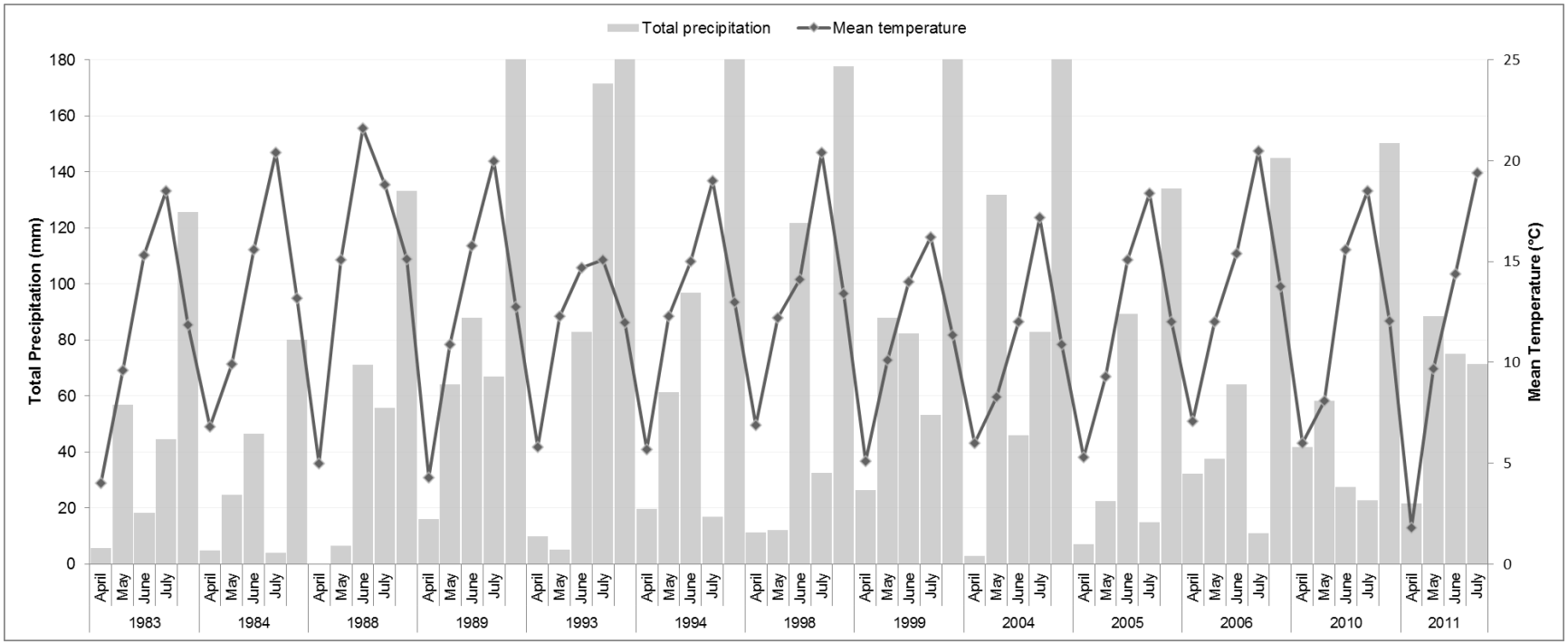

Fig. 5.3 Monthly (April-July) mean temperature (°C) and total precipitation (mm) in the study area for each selected historical year and the year preceding it. Data for Val Marie weather station (Source: Environment Canada) were compiled for the peak vegetative growth period (June-July) and 2-months prior to it. Note: Precipitation data unavailable for April, 1988.

5.3 RESULTS AND DISCUSSION

5.3.1 MESMA with 2-endmember models on historical imagery

In Chapter 4, the performance and usefulness of image unmixing using MESMA with 2- and 3-endmember models on a Landsat-5 TM image (acquired on 17 July 2006; Table 5.1) for the same study area has been described in detail. Using the same unmixing approach on the seven historical time-series Landsat-5 TM imagery, similar vegetation distribution trends as those reported by Michalsky and Ellis (1994) and He (2008) were observed over the study area (Fig. 5.4). The mapped vegetation distribution patterns from spectral unmixing were similar in all the historical imagery. This is to be expected as all the images were acquired for phenologically comparable time points (June-July) and made spectrally comparable using radiometric calibration and atmospheric correction. Therefore, the optimal GV, NPV and soil endmembers used in MESMA were spatially and temporally representative of the land cover seen in the study area. The similarity of the vegetation mapping patterns in the historical images indicate that MESMA can be effectively used as a standard semi-automated approach by developing comprehensive region-specific spectral libraries to identify the major vegetation types and their spatial distribution.

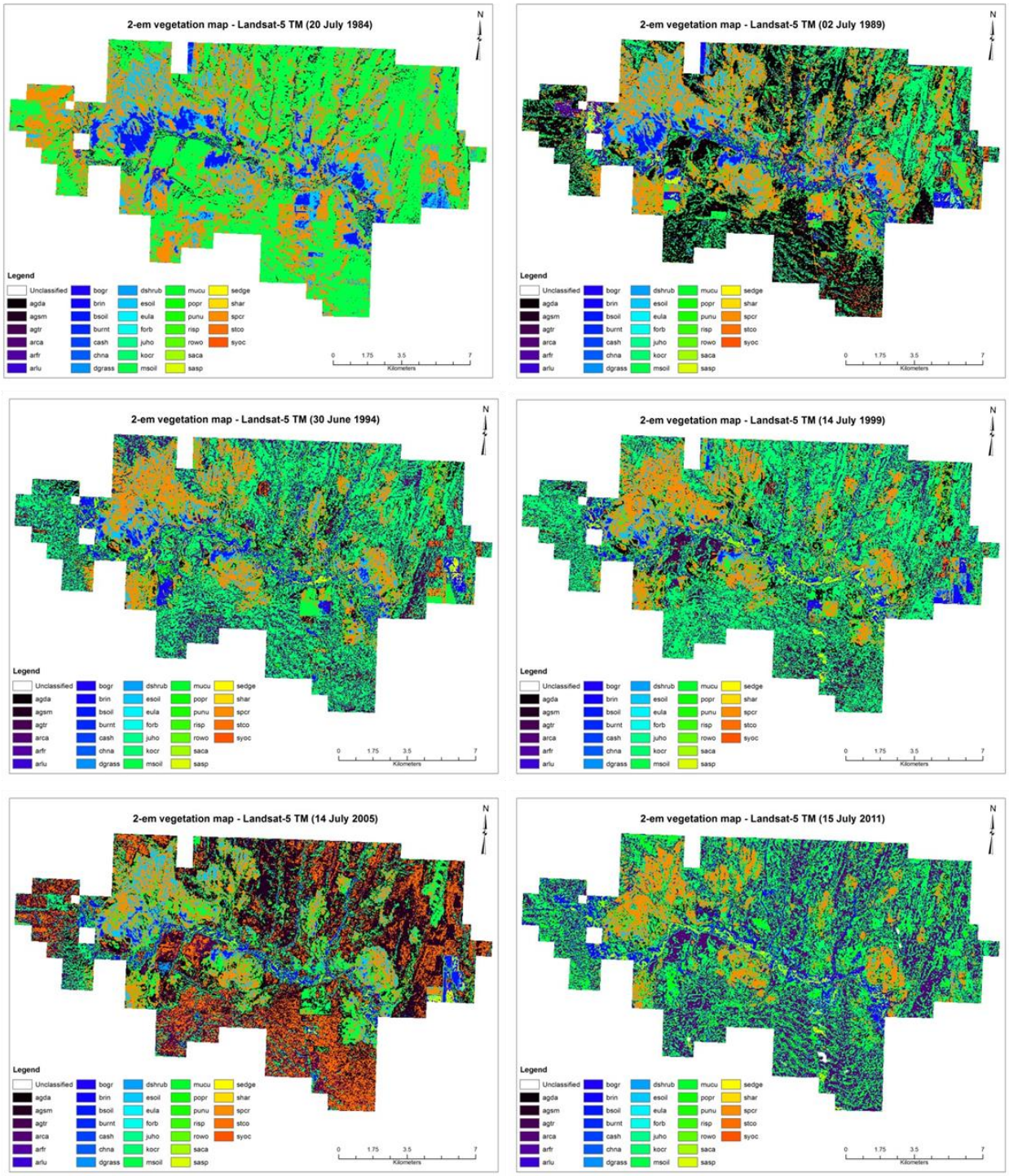

Fig. 5.4 Land cover mapped in the Landsat-5 time-series imagery (1984, 1989, 1994, 1999, 2005, 2011) using 2-em MESMA. Legend in each image shows the same 32 land cover classes.

The 97 2-em unmixing models individually tested on each of the historical images showed similar numbers of successful 2-em models, except for the 1984 image (Table 5.2). The number

of successful models differed between the images and ranged from 49 models (1984 image) to 84 models (2011 image). The numbers of successful models are comparable, except for the 1984 (49 models) and the 2005 (64 models) images. The 2011 image had 84 successful models which is highest than all the other years, and this might be due to 2011 being a 'wet year' and resulted in higher plant productivity and vegetation cover in the study area (Fig. 5.3). Similarly, NDVI values throughout the study area for 2011 were higher than the other years (Table 5.3). The similarity in the number of successful models further suggests that the compiled spectral library was effective in capturing the spectral variability on the landscape and representative of the materials in the images.

The image dates range from 30th of June to 20th of July (Table 5.2), however as the same set of endmembers were used to model the seven images, the difference in the number of successful 2-em unmixing models between the time-series images may be attributed to the spectral variability arising from plant phenology in the study area (Li and Guo, 2012). The effect of plant phenology on endmember selection and its impact on vegetation mapping have been discussed by Dennison and Roberts (2003b).The slight differences in the number of successful models may also be due to the variations in vegetation productivity associated with the trends in total precipitation or mean temperature (Fig. 5.3). This is clearly evident in the 2011 image when there is higher total precipitation leading to the development of sloughs and increased water levels in the creeks and streams and seen as unclassified pixels in the image. Research has indicated that soil moisture is the most important factor controlling plant growth in the study area, and vegetation productivity can increase under higher moisture availability.

Table 5.2 The number of successful 2-endmember models out of 97 models tested for each selected Landsat imagery.

Satellite image	**Date of acquisition**	**Number of successful models**
Landsat-5 TM	20 July 1984	49
Landsat-5 TM	02 July 1989	79
Landsat-5 TM	30 June 1994	79
Landsat-5 TM	14 July 1999	83
Landsat-5 TM	14 July 2005	64
Landsat-5 TM	17 July 2006	70
Landsat-5 TM	15 July 2011	84

The average of mean monthly (April-July) temperature and total precipitation (Fig. 5.3) showed that 2005 and 2006 coincided with low rainfall (134 mm and 145.1 mm) and slightly higher temperatures (12 ˚C and 13.8 ˚C). 1984 had the lowest rainfall (80.2 mm) and highest temperature (13.2 ˚C). Other than 1984, 2005 and 2006 showed the lowest NDVI values over the 27-year period. Rainfall was highly variable over the 27-year period. Therefore, the analysis of climatic trends suggests that rainfall and temperature are the most influencing factors for vegetation growth, and also explains the success of only 49 out of 97 models for the 1984 image.

Comparison of mean NDVI values (Table 5.3) for the study area against total precipitation revealed that higher NDVI values were seen for the years with higher precipitation (Fig. 5.3). Trends for NDVI are also positively related to the amount of precipitation received in the preceding year. This might be because the precipitation is stored as soil moisture and available for plant growth in the succeeding year. Analysis of mean NDVI values for the whole study area for the selected historical years (Table 5.3) revealed that NDVI values were lower in 1984, 2005, and 2006 (0.248, 0.360, 0.321, respectively). This trend further coincides with the number of successful 2-em models: 1984 showed the lowest number of successful models (49) when the mean NDVI in the study area was 0.248. Mean NDVI in 2011 was 0.518 and showed the highest number of 2-em models (84).

Table 5.3 Descriptive statistics (mean, minimum, maximum, and standard deviation) for NDVI and cover fraction estimated for the West Block of GNPC in the Landsat-5 TM time-series imagery.

Image date	**NDVI**				**Fractional cover**			
	Min.	Max.	Mean	S.D.	Min.	Max.	Mean	S.D.
20 July 1984	0.040045	0.844039	0.248012	0.073289	0.000000	1.049999	0.566372	0.474717
02 July 1989	0.073881	0.912966	0.380472	0.124053	0.000000	1.049999	0.555296	0.466955
30 June 1994	0.002381	0.937477	0.435184	0.137156	0.000000	1.049998	0.533489	0.450910
14 July 1999	0.09434	1.000000	0.431552	0.137763	0.000000	1.049999	0.533662	0.451473
14 July 2005	0.091686	0.917435	0.360097	0.118682	0.000000	1.049999	0.541122	0.457112
17 July 2006	0.087578	0.882840	0.321208	0.100141	0.000000	1.050000	0.546644	0.459510
15 July 2011	0.004310	1.000000	0.518098	0.129769	0.000000	1.049994	0.499826	0.427292

5.3.2 Land cover mapped in the satellite images

The major vegetation types and extent of dominant land cover were identified in each of the historical imagery (Fig. 5.4). The temporal variations in the proportion of land cover classes between images, if any, may be attributed to plant phenology, climatic events, natural- or anthropogenic-induced disturbances, or those arising due to the effects of climate change. Overall, the images were modeled with reasonable accuracy and the vegetation types were identified along the topographical and moisture gradients; the sparser native grasses were identified in the uplands and the riparian shrubs and invasive grasses were mapped along the river valley. Thus, the optimal endmembers included in the spectral library were effective in capturing the spectral diversity of the surface materials in the study area. A few of the unmodeled pixels were water (the Frenchman River). High residuals were seen for the very bright pixels, i.e. in the bad lands and densely vegetated areas. Unmixing with 2-em models showed that native prairie grasses, shrubs, and forbs as the dominant land cover (>80 % of the images); however this is slightly over-estimated and the bad lands are underestimated (Fig. 5.4). This result is similar to Okin et al. (2001) who found that MESMA overestimates vegetation in semi-arid environments with low vegetative cover. Nevertheless, these estimates from 2-em unmixing are reasonable taking into consideration that the soil or NPV classes are often seen mixed with GV.

5.3.3 Spatio-temporal vegetation changes in the northern mixed prairie

Change-detection analysis revealed that there were significant changes to the vegetation in the study area over the 27-year period. GNPC was acquired by Parks Canada in 1984 and since its acquisition, the Park has been actively following ecosystem management strategies such re-seeding of native prairie grasses, prescribed burning, and introducing plains bison (since 2006) for restoring and maintaining the native prairie biodiversity. Change-detection using NDVI images (Fig. 5.5) revealed that the vegetation trends are relatively stable in the GNPC area – see maps for image differencing of each historical NDVI image (Fig. 5.5a-5.5e) or land cover map (Fig. 5.6a-5.6e) from the 1984 NDVI image or land cover map. Of interest are the NDVI change-images for 1989, 1994, and 2011 that correspond to unique climatic events (Fig. 5.3). 2011 was a wet year with abundant moisture available for plant growth, hence increased NDVI values are seen throughout the park.

Comparison of Fig. 5.5f and 5.6f shows that similar spatial trends are seen in the NDVI and MESMA difference images. Both NDVI and MESMA images clearly picked out bad lands as areas of no or very minor change, and this is to be expected due to very low vegetation cover. Overall, it appears that the vegetation inside the park is stable, however much of the change pressure is in the southern portion of the park.

Fig. 5.5 Change-detection using NDVI images. 1984-1989 (5.5a), 1984-1994 (5.5b), 1984-1999 (5.5c), 1984-2005 (5.5d), 1984-2011 (5.5e). Areas (colored polygons) showing consistent NDVI change are shown in Fig. 5.5f.

Fig. 5.6 Change-detection using land cover maps from 2-em MESMA. 1984-1989 (5.6a), 1984-1994 (5.6b), 1984-1999 (5.6c), 1984-2005 (5.6d), 1984-2011 (5.6e). Areas (colored polygons) showing consistent land cover change are shown in Fig. 5.6f.

5.4 CONCLUSIONS

MESMA was found to be a reasonably effective technique for identifying spatio-temporal vegetation changes in the northern mixed prairie. Unlike the previous studies that have used NDVI-time series derived from Landsat, SPOT VEGETATION 10-day composites, or NOAA AVHRR maximum value composites (MVC), this study was more effective in identifying the vegetation change over the 27-year period.

The development of a comprehensive region-specific endmember spectral library greatly helped to identify the land cover or vegetation types in the historical imagery. The consistent unmixing and the similarity of vegetation patterns identified and mapped across all seven TM images indicates that MESMA is an effective mapping technique to use with time-series imagery to monitor ecosystem changes. However, future research should consider the effects of vegetation phenology and account for extreme climatic events.

The results obtained from unmixing and spatio-temporal change analysis can be used in identifying the success of biodiversity conservation efforts, identifying zones of major threat, and developing ecosystem prediction models. However, it should be stressed that the success of MESMA greatly depends on the selection of optimum number and type of endmembers which are region-specific and also those that take into account the spectral diversity on the landscape. Spectral variability is problematic in semi-arid regions and this can be overcome to a certain extent by collecting vegetation endmembers throughout the vegetation growth period. However, if the goal is to identify plants at the species-level, researchers should take into plant phenology and acquire imagery for time periods that will permit the greatest discrimination among the different vegetation types.

Overall, this study was successful in using MESMA with medium-resolution multispectral imagery such as Landsat-5 TM. Archived Landsat imagery since 1972 from MSS, TM, and ETM+ sensors is openly available. Note that the Landsat-5 TM sensor failed in 2011 and the Landat-7 ETM+ sensor has striping issues since 2003. The Landsat program has provided 40 years of imagery for earth observation and monitoring, Landsat-8 launched by USGS and NASA in February 2013 continue to provide free imagery as part of the Landsat data continuity mission (LDCM; Irons et al., 2012). Using a similar approach, future studies may employ MESMA on Landsat-8 imagery to other ecosystems or environments to identify ecosystem changes over

space and time. Data sources such as RapidEye and WorldView with finer temporal resolution and a vegetation specific red-edge band provide enhanced opportunities for ecosystem monitoring.

5.5 ACKNOWLEDGEMENTS

Financial support for this study was provided by the University of Saskatchewan, Saskatchewan Environment, and Nature Saskatchewan. Fieldwork assistance of Jesse Nielsen, Randy Bonin, Chunhua Zhang and Yuhong He is gratefully acknowledged. Xulin Guo (U of S), Joseph Piwowar (Univ. of Regina), and Greg McDermid (Univ. of Calgary) shared instruments. Open-source imagery from USGS and GeoBase were used in this study, and is greatly appreciated.

5.6 REFERENCES

Adams, J.B., Smith, M.O., and Gillespie, A.R. 1993. Imaging spectrometry: interpretation based on spectral mixture analysis, In Pieters CM, Englert P, editors. Remote geochemical analysis: elemental and mineralogical composition. New York: Cambridge Univ. Press, 7: 145-166.

Anderson, G.P., Pukall, B. Allred, C.L. Jeong, L.S. Hoke, M. Chetwynd, J.H. Adler-Golden, S.M. Berk, A. Bernstein, L.S. Richtsmeier, S.C. Acharya, P.K.. and Matthew, M.W. 1999. FLAASH and MODTRAN4: state-of-the-art atmospheric correction for hyperspectral data. *IEEE Proceedings of Aerospace Conference*, pp. 177-181, Snowmass at Aspen, CO, USA.

Ballantine, J-A C., Okin, G.S., Prentiss, D.E., and Roberts, D.A. 2005. Mapping African landforms using continental scale unmixing of MODIS imagery. *Remote Sensing of Environment*, 97(4): 470-483.

Beyer, H.L. 2010. Geospatial Modelling Environment (version 0.5.2 Beta). (software). URL: http://www.spatialecology.com/gme.

Blood, D.A., and Ledingham, G.F. 1986. *An evaluation of interim range management options on lands acquired for the purpose of establishing Grasslands National Park.* Prepared for Parks Canada by D.A. Blood and Associates Ltd. 189 pp.

Boardman, J.W., Kruse, F.A., and Green, R.O. 1995. Mapping target signatures via partial unmixing of AVIRIS data in Summaries of the 5th JPL Airborne Earth Science Workshop, JPL Publication 95-1, Vol 1, Jet Propulsion Laboratory, Pasadena, CA pp. 23-26.

Chander, G., Markham, B.L., and Helder, D.L. 2009. Summary of current radiometric calibration coefficients for Landsat MSS, TM, ETM+, and EO-1 ALI sensors. *Remote Sensing of Environment*, 113(5): 893-903.

Coppin, P., Jonckheere, I., Nackaerts, K., and Muys, B. 2004. Digital change-detection methods in ecosystem monitoring: A review. *International Journal of Remote Sensing*, 25(9): 1565-1596.

Davidson, A., and Csillag, F. 2001. The influence of vegetation index and spatial resolution on a two-date remote sensing-derived relation to C4 species coverage. *Remote Sensing of Environment,* 75(1): 138-151.

Dennison, P.E., Charoensiri, K., Roberts, D.A., Peterson, S.H., and Green, R.O. 2006. Wildfire temperature and land cover modeling using hyperspectral data. *Remote Sensing of Environment*, 100(2): 212-222.

Dennison, P.E., and Roberts, D.A. 2003a. Endmember selection for multiple endmember spectral mixture analysis using endmember average RMSE. *Remote Sensing of Environment*, 87: 2-3, 123-135.

Dennison, P.E., and Roberts, D.A. 2003b. The effects of vegetation phenology on endmember selection and species mapping in Southern California chaparral. *Remote Sensing of Environment*, 87(2-3): 295-309.

Dennison, P.E., Halligan, K.Q., and Roberts, D.A. 2004. A comparison of error metrics and constraints for multiple endmember spectral mixture analysis and spectral angle mapper. *Remote Sensing of Environment*, 93(3): 359-367.

Dennison, P.E., Roberts, D.A., and Peterson, S.H. 2007. Spectral shape-based temporal compositing algorithms for MODIS surface reflectance data. *Remote Sensing of Environment,* 109(4): 510-522.

Elmore, A.J., Mustard, J.F., Manning, S.J., and Lobell, D.B. 2000. Quantifying vegetation change in semiarid environments: precision and accuracy of spectral mixture analysis and the normalized difference vegetation index, *Remote Sensing of Environment,* 73: 87-102.

Franke, J., Roberts, D.A., Halligan, K., and Menz, G. 2009. Hierarchical Multiple Endmember Spectral Mixture Analysis (MESMA) of hyperspectral imagery for urban environments. *Remote Sensing of Environment*, 113(8): 1712-1723.

Fraser, R.H., Olthof, I., and Pouliot, D. 2009. Monitoring land cover change and ecological integrity in Canada's national parks. *Remote Sensing of Environment*, 113(7): 1397-1409.

Gardner, M. 1997. *Mapping chaparral with AVIRIS using Advanced Remote Sensing Techniques*. M.Sc. Thesis, University of California, Santa Barbara.

García-Haro, F.J., Sommer, S., and Kemper, T. 2005. A new tool for variable multiple endmember spectral mixture analysis (VMESMA). *International Journal of Remote Sensing*, 26(10): 2135-2162.

Gauthier, D.A., Lafon, A., Toombs, T., Hoth, J., and Wiken, E. 2003. Grasslands: Toward a North American Conservation Strategy. Canadian Plains Research Center, University of Regina, Regina, Saskatchewan, and Commission for Environmental Co-operation, Montreal, Quebec, Canada.

Halligan, K.Q. 2002. *Multiple endmember spectral mixture analysis of vegetation in the northwest corner of Yellowstone National Park*. M.Sc. Thesis, University of California, Santa Barbara.

Harms, V.L. 2006. *Annotated catalogue of Saskatchewan vascular plants*. 116 pp.

He, Y., Guo, X., and Wilmshurst, J. 2006. Studying mixed grassland ecosystems I: suitable hyperspectral vegetation indices. *Canadian Journal of Remote Sensing*, 32(2): 98-107.

He, Y., Guo, X., and Si, B.C. 2007. Detecting grassland spatial variation by a wavelet approach. *International Journal of Remote Sensing*, 28(7): 1527-1545.

He, Y., Guo, X. and Wilmshurst, J.F. 2007. Comparison of different methods for measuring leaf area index in a mixed grassland. *Canadian Journal of Plant Science*, 87(4): 803-813.

He, Y. 2008. *Modeling Grassland Productivity through Remote Sensing Products.* Ph.D. Thesis, University of Saskatchewan, Saskatoon.

Irons, J.R., Dwyer, J.L., and Barsi, J.A. 2012. The next Landsat satellite: The Landsat data continuity mission. *Remote Sensing of Environment*, 77(2): 212-225.

Looman, J., and Best, K.F. 1987. *Budd's flora of the Canadian Prairie Provinces.* Research branch, Agriculture Canada, Publication 1662. 863 pp.

Li, Z., and Guo, X. 2010. A suitable vegetation index for quantifying temporal variations of LAI in semi-arid mixed grassland. *Canadian Journal of Remote Sensing*. 36(6): 709-721.

Li, Z., and Guo, X. 2012. Detecting climate effects on vegetation in northern mixed prairie using NOAA AVHRR 1-km time-series NDVI data. *Remote Sensing*. 4(1): 120-134.

Lu, D., Mausel, P., Brondízio, E., and Moran, E. 2004. Change-detection techniques. *International Journal of Remote Sensing*, 25(12): 2365-2401.

Michalsky, S.J., and Ellis, R.A. 1994. Vegetation of Grasslands National Park. DA Westworth and Associates, Calgary.

Okin, G.S., Roberts, D.A., Murray, B., and Okin, W.J. 2001. Practical limits on hyperspectral vegetation discrimination in arid and semiarid environments. *Remote Sensing of Environment*, 77(2): 212-225.

Ollinger, S.V. 2011. Sources of variability in canopy reflectance and the convergent properties of plants. *New Phytologist*, 189(2): 375-394.

Painter, T.H., Dozier, J., Roberts, D.A., Davis, R.E., and Green, R.O. 2003. Retrieval of subpixel snow-covered area and grain size from imaging spectrometer data. *Remote Sensing of Environment*, 85: 64-77.

Painter, T.H., Roberts, D.A., Green, R.O., and Dozier, J. 1998. The effect of grain size on Spectral Mixture Analysis of snow-covered area from AVIRIS data. *Remote Sensing of Environment*, 65(3): 320-332.

Powell, R. 2006. Long-term monitoring of urbanization in the Brazilian Amazon using remote sensing. Ph.D. Thesis, University of California, Santa Barbara.

Powell, R., Roberts, D.A., Dennison, P.E., and Hess, L.L. 2007. Sub-pixel mapping of urban land cover using multiple endmember spectral mixture analysis: Manaus, Brazil. *Remote Sensing of Environment*, 106(2): 253-267.

Rashed, T., Weeks, J.R., Roberts, D., Rogan, J., and Powell, R. 2003. Measuring the physical composition of urban morphology using multiple endmember spectral mixture models. *Photogrammetric Engineering & Remote Sensing*, 69(9): 1011-1020.

Roberts, D.A., Adams, J.B., and Smith, M.O. 1993. Discriminating green vegetation, non-photosynthetic vegetation and soils in AVIRIS Data. *Remote Sensing of Environment*, 44: 255-269.

Roberts, D.A., Batista, G., Pereira, J., Waller, E., and Nelson, B. 1998. Change identification using multitemporal spectral mixture analysis: Applications in Eastern Amazonia, Chapter 9 in Remote Sensing Change Detection: Environmental Monitoring Applications and Methods, (Elvidge, C. and Lunetta R., Eds.), Ann Arbor Press, Ann Arbor, MI, pp. 137-161.

Roberts, D.A., Brown, K.J., Green, R., Ustin, S., and Hinckley, T. 1998. Investigating the relationship between liquid water and leaf area in clonal Populus, Proc. 7th AVIRIS Earth Science Workshop JPL 97-21, Pasadena, CA 91109: 335-344.

Roberts, D.A., Dennison, P.E., Gardner, M., Hetzel, Y., Ustin, S.L., and Lee, C. 2003. Evaluation of the potential of Hyperion for fire danger assessment by comparison to the Airborne Visible/Infrared Imaging Spectrometer. *IEEE Transactions on Geoscience and Remote Sensing*, 41(6): 1297-1310.

Roberts, D.A., Gardner, M., Church, R., Ustin, S.L., and Green, R.O. 1997. Optimum Strategies for mapping vegetation using multiple endmember spectral mixture models, in SPIE Conf. Vol 3118, Imaging Spectrometry III, 108-119., San Diego, CA July 27-Aug 1, 1997.

Roberts, D.A., Gardner, M., Church, R., Ustin, S., Scheer, G., and Green, R.O. 1998. Mapping Chaparral in the Santa Monica Mountains using Multiple Endmember Spectral Mixture Models. *Remote Sensing of Environment*, 65(3): 267-279.

Roberts, D.A., Green, R.O., and Adams, J.B. 1997. Temporal and spatial patterns in vegetation and atmospheric properties from AVIRIS. *Remote Sensing of Environment*, 62(3): 223-240.

Roberts, D.A. and Herold, M. 2004. Imaging Spectrometry of Urban Materials, in Molecules to Planets: Infrared Spectroscopy in Geochemistry, Exploration Geochemistry and Remote Sensing (P. King, M. Ramsey and G. Swayze, Ed), Mineral Association of Canada, 155-183.

Roberts, D.A., Numata, I., Holmes, K.W., Batista, G., Krug, T., Monteiro, A., Powell, B., and Chadwick, O. 2002. Large area mapping of land-cover change in Rondônia using multitemporal spectral mixture analysis and decision tree classifiers. *Journal of Geophysical Research: Atmospheres,* 107: LBA 40-1-LBA 40-18.

Roberts, D.A., Ustin, S.L., Ogunjemiyo, S., Greenberg, J., Dobrowski, S.Z., Chen, J. and Hinckley, T.M. 2004. Spectral and structural measures of Northwest forest vegetation at leaf to landscape scales. *Ecosystems*, 7(5): 545-562.

Samson, F., and Knopf, F. 1994. Prairie conservation in North America. *Bioscience*, 44(6): 418-421.

Samson, F., and Knopf, F. 1996. Prairie conservation: Preserving North America's most endangered ecosystem. Island Press. Washington D.C. and Covello, California, USA.

Sonnetag, O., Chen, J.M., Roberts, D.A., Talbot, J., Halligan, K.Q., and Govind, A., 2007. Mapping tree and shrub leaf area indices in an ombrotrophic peatland through multiple endmember spectral unmixing. *Remote Sensing of Environment*, 109(3): 342-360.

Saskatchewan Institute of Pedology, 1992. Grasslands National Park Soil Survey, University of Saskatchewan, Saskatoon.

Settle, J.J., and Drake, N.A. 1993. Linear mixing and the estimation of ground cover proportions, *Int. J. Remote Sens.*, 14(6): 1159-1177.

Singh, A. 1989. Digital change-detection techniques using remotely sensed data. *International Journal of Remote Sensing*, 10(6): 989-1003.

Somers, B., Asner, G.P., Tits, L., and Coppin, P. 2011. Endmember variability in spectral mixture analysis: A review. *Remote Sensing of Environment*, 115(7): 1603-1616.

Song, C. 2005. Spectral mixture analysis for subpixel vegetation fractions in the urban environment: How to incorporate endmember variability? *Remote Sensing of Environment*, 95(2): 248-263.

Tompkins, S., Mustard J.F., Pieters, C.M., and Forsyth, D.W. 1997. Optimization of endmembers for spectral mixture analysis. *Remote Sensing of Environment*, 59(3): 472-489.

Ustin, S.L., Roberts, D.A., Gamon, J.A., Asner, G.P., and Green, R.O. 2004, Using imaging spectroscopy to study ecosystem processes and properties. *Bioscience*, 54(6): 523-534.

Zhang, C., and Guo, X. 2007. Measuring biological heterogeneity in the northern mixed prairie: a remote sensing approach. *The Canadian Geographer*, 51(4): 462-474.

Zhang, C. 2008. *Monitoring Biological Heterogeneity in a Northern Mixed Prairie Using Hierarchical Remote Sensing Methods.* Ph.D. Thesis, University of Saskatchewan, Saskatoon.

Zhou, W. 2007. *Assessing Remote Sensing Application on Rangeland Insurance in Canadian Prairies.* M.Sc. Thesis, University of Saskatchewan, Saskatoon.

CHAPTER 6

6.1 SUMMARY

Scale and scaling are fundamental topics of interest and active research in ecology, remote sensing, and GIScience (Chave, 2013; Turner, 1989; Urban, 2005; Wessman, 1992; Goodchild, 2001). Often, ecological data are collected at a single measurement scale or dependent on the sampling methods used, and the analysis scale is determined by the specific purpose of the study or by the data sets used in the study. Also, scientists frequently require upscaling or downscaling to obtain predictions or information at alternate scales. These situations introduce discrepancy between the scale at which data is collected or analyzed and the scale at which conclusions have to be derived for management action or decision-making. Several researchers have confirmed that conclusions and observed patterns change with scale and there are direct implications by selecting an arbitrary scale of study (Wiens, 1989; Wu, 1999; Wessman, 1992; Turner, 1989; Dungan et al., 2002; Urban, 2005; Wu et al., 2006). Therefore, a rational choice would be to adopt a multi-scalar approach thereby making it possible to identify the limitations of the specific scale used in the study or to identify the scales at which patterns, processes, or phenomena become relevant.

Remotely sensed (RS) data sets are increasingly being used in ecological studies and ecosystem monitoring due to their ability to provide multi-scalar ecological and environmental information for large areas in an instantaneous and cost-effective manner. Thus, as the science and technology of RS advances, ecologists and scientists have access to wide selection of multi-scalar RS data sets from different platforms (ground-, airborne-, or satellite). Hence, it is important to identify how they compare and which scales of RS data can provide relevant information while maintaining a high benefit-to-cost ratio.

In this dissertation, I specifically examined the implications of scale of RS data for vegetation analysis in the northern mixed prairie. My research utilized RS data sets at different spatial, spectral, and temporal scales: plot-level spectroradiometer data to landscape-level satellite imagery with varying spatial and spectral resolutions and over a 27-year time frame. These RS

data sets were supplemented with field-collected vegetation data such as plant cover, aboveground biomass, leaf area index (LAI), dominant species, and plant height.
The fundamental research hypothesis tested was that multi-scalar RS data can be useful and successfully exploited to reveal important spatial patterns, biophysical characteristics, and dynamics of the northern mixed prairie vegetation. Specifically, I tested the following hypotheses: 1) RS data sets can be used to identify the spatial variation and spatial scales of plant biophysical variables representing greenness and wetness; 2) a simultaneous comparison of RS data at different scales helps to identify the limitations of scale; 3) implications exist when upscaling RS data from finer to coarser spatial scales; 4) effects of spatial autocorrelation are evident in RS data sets acquired for the northern mixed prairie; 5) spectral unmixing approaches are better suited for incorporating the spatial- and spectral-heterogeneity of vegetation in the northern mixed prairie; and 6) developing a region-specific and comprehensive (spatial-temporal) endmember library is useful for change-detection of vegetation.

My research specifically focused on the lowland vegetation types that have been ignored in previous studies, but are considered ecologically significant by ecologists and conservationists, and therefore deserved detailed study. Fundamental biophysical and spectral characteristics of the lowland vegetation identified in this research are an important outcome of my study. Though previous research has tested the effects of scale to some extent, none has considered the implications of using RS data at multiple scales or by comparing them in tandem. The results from my study indicate that the spatial patterns of vegetation change with scale, thus a multi-scalar approach can identify important characteristics about the mixed prairie vegetation.

6.2 CONCLUSIONS

My research as a whole has advanced the understanding of RS of the northern mixed prairie vegetation, especially in the context of effects of scale and scaling. From an eco-management perspective, this research has provided cost- and time-effective methods for vegetation monitoring. The following four sections summarize the major findings:

6.2.1 Multi-scalar comparison of plant biophysical properties along topographical gradients

RS data at all data scales successfully captured the spatial variation of biophysical properties along topographical gradients. An inverse relationship was observed for plant cover, LAI, and VI to topographic gradients. VI at all spatial scales showed significant relationships to plant cover and LAI; however VI at finer scales showed the strongest relationship. The spatial scales of variation were different for VI_n, VI_b, and LAI and ranged between 35 and 200 m. Pixel size of imagery finer than 20 m is recommended as ideal for studying the biophysical properties of the mixed prairie vegetation.

6.2.2 Spatial scale and effects of upscaling in the northern mixed prairie

Comparison of RS data at different spatial scales from four remote sensors revealed that VI_n, VI_b, and LAI increased withelevation and slope. RS data at finer scales showed the strongest ability than coarser scales to estimate ground vegetation. VI_n were found to be better predictors than VI_b in estimating LAI, and upscaling from all four spatial scales showed similar weakening trends for VI_b to predict LAI. Spatial autocorrelation was present in the data sets, violating the conditions of global regression models. However, the use of spatial regression models in-lieu of global regression models accounted for spatial- autocorrelation and dependency in the RS data and significantly improved the prediction results.

6.2.3 Vegetation mapping using spectral unmixing approaches

Compared to whole pixel-based and object-oriented classifiers, MESMA was found to be more effective than simple SMA and produced improved vegetation maps. MESMA successfully captured the spatial heterogeneity of vegetation and incorporated the spectral variability of land cover within the study area. By developing a comprehensive region-specific endmember library and identifying optimal endmembers, MESMA successfully mapped the dominant vegetation types and estimated sub-pixel fractions of GV, NPV, and soil for the study area. The efficiency of spectral unmixing was found to be highly dependent on the identification of optimal endmembers, however not all endmembers were successfully modeled. Comparison of MESMA on the three imagery types showed spectral resolution to be important over spatial resolution. 3-

em models were found to be better suited than the 2-em models for modeling vegetation types in the study area, however the availability of only multispectral imagery limited the full unmixing capability. The methodology presented would be more effectively used on hyperspectral imagery if it becomes available for the northern mixed prairie. Nevertheless, map products derived from spectral unmixing are useful for monitoring and management of native and invasive vegetation, habitat- and fire-modeling, and effective park management.

6.2.4 Spatio-temporal changes to the northern mixed prairie vegetation

Image unmixing and change-detection analysis showed that MESMA can be used as a standard tool for identifying spatio-temporal changes on time-series imagery. MESMA was effective in mapping the dominant vegetation types and produced comparable mapping results for each image in the time-series. Climatic variables of temperature and precipitation were found to affect the number of successful image unmixing models, with fewer successful unmixing models for years of climatic extremes. Change-detection showed the effectiveness of biodiversity conservation practices of GNPC since establishment and suggests that its managementstrategies are effective in maintaining heterogeneity of vegetation in the park region. The methodology presented can be continued to be used to monitor spatio-temporal changes in the northern mixed prairie, and may be tested in other ecosystems to gain valuable insight into their dynamics.

6.3 FUTURE RESEARCH AND OPPORTUNITIES

My research utilized RS data at multiple scales (field- and satellite-level) and compared them for studying the northern mixed prairie vegetation. Though the methods were somewhat effective with multispectral imagery (10 m or coarser), future research should be able to achieve better success with the methods presented in this study using airborne or satellite hyperspectral imagery, should they become available for the northern mixed prairie. Regardless, the current availability of finer spatial and temporal resolution multispectral data sets such as WorldView-2 (0.5 m, 8 bands), RapidEye (5 m, 5 bands), and Landsat-8 (30 m, 11 bands) with their vegetation-specific red-edge band offer immediate opportunities to re-test the methods used in this study.

The East Block of GNPC has slightly different vegetation types compared to the West Block, and therefore an elaborate and comprehensive spectral library development will be useful as the same mapping methodology can be applied for the East Block. Unmixing methods have been shown to be effective for mapping soils in semi-arid regions (Okin et al., 2001). Therefore, the incorporation of more soil endmembers might be helpful in the image unmixing as exposed soil (bad lands) is seen in some parts of the study area. This research focused only on the area within the GNPC, i.e. conserved lands. Future research could explore spatio-temporal dynamics outside the park, however this will require spectral reflectance data for the land cover and land use (cultivated crops and forage) outside the park. Therefore, understanding of the land use-land cover around the park and the development of spectral libraries specific to those cover classes may help to identify spatio-temporal changes beyond the park boundary. It might be useful to explore different field sampling approaches to identify their effects on scaling.

The short vegetation growth period and the effect of plant phenology in the northern mixed prairie (Zhang, 2008; Li and Guo, 2012) should be considered while identifying and selecting imagery for any vegetation analysis and for spectral unmixing. Though the general plant phenological trends in the region are known at coarser temporal scales, future studies could research the differences in the spectral response arising due to phenology of the dominant grass vegetation with multiple field spectral acquisitions (spectroradiometry) throughout the vegetative growth period, i.e. at finer temporal scales. Ideally, green vegetation endmembers corresponding with the vegetative growth period should be incorporated into the unmixing models. Having knowledge of vegetation phenology, one might be able to select phenology-specific endmembers for a particular plant species and utilize in the endmember model building and spectral unmixing. The current study was interested in the general mapping of the dominant vegetation types, however any particular vegetation types of interest may be better identified by using imagery in the latter vegetation growth period (e.g., shrubs or smooth brome might be better mapped in the August or September imagery when the native prairie grasses have completely senescenced).

This study used multispectral imagery and 2- and 3-em models for unmixing. Future research may utilize the spectral unmixing methodology with hyperspectral imagery with hundreds of

continuous narrow bands to an even greater level of success (Schaepman et al., 2009). With the availability of hyperspectral imagery, 3- or even 4-em models could be tested. Okin et al. (2001) found that even 4-em MESMA is deficient in reliably estimating vegetation fractions when plant cover is <30% and seen mixed with soil. Further research needs to be attempted in other semi-arid regions to develop more robust spectral unmixing techniques that can account for non-linear mixing. However, this will require better understanding of the interaction of reflectance spectra of vegetation and background materials. In general, higher awareness about the processing and calibration of hyperspectral data sets is needed (Kokaly et al., 2009; Plaza et al., 2009). Increased education about the usefulness of hyperspectral data sets is also needed (Goetz, 2009). The free availability of hyperspectral data sets such as EO-1 ALI and Hyperion from USGS and AVIRIS from JPL are good initiatives.

Hyperspectral imagery can give insight into important biophysical characteristics and biochemical properties, and also provide vegetation maps at the species-level. However with the use of hyperspectral imagery, consideration will need to be given for data redundancy, data reduction, and the identification of optimum bands for vegetation mapping, species identification, and also in the development of more robust VI*n* (i.e. those compensating for background effects) for studying specific vegetation properties. Integration of spectral and spatial information for image classification and object-identification and mapping seems to be the direction in the current state-of-research (Plaza et al., 2009). Integration of diverse data sets such as multispectral or hyperspectral data with LiDAR and improvements in object-oriented and knowledge-based classifiers are worth mentioning.

Results showed that the field endmembers do not effectively upscale to those acquired through satellite RS. Further research may be undertaken with field spectroscopy to understand the degree or level of spectral mixing (pixel aggregation) by varying the field-of-view (FOV) of the remote sensor and how the contribution of background materials change with variation to FOV of the sensor. Milton et al. (2007) and Schaepman et al. (2009) provide comprehensive reviews on the advancements made in the field of field spectroscopy, especially in the context of earth science applications.

Spectral unmixing with hyperspectral imagery has been used in several applications, however unmixing with multispectral imagery has not been greatly exploited. This study showed that it is possible to derive landscape-level vegetation maps that are useful for multiple applications with the development of comprehensive endmember spectral libraries. Unlike the huge costs for objected-oriented classifier tools and their specificity, the availability of open-source tools such as VIPER (Roberts et al., 2007) and VMESMA (Garcia-Haro, 1998) allow unmixing and mapping using hyperspectral and multispectral images. Also worth mentioning are free tools such as SPRING and OTB.

Many of the publically-available spectral library databases (USGS, JPL) lack endmember spectra for native prairie vegetation. Therefore, by developing and sharing comprehensive spectral libraries for the prairie vegetation, researchers working in other similar ecosystems (such as steppes in Eurasia and pampas in South America) may benefit by utilizing the same approach for vegetation mapping, analysis, and monitoring. Obviously, spectral library standardization and metadata procedures will also need to be improved. Efforts such as SPECNET (Spectral Network; Gamon et al., 2006), SPECCHIO (Spectral Input/Output; Bojinski et al., 2003), and open-source spectral library initiatives should be encouraged (Hueni et al., 2009).

Grasslands are significant carbon sinks. Future research may use spectral unmixing methods to identify the effects of grazing by natural- and introduced-herbivores to understand how grazing affects the carbon sequestration process in grasslands (see Yang and Guo (2011) and Yang et al. (2012)). Mapping of standing dead biomass (non-photosynthetic vegetation) through spectral unmixing may be attempted as it might help in the prediction and management of natural fires in the region.

Scaling is an on-going topic of research in RS. Though the general spectral reflectance behavior of vegetation, soil, and water is understood at the leaf-level (Jacquemond et al., 2000), robust scaling laws and algorithms need to be developed at canopy scales. Scientists believe that the uncertainties with scaling relationships or processes from leaf-to-canopy-to-ecosystem may be better understood by using imaging spectroscopy (Kokaly et al., 2009; Blackburn, 2007; Schaepman et al., 2009).

The Landsat project since 1972 has become the longest imaging program for terrestrial or earth-observation data (Wulder et al., 2008; Wulder et al., 2012 Roy et al., 2014). Therefore, earth observation and vegetation monitoring should be more readily feasible with the availability of RS data sets such as Landsat-8 from the LDCM (Irons et al., 2012) and Sentinel missions. Leimgruber et al. (2005) has discussed the impact of Landsat for conservation biology. Perhaps, there needs to be more collaborative and inter-disciplinary studies among ecologists and RS scientists so that these archived time-series data sets are utilized more readily and effectively. Availability of DMC and RapidEye data sets at very fine temporal resolution provides better opportunities for monitoring. Though the approaches described in this study can be readily replicated on Landsat-8 imagery, readers should be aware about the band changes to the imagery (Irons et al., 2012).

Researchers have worked specifically on plant spectral signatures to identify important canopy traits and plant biophysical characteristics (Blackburn, 2007; Ollinger, 201; Asner et al., 2009; Kokaly et al., 2009; Ustin and Gamon, 2010). Grasslands being important carbon fixers, RS may be attempted to explore as to how foliar pigment and water content, nutrient and forage quality may be estimated. Future imaging spectrometer missions such as the Hyperspectral Environment and Resource Observer (HERO), Environmental Mapping and Analysis Program (EnMAP; Blackburn, 2007), the Accelerated Canopy Chemistry Program (ACCP, 1994) of NASA (National Aeronautics and Space Administration), the European Global Monitoring for Environment and Security (GMES) program , and the HyspIRI (Hyperspectral Infrared Imager) projects may facilitate the development of a greater range of scientific and practical applications of hyperspectral vegetation analysis.

Ecologists, as they are increasingly inclined to use finer spatial resolution RS data sets for large-scale research, need to account for the spatial effects (spatial- autocorrelation and dependency) and how it may impact their results or predictions. Many software packages such as ArcGIS, GeoDA, GWR (Geographically Weighted Regression), QGIS, Surfer, SAGA (System for Automated Geoscientific Analyses), SpaceStat, R, SAM (Spatial Analysis for Macroecology;

Rangel et al., 2010), and PASSAGE (Pattern Analysis, Spatial Statistics and Geographic Exegesis; Rosenberg and Anderson, 2011) have tools to incorporate spatial effects.

RS is increasingly gaining popularity as data sources for ecological and environmental studies for its non-destructive, synoptic, repetitive, and cost-effective advantages. Optics and sensor technology and data processing methods are developing at a rapid pace. As the science and technology of RS grows, there will be enhanced availability of RS data from multiple sources at multiple resolutions that will open tremendous opportunities for multi-scalar studies on ecosystem analysis and environmental monitoring. That being said, serious consideration needs to be given to the selection, analysis, and conclusions of scale of study as it can directly impact the information derived from them.

6.4 REFERENCES

ACCP. 1994. Accelerated canopy chemistry program final report to NASA-EOS-IWG. Washington, DC USA: National Aeronautics and Space Administration [*http://daac.ornl.gov/ACCP/accp.html*].

Asner, G.P., Martin, R.E., Ford, A.J., Metcalfe, D.J., and Liddell, M.J. 2009. Leaf chemical and spectral dversity in Australian tropical forests. *Ecological Applications*, 19(1): 236-253.

Atkinson, P.A. and Tate, N.J. 2000. Spatial Scale Problems and Geostatistical Solutions: A Review. *The Professional Geographer*, 52(4): 607-623.

Blackburn, G.A. 2007. Hyperspectral remote sensing of plant pigments. *Journal of Experimental Botany*, 58(4): 855-867.

Bojinski, S., Schaepman, M., Schläpfera, D., and Itten, K. 2003. SPECCHIO: a spectrum database for remote sensing applications. *Computers & Geosciences*, 29(1): 27-38.

Briggs, J.M., Knapp, A.K., and Collins, S.L. 2008. Steppes and Prairies. *Encyclopedia of Ecology*, 3373-3382.

Chave, J. 2013. The problem of pattern and scale in ecology: what have we learned in 20 years? *Ecology Letters*, 16(s1): 4-16.

Dungan, J.L., Perry, J.N., Dale, M.R.T., Legendre, P., Citron-Pousty, S., Fortin, M.J., Jakomulska, A., Miriti, M., and Rosenberg, M.S. 2002. A balanced view of scale in spatial statistical analysis. *Ecography*, 25(5): 626-640.

Gamon, J.A., Rahman, A.F., Dungan, J.L., Schildhauer, M., and Huemmrich, K.F. 2006. Spectral Network (SpecNet): What is it and why do we need it? *Remote Sensing of Environment*, 103: 227-235.

García-Haro, F. J., Sommer, S., and Kemper, T. 2005. A new tool for variable multiple endmember spectral mixture analysis (VMESMA). *International Journal of Remote Sensing*, 26(10): 2135-2162.

Goetz, A.F.H. 2009. Three decades of hyperspectral remote sensing of the Earth: A personal view. *Remote Sensing of Environment*, 113: S5-S16.

Goodchild, M.F. 2001. Models of scale and scales of modelling. In: Tate, N.J., Atkinson, P.M. (Eds.), Modelling Scale in Geographical Information Science. John Wiley & Sons, Chichester.

Hueni, A., Nieke, J., Schopfer, J., Kneubuhler, M., and Itten, K.I. 2009. The spectral database SPECCHIO for improved long-term usability and data sharing. *Computers and Geosciences*, 35(3): 557-565.

Irons, J.R., Dwyer, J.L., and Barsi, J.A. 2012. The next Landsat satellite: The Landsat data continuity mission. *Remote Sensing of Environment*, 77(2): 212-225.

Jacquemoud, S., Bacour, C., Poilve, H., and Frangi, J. P. 2000. Comparison of four radiative transfer models to simulate plant canopies reflectance: Direct and inverse mode. *Remote Sensing of Environment*, 74(3): 471-481.

Kokaly, R.F., Asner, G.P., Ollinger, S.V., Martin, M.E., and Wessman, C.A. 2009. Characterizing canopy biochemistry from imaging spectroscopy and its application to ecosystem studies. *Remote Sensing of Environment*, 113: S78-S91.

Leimgruber, P., Christen, C.A., and Laborderie, A. 2005. The impact of Landsat satellite monitoring on conservation biology. *Environmental Monitoring and Assessment*, 106(1-3): 81-101.

Li, Z., and Guo, X. 2012. Detecting climate effects on vegetation in northern mixed prairie using NOAA AVHRR 1-km time-series NDVI data. *Remote Sensing*. 4(1): 120-134.

Milton, E.J., Schaepman, M.E., Anderson, K., Kneubühler, M., and Fox, N. 2009. Progress in field spectroscopy. *Remote Sensing of Environment*, 113(1): S92-S109.

Okin, G.S., Roberts, D.A., Murray, B., and Okin, W.J. 2001. Practical limits on hyperspectral vegetation discrimination in arid and semiarid environments. *Remote Sensing of Environment*, 77(2): 212-225.

Ollinger, S.V. 2011. Sources of variability in canopy reflectance and the convergent properties of plants. *New Phytologist*, 189(2): 375-394.

Plaza, A., Benediktsson, J.A., Boardman, J.W., Brazile, J., Bruzzone, L., Camps-Valls, G., Chanussot, J., Fauvel, M., Gamba, P., Gualtierii, A., Marconcini, M., Tilton, J. and Trianni, G. 2009. Recent advances in techniques for hyperspectral image processing. *Remote Sensing of Environment*, 113(1): S110-S122.

Rangel, T.F., Diniz-Filho, J.A.F., and Bini, L.M. 2010. SAM: A comprehensive application for spatial analysis in Macroecology. *Ecography*, 33(1): 46-50.

Roberts, D. Halligan, K., and Dennison, P. 2007. VIPER Tools User Manual Version 1.5. 91 pp.

Rosenberg, M.S., and Anderson, C.D. 2011. PASSaGE: Pattern Analysis, Spatial Statistics and Geographic Exegesis. *Methods in Ecology and Evolution*, 2(3): 229-232.

Roy, D.P., Wulder, M.A., Loveland, T.R., Woodcock, C.E., Allen, R.G., Anderson, M.C., Helder, D., Irons, J.R., Johnson, D.M., Kennedy, R., Scambos, T.A., Schaaf, C.B., Schott, J.R., Sheng, Y., Vermote, E.F., Belward, A.S., Bindschadler, R., Cohen, W.B., Gao, F., Hipple, J.D., Hostert, P., Huntington, J., Justice, C.O., Kilic, A., Kovalskyy, V., Lee, Z.P., Lymburner, L., Masek, J.G., McCorkel, J., Trezza, R., Vogelmann, J., Wynne, R.H., and Zhu, Z. 2014. Landsat-8: Science and product vision for terrestrial global change research. *Remote Sensing of Environment*, 145: 154-172.

Schaepman, M.E., Ustin, S.L., Plaza, A.J., Painter, T.H., Verrelst, J., and Liang, S. 2009. Earth system science related imaging spectroscopy – An assessment. *Remote Sensing of Environment*, 113: S123-S137.

Turner, M.G. 1989. Landscape Ecology: The Effect of Pattern on Process. *Annual Review of Ecology and Systematics*, 20: 171-197.

Turner, M.G., Dale, V.H., and Gardner, R.H. 1989. Predicting across scales: Theory development and testing. *Landscape Ecology*, 3(3-4): 245-252.

Urban, D.L. 2005. Modeling ecological processes across scales. *Ecology*, 86, 1996-2006.

Ustin, S.L., Roberts, D.A., Gamon, J.A., Asner, G.P., and Green, R.O. 2004. Using imaging spectroscopy to study ecosystem processes and properties. *Bioscience*, 54(6): 523-534.

Wessman, C.A. 1992. Spatial scales and global change: Bridging the gap from plots to GCM grid cells. *Annual Review of Ecology and Systematics*, 23: 175-200.

Wiens, J.A., and Milne, B.T. 1989. Scaling of 'landscapes' in landscape ecology, or landscape ecology from a beetle's perspective. *Landscape Ecology*, 3(2): 87-96.

Wu, J. 1999. Hierarchy and scaling: extrapolating information along a scaling ladder. *Canadian Journal of Remote Sensing*, 25(4): 367-380.

Wu, J., Jones, K.B., Li, H., and Loucks, O.L. 2006. *Scaling and Uncertainty Analysis in Ecology: Methods and Applications*. Springer, 3-15.

Wulder, M.A., White, J.C., Goward, S.N., Masek, J.G., Irons, J.R., Herold, M., Cohen, W.B., Loveland, T.R., and Woodcock, C.E. 2008. Landsat continuity: Issues and opportunities related to Landsat continuity. *Remote Sensing of Environment*, 112(3): 955-969.

Wulder, M.A., Masek, J.G., Cohen, W.B., Loveland, T.R., and Woodcock, C.E. 2012. Opening the archive: How free data has enabled the science and monitoring promise of Landsat. *Remote Sensing of Environment*, 122: 2-10.

Yang, X., and Guo, X. 2011. Investigating vegetation biophysical and spectral parameters for detecting light to moderate grazing effects: a case study in mixed grass prairie. *Central European Journal of Geosciences*, 3(3): 336-348.